Gram-positive heme acquisition

by

Yan Shipelskiy

B.S., The Pennsylvania State University, 2010

An abstract of a dissertation

submitted in partial fulfillment of the requirements for the degree

Doctor of Philosophy

Department of Biochemistry and Molecular Biophysics
College of Arts and Sciences

Kansas State University
Manhattan, Kansas

2017

Abstract

Gram-positive bacteria are characterized by a single lipid bilayer with a thick peptidoglycan layer. This group of organisms contains bacteria commonly associated with human infection, including: *Staphylococcus aureus, Listeria monocytogenes, Bacillus anthracis* and *Streptococcus pneumoniae* among others. These bacteria have a common system for importing iron in the form of heme, which is acquired by proteins containing heme-binding NEAT (**NEA**r iron **T**ransporter) domains. The heme acquisition system in *S. aureus* is termed the **I**ron **S**urface **De**terminant (Isd) system and in *L. monocytogenes* is termed **H**eme **B**inding **P**rotein (Hbp) and **H**eme/Hemoglobin **Up**take Protein (Hup). These proteins work together to obtain heme from hemoglobin and then transport the heme into the cytoplasm via well characterized ABC-transporters.

Although there have been clinical trials with antibodies directed against Isd proteins, there are currently no antibiotics targeting iron uptake systems in bacteria in general. Building upon fluorescent approaches for detection of iron uptake in Gram-negative organisms, this work develops fluorescent heme acquisition detection in Gram-positive organisms. The spectrofluorimetric methodology facilitates the understanding of heme acquisition protein interactions and mechanisms in bacteria. This work could subsequently be used to identify inhibitors of Gram-positive bacterial iron uptake systems, and develop a new target for antibiotic action.

Gram-positive heme acquisition

by

Yan Shipelskiy

B.S., The Pennsylvania State University, 2010

A dissertation

submitted in partial fulfillment of the requirements for the degree

Doctor of Philosophy

Department of Biochemistry and Molecular Biophysics
College of Arts and Sciences

Kansas State University
Manhattan, Kansas

2017

Approved by:

Major Professor
Philip E. Klebba, PhD

Abstract

Gram-positive bacteria are characterized by a single lipid bilayer with a thick peptidoglycan layer. This group of organisms contains bacteria commonly associated with human infection, including: *Staphylococcus aureus, Listeria monocytogenes, Bacillus anthracis* and *Streptococcus pneumoniae* among others. These bacteria have a common system for importing iron in the form of heme, which is acquired by proteins containing heme-binding NEAT (**NEA**r iron **T**ransporter) domains. The heme acquisition system in *S. aureus* is termed the **I**ron **S**urface **De**terminant (Isd) system and in *L. monocytogenes* is termed **H**eme **B**inding **P**rotein (Hbp) and **H**eme/Hemoglobin **Up**take protein (Hup). These proteins work together to obtain heme from hemoglobin and then transport the heme into the cytoplasm via well characterized ABC-transporters.

Although there have been clinical trials with antibodies directed against Isd proteins, there are currently no antibiotics targeting iron uptake systems in bacteria in general. Building upon fluorescent approaches for detection of iron uptake in Gram-negative organisms, this work develops fluorescent heme acquisition detection in Gram-positive organisms. The spectrofluorimetric methodology facilitates the understanding of heme acquisition protein interactions and mechanisms in bacteria. This work could subsequently be used to identify inhibitors of Gram-positive bacterial iron uptake systems, and develop a new target for antibiotic action.

Table of Contents

List of Figures……ix

List of Tables……xii

Acknowledgements……xiii

Dedication……xiv

Chapter 1: Introduction……1

1.1 The Importance of Iron for Bacteria……1

1.2 Iron Uptake in *Escherichia coli* and Other Gram-negative Bacteria……2

1.3 A model of the Gram-positive cell wall with NEAT-domain based heme uptake……7

1.4 NEAT-domain Dependent Iron Uptake in *Listeria monocytogenes*……11

1.5 NEAT-domain Dependent Iron Uptake in *Staphylococcus aureus*……13

1.6 NEAT-domain Dependent Iron Uptake in *Bacillus anthracis*……14

1.7 NEAT-domain Dependent Iron Uptake in *Streptococcus pyogenes*……16

1.8 NEAT-domain Independent Iron Uptake in Gram-positive Bacteria……19

1.9 Genetic Regulation of Iron Uptake……22

1.10 Development of the Universal Assay……24

1.11 Clinical Relevance of Iron Uptake by Pathogenic Bacteria……25

Chapter 2: Materials and Methods……29

2.1 Bacterial Strains and Plasmids……29

2.2 Growth Media……33

2.3 Oligonucleotides……34

2.4 Genetic Constructs……36

2.5 Verification of *hbp1* Deletion from *L. monocytogenes* Strain EGD-e……38

2.6 Verification of *hbp2* Deletion from *L. monocytogenes* Strain EGD-e……39

2.7 Preparation of Competent *E. coli* and *L. monocytogenes* Competent Cells….40

2.8 Transformation of *E. coli* and *L. monocytogenes* Competent Cells……41

2.9 Verification of Plasmid Uptake……42

2.10 Selection of Sites in Hbp2 for Mutation……44
2.11 Expression and Purification of His-tagged Heme Uptake Proteins……47
2.12 Expression and Purification of Hbp2 from *L. monocytogenes*……48
2.13 Preparation and Quantification of Fluorescein Maleimide, Coumarin Maleimide, Heme and FeEnt……49
2.14 Labeling Cysteine Mutations in Hbp2……51
2.15 Fluorometric Analysis of Heme Binding to Hbp2……51
2.16 Iron Starvation of Gram-positive Cells and *In vivo* Heme Uptake Experiments……52
2.17 Fluorescence Labeling and Analysis of FeEnt Uptake in *E. coli*……53
2.18 Fractionation of the *Caulobacter crescentus* Inner and Outer Membranes.55

Chapter 3: Expression of NEAT-domain Containing Proteins, their Interactions and *in vivo* Heme Uptake by Gram-positive Cells……56
3.1 Expression of Hbp2 Using the pPL2 Plasmid in *L. monocytogenes*……56
3.2 Expression of Hbp2 Using the pAT28 Plasmid in *L. monocytogenes*……58
3.3 Labeling of *in vivo* Hbp2 in *L. monocytogenes*……59
3.4 Expression and Purification of Hbp2 from *E. coli* Using pET28……62
3.5 Expression and Purification of Hbp2(S154C) from *L. monocytogenes*……65
3.6 Spectroscopic Analysis of Coumarin-Labeled Hbp2(S154C)……66
3.7 Analysis of Total Quenching During Heme Binding to Hbp2……70
3.8 Titration of Heme into Hbp2 to Determine K_d……72
3.9 Heme Transfer from Hbp2 to Hbp1, HupD and IsdC, IsdB and IsdH……75
3.10 Heme Uptake from Hbp2(S154C) by *B. subtilis*, *L. monocytogenes* and *S. aureus*……83

Chapter 4: Concerted Loop Motion Triggers Induced Fit of FepA to Ferric Enterobactin..85
4.1 Introduction……85

4.2 Results……87

Chapter 5 – High-Throughput Screening Assay for Inhibitors of TonB-Dependent Iron Transport……97

5.1 Introduction……97

5.2 Results……98

Chapter 6 – TonB-Dependent Heme/Hemoglobin Utilization by *Caulobacter crescentus* HutA……104

6.1 Introduction……104

6.2 Results……106

References……119

List of Figures

Figure 1-1: Model of the Gram-negative system for TonB-dependent nutrient uptake…..4

Figure 1-2: Enterobactin, ferrichrome, rhodotorulic acid, and aerobactin: Small compounds used by bacteria to acquire iron……6

Figure 1-3: A model of the Gram-positive *Listeria monocytogenes* NEAT-domain based heme uptake……8

Figure 1-4: Alignment of crystal structures of NEAT-domains from *S. aureus*……10

Figure 1-5: Chromosomal map of *Listeria monocytogenes* genes responsible for heme uptake……12

Figure 1-6: Heme Acquisition Operon of *S. aureus*……14

Figure 1-7: Heme Acquisition Operon of *B. anthracis*……15

Figure 1-8: Heme Acquisition Operon of *S. pyogenes*……17

Figure 1-9: Comparison of *S. aureus* IsdC and *S. pyogenes* Shp crystal structures……18

Figure 1-10: Coordination of Heme by *S. pyogenes* Shp residues M66 and M153……19

Figure 2-1: Plasmid Maps of His-tag expression vector pET28a, the integration-shuttle vector pPL2, shuttle vector pAT28, and *E. coli* expression vector pHSG575……32

Figure 2-2: Chromosomal annotation of genes vital for the transport of heme and ferrichrome in the *L. monocytogenes* genome.……37

Figure 2-3: Chromosomal sequence of *hbp1* and *hbp2*, with the upstream primer……37

Figure 2-4: pET28a-Hbp2Δ30(S154C) Sequencing Confirmation……38

Figure 2-5: Map of WT *hbp2* Inserted into pAT28……38

Figure 2-6: Sequence of *hbp2* in pAT28 Plasmid……39

Figure 2-7: Double Digest of pAT28-Hbp2(K62C)……43

Figure 2-8: Alignment of pAT28-Hbp2 to pAT28-Hbp2(K62C)……44

Figure 2-9: Clustal Omega Alignment of NEAT-domains with Available Structures to *L. monocytogenes* Hbp2 NEAT-domain 1……45

Figure 2-10: Location of Cysteine Mutants in Hbp2 NEAT1……46

Figure 2-11: Inhibition of *E. coli* FeEnt Uptake by Different Concentrations of the Energy Poison CCCP……54

Figure 3-1: Expression of Hbp2 from WT EGD-e. Lack of Expression from *Δhbp2* Strain and Integrated pPL2-Hbp2 Plasmids……..57

Figure 3-2: Western Blot Showing the Expression of WT Hbp2 and the K62C and S154C Mutants from the pAT28 Vector……59

Figure 3-3 Fluorescent Labeling and Heme Response of *L. monocytogenes* Cells Expressing Cysteine-containing Hbp2……60

Figure 3-4: Coomassie Stained Gel of 40mM imidazole Wash and Eluted Fractions of His-tagged Hbp2Δ30(S154C)……63

Figure 3-5: Spectroscopic Analysis of Heme Binding to His-Hbp2(S154C)……..64

Figure 3-6: Dialysis of His-Tagged Hbp2Δ30(S154C)……65

Figure 3-7: Fluorescent Gel (A) and Coomassie Stain (B) of S300HR-purified Hbp2……66

Figure 3-8: 50x Dilution of Coumarin Labeled Hbp2(S154C) from Fraction 43……68

Figure 3-9: Absorbance of Free Coumarin-maleimide in Methanol and PBS, Compared to Coumarin Maleimide Reacted with Cysteine in PBS……69

Figure 3-10: 30nM of Labeled Hbp2(S154C) with 100nM Heme……71

Figure 3-11: Titration of Heme into 30nM of Coumarin Labeled Hbp2(S154C)……..73

Figure 3-12: Fluorescence Drop from Heme Binding to Hbp2……74

Figure 3-13: Heme Transfer from holo-Hbp2 to apo-Hbp1……76

Figure 3-14: Heme Transfer from holo-Hbp2 to apo-HupD……77

Figure 3-15: Heme Transfer from Holo-Hbp2 to apo-Hbp1 then apo-HupD……78

Figure 3-16: Heme Transfer from holo-Hbp2 to apo-IsdC……..80

Figure 3-17: Heme Transfer from holo-Hbp2 to apo-IsdB……..81

Figure 3-18: Heme Transfer from holo-Hbp2 to apo-IsdH……82

Figure 3-19: Fluorescence recovery during heme uptake in *B. subtilis*, *L. monocytogenes* and *S. aureus*……..84

Figure 4-1: Labeling Efficiency of WT and S271C FepA Under Various Time, Concentration and pH Conditions……88

Figure 4-2: Fluorescence Response from FeEnt Binding to FepA with Different Cysteine Mutations……89

Figure 4-3: Evaluation of FepA Expression and Fluoresceination in Strains Expressing or Lacking TonB……..93

Figure 4-4: Fluorescent Microscopy of GFP-TonB and FepA(S271C) Labeled with Alexa Fluor 546 upon FeEnt Binding……96

Figure 5-1: Fluorescence Quenching and Recovery from Ferric-enterobactin Binding to FepA……..101

Figure 5-2: Evaluation of *E. coli* Ability to Take up FeEnt after Storage on Ice and Z-factor Analysis of the Microtiter Assay……102

Figure 6-1: Siderophore Nutrition Tests for *C. crescentus*……..107

Figure 6-2: *C. crescentus* Growth in Iron limiting Conditions and Recovery when Supplemented with Utilizable Iron……..109

Figure 6-3: Binding and Transport of Radiolabeled Ferrichrome and Ferric-citrate…….111

Figure 6-4: Phylogenetic Analysis of TBDTs from *E. coli* and *C. crescentus*……..112

Figure 6-5: Sucrose Gradient Separation of *C. crescentus* Cell Envelope……..116

Figure 6-6: Separation of *C. crescentus* Cell Envelope into Inner and Outer Membrane Fractions……..117

Figure 6-7: Deletion of ccr02277 Shows a Loss of Ability for *C. crescentus* to Produce HutA or Take up Heme……..118

List of Tables

Table 1-1: TonB-dependent Receptors in *E. coli*……..5

Table 2-1: Bacterial Strains……30-31

Table 2-2: Plasmids……31

Table 2-3: Media……33

Table 2-4: Oligonucleotides……34-36

Table 3-1: Fluorescence quenching from heme being added to purified Hbp2(S154C) labeled with coumarin……73

Table 4-1: Phenotypes of FepA cysteine mutants……92

Table 4-2: Binding Kinetics During FeEnt Binding to Different Loops of FepA……94

Table 5-1: Inhibitory Concentrations of Various Energy Poisons for TonB-dependent Reactions……103

Table 6-1: Summary and Quantification of Halos for Siderophore Nutrition Tests with *C. crescentus*……..108

Acknowledgements

I would like to take this opportunity to thank Dr. Philip Klebba for his mentoring. The path forward in this research was not always clear and there were set-backs throughout my experience, despite any problems Phil was there to offer support, guidance and inspiration. In trying times, interaction with Phil always left me feeling better. I would also like to thank Dr. Salete Newton. Sally has been there to offer advice and guidance in situations good and bad. Her upbeat attitude and the exquisite treats she regularly brought for us gave me and the students in Phil's lab a home-away-from-home. I would like to thank Dr. Michal Zolkiewski, who is incredibly supportive and knowledgeable. Dr. Zolkiewski has a talent for communicating complicated material in an easy to understand manner. I would like to thank Dr. Brian Geisbrecht, who is tremendously knowledgeable and supportive. Dr. Geisbrecht's expertise on structures and infectious diseases were vital. I would like to thank Dr. Ruth Welti, whose support has been incredibly comforting. Dr. Welti has a very warm and personal touch that is uplifting in a technical environment. I would also like to thank Dr. Yoonseong Park, whose acceptance of the outside chair position in a timely manner is greatly appreciated. Additionally, I would like to thank Dr. Larry Davis, Dr. Maureen Gorman, Lisa Brummet, Dr. Stephen Chapes, David Manning, Dr. John Tomich, Sue-Yi Huang, Dr. Om Prakash, Dr. Lorne Jordan, Noah Long and countless others for their support, advice, friendship.

Dedication

My grandmother, Sonya Kaplun, is a wonderful educator and a tremendous researcher. Her research thesis was on the bacterial genus Azotobacter. She overcame great odds to become one of the first Jewish women to attain her advanced degree in microbiology, and most of life's trouble pale in comparison with the adversity she has risen above. Grandma Sonya is a great role model and an inspiration. As of this publication she is going strong at the sprightly young age 91.

I would like to thank my mom Rimma, my dad Boris, my granddad Shura, grandma Genya, grandma Bertha, my sister Beccah and my girlfriend Emily. Their love and support is precious. Their making fun of me when I fall short of being an esteemed biochemist is less-appreciated.

Chapter 1: Introduction

1.1 The Importance of Iron for Bacteria.

Iron is the most abundant trace element in mammals and is essential to all life on earth, including bacteria. Iron is important for bacteria because of its critical role in metabolic pathways, detoxification and energy generation. While ferrous iron is soluble in water, in the presence of oxygen iron is oxidized and forms iron oxides which have exceedingly low solubility in water. Whereas bacteria need micromolar concentrations of iron for growth, the concentration of ferrous iron in solution is estimated at 10^{-18} M (Raymond et al 2003, Sheldon and Heinrichs 2015). In addition to poor solubility in aqueous environments, animals have further strategies for limiting the iron available to bacteria during infection. Circulating ferric iron is complexed by transferrin or lactoferrin. Heme, which is the largest source of iron in the body, accounting for two thirds of total iron stores, is bound by hemoglobin and sequestered within red blood cells (Skaar et al, 2004; Pishchany et al, 2013). If heme or hemoglobin are found in circulation, they are complexed by hemopexin or haptoglobin respectively (Sheldon and Heinrichs 2015). This tight control of iron in eukaryotes helps prevent bacteria from acquiring an essential nutrient for proliferation, and is referred to as “nutritional immunity.” Both infectious and free-living bacteria have developed multiple systems for acquiring iron from the host or the environment.

However, iron also poses a potential threat to organisms because of its tendency to generate reactive oxygen species (ROS) via Fenton chemistry. Both eukaryotic organisms and bacteria have extensive approaches to limiting ROS generation by iron. In eukaryotes, iron is sequestered using transferrin and heme binding proteins in the extracellular environment, whereas intracellular iron can be stored in a non-reactive state in ferritin, a large protein complex. Bacteria also have a ferritin-like intracellular iron storage structure, along with efflux pumps to excrete iron if it's concentration is excessive (Pi et al, 2016).

1.2 Iron Uptake in *Escherichia coli* and Other Gram-negative Bacteria.

Bacterial iron uptake mechanisms vary based on the presence of an outer membrane. Gram-negative bacteria include common pathogenic genera like Enterococcus, Klebsiella, Acinetobacter, Pseudomonas and Enterobacter. Gram-negative bacteria are characterized by an inner membrane and outer membrane with a thin peptidoglycan layer in the periplasmic space. The outer membrane is porous up to 600Da, due to the presence of Outer membrane proteins (OMPs), which allow for passive diffusion of small molecules at high concentrations (Newton et al, 1999; Smallwood et al, 2014). Nutrients which are larger than 600Da or found in low concentration within the environment, including iron, must be actively transported across the Gram-negative outer membrane. Gram-negative bacteria power this active transport using the TonB system, which is composed of a three-protein transmembrane complex composed of

TonB/ExbB/ExbD located in the inner membrane (Higgs et al, 2002; Celia et al, 2016). ExbB has three transmembrane domains, with a cytoplasmic loop, whereas both TonB and ExbD have a single transmembrane domain with a periplasmic domain. ExbB:ExbD:TonB are proposed to associate in a 7:2:1 stoichiometry respectively, with ExbB functioning as a scaffold, within which TonB and ExbD associate (Baker and Postle, 2013). This complex utilizes the electrochemical gradient found across the inner membrane to drive the import of nutrients across the unenergized outer membrane, by interacting with ligand gated outer membrane proteins (Figure 1-1).

Outer membrane ligand gated porins that interact with TonB are called Ton-B dependent transporters (TBDTs) and are characterized by a C-terminal 22-strand beta-barrel structure with an N-terminal "cork" region in the middle, which blocks passive diffusion of nutrients (Figure 1-1). The N-terminal portion of TBDT additionally has a TonB-box region which interacts with TonB directly during nutrient transport (Jordan et al, 2013). The TBDTs bind and transport nutrients in two separate stages, the first energy independent stage involves nutrient binding, and the second energy dependent stage involves the transfer of the nutrient to the periplasmic space (Smallwood et al, 2014; Celia et al, 2016). During the first energy independent step, the outer loops of the TBDTs have been shown to close around the ligand, localizing the ligand in a vestibule (Smallwood et al, 2014). Binding of the ligand to the TBDT exposes the TonB box, which can directly interact with TonB. During the second step of outer membrane transport, TonB transiently associates with the Ton Box and transduces the energy from the inner membrane electrochemical gradient to drive a conformational change in the TBDR which

allows for the transport of the ligand from the TBDT vestibule into the periplasmic space (Ma et al, 2007). This second step is considered energy dependent since it requires a PMF across the inner membrane. Energy uncouplers like cyanide and CCCP disrupt the PMF and inhibit TonB-dependent uptake of nutrients (Hanson et al, 2016). Once inside the periplasmic space, the ligand interacts with periplasmic carrier proteins that shuttle the ligand to well characterized ATP-binding cassette (ABC) transporters, which hydrolyze ATP to drive transport into the cytoplasm (Newton et al, 2010; Roe et al, 2013).

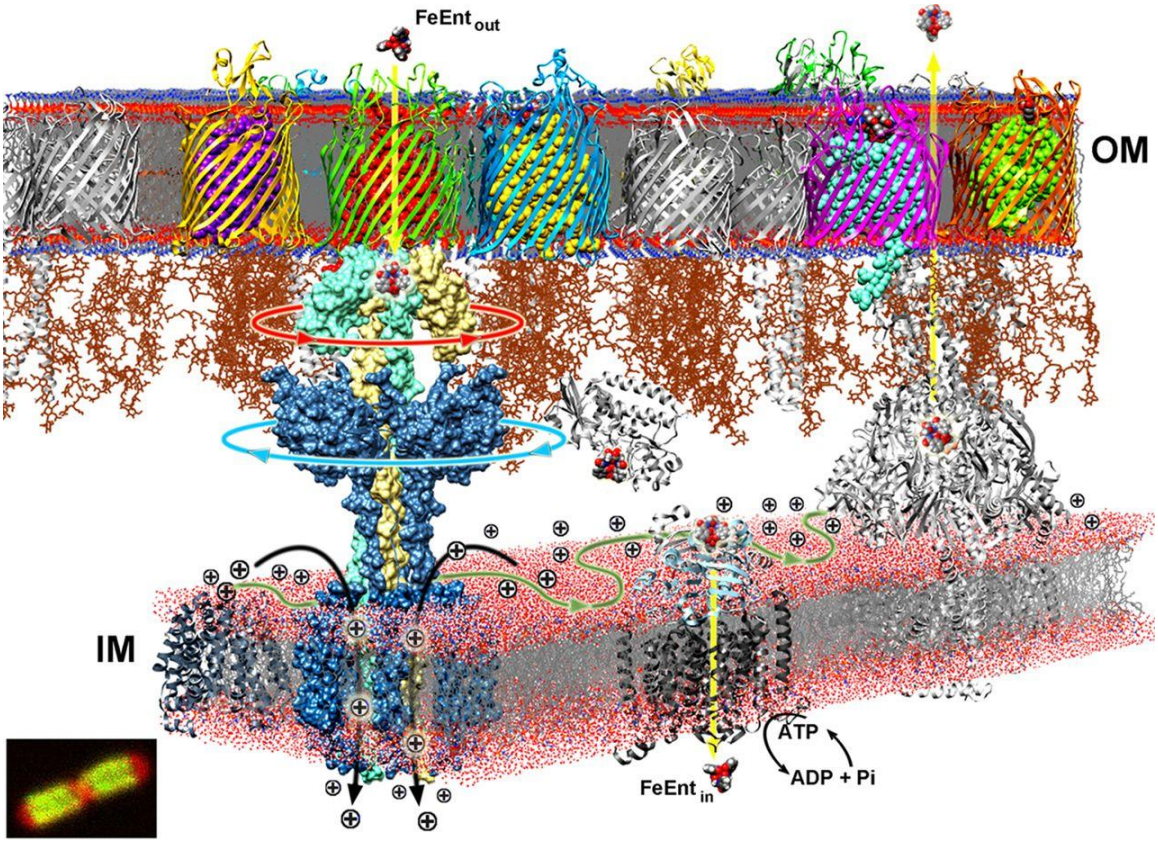

Figure 1-1: Model of the Gram-negative system for TonB-dependent nutrient uptake (Klebba, 2016. Figure reprinted with permission from the American Society for Microbiology).

E. coli has eight TBDTs, including FepA, which transports ferric enterobactin, FhuA which transports ferrichrome and BtuB which transports vitamin B12. A complete list is

provided in Table 1-1 (Balhesteros et al, 2016). Enterobactin and ferrichrome are two prototypical siderophores among an exhaustive library. Siderophores are small molecules synthesized in non-ribosomal pathways from amino acids. They are secreted by bacteria to bind iron with high affinity for subsequent uptake. These iron scavenging molecules were discovered by Dr. Neilands and are also produced by Gram-positive organisms (Neilands 1981). Siderophores can be categorized by their functional groups which interact with the iron in a hexacoordinated fashion. Siderophores commonly have three of these functional groups and they can be composed of hydroxamates (Figure 1-2B), catecholates (Figure 1-2A) or mixed-type siderophores (Figure 1-2D).

Table 1-1: TonB-dependent Receptors in *E. coli*.

Receptor	Ligand	Reference
FepA	Ferric Enterobactin	Smallwood et al, 2014
FecA	Iron-citrate	Ferguson et al, 2002
BtuB	Vitamin B12 (cobalamin)	Chimento et al, 2003
Cir	Iron catecholate	Nikaido and Rosenberg, 1990
Fiu	Iron catecholate	Nikaido and Rosenberg, 1990
FhuA	Ferrichrome	Pawelek et al, 2006
FhuE	Coprogen & Rhodotorulate	Hantke, 1983
IutA	Aerobactin	de Lorenzo et al, 1986

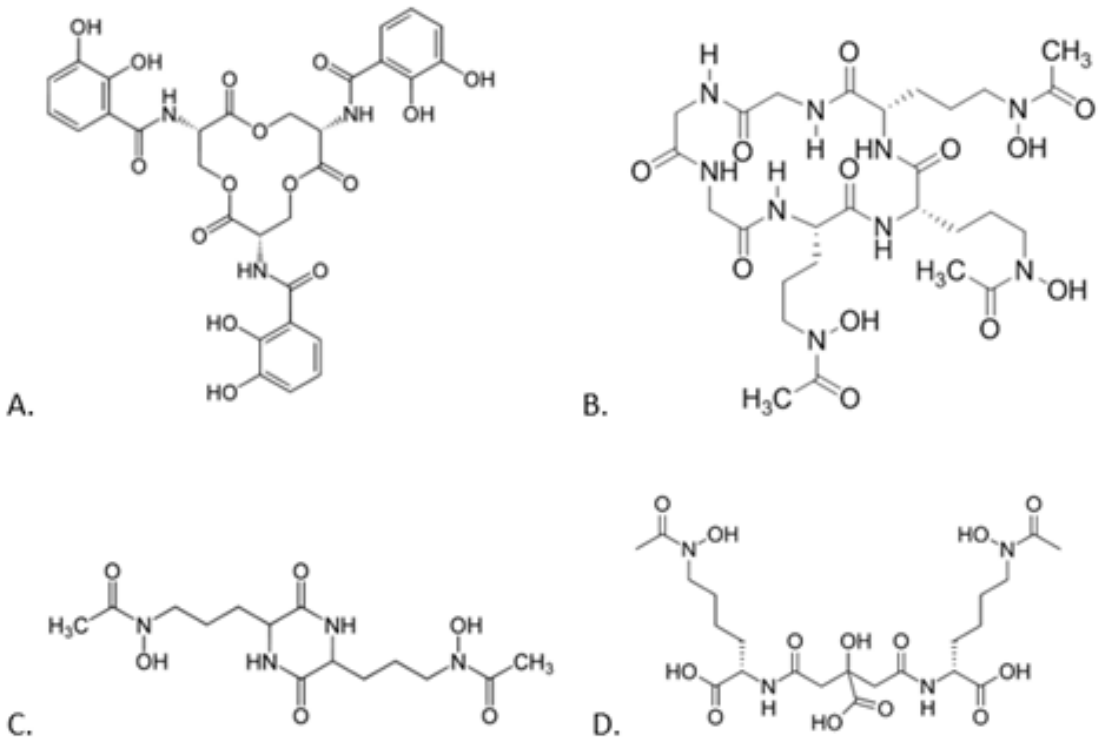

Figure 1-2: Enterobactin (A), Ferrichrome (B), Rhodotorulic acid (C), and aerobactin (D): Small compounds used by bacteria to acquire iron.

While the *E. coli* TonB system is best characterized, there are variations in other organisms. *Caulobacter crescentus* has upwards of 60 TBDRs (Balhesteros et al, 2016), presumably because of the dilute environment the free-living organism occupies. The low-nutrient conditions in freshwater lakes necessitates a high level of active nutrient uptake compared to *E. coli*. *Vibrio cholera* and *Actinobacillus pleuropneumoniae* have two copies of TonB/ExbB/ExbD energy transducing complex (Occhino et al, 1998; Beddek et al, 2004).

The substrates that bacteria can import using the TonB system are not limited to siderophore-bound iron, but also include sugars, heme, vitamins and other metals

(Neugebauer et al, 2005; Schauer et al, 2008; Mirus et al, 2009). Even in *E. coli* BtuB is responsible for taking up the porphyrin vitamin B12, and uropathogenic strains of *E. coli* have been reported to contain two distinct TBDT heme uptake proteins, Hma and ChuA (Hagan and Mobley, 2009). Numerous reports have shown that heme acquisition is a common role for TBDT. *Serratia marcescens* produces and secretes a heme binding protein, HasA, which transfers heme to the TBDT HasR (Létoffé et al, 2004; Huché et al, 2006). *Haemophilus ducreyi* also expresses a hemoglobin binding and heme acquisition protein HgbA which is a TBDT (Fusco et al, 2013). Likewise, *Leptospira interrogans* produces a heme binding protein HbpA (Asuthkar et al, 2007). *Caulobacter crescentus* also expresses a heme uptake and utilization TBDT HutA (Balhesteros et al, 2016).

1.3 Iron Uptake in Gram-positive Bacteria via NEAT-domain Containing Proteins.

Gram-positive bacteria are characterized by a single lipid bilayer with a thick peptidoglycan layer, and no outer membrane. This group of bacteria contains common human pathogens, including: *Staphylococcus aureus*, *Listeria monocytogenes, Bacillus anthracis* and *Streptococcus pneumoniae* among others. These bacteria don't need to power nutrient import across an outer membrane, and can take up heme or siderophores directly via ABC transporters at high concentrations (Drazek et al, 2000; Xiao et al, 2011). Despite having a single membrane, Gram-positive bacteria have an extensive peptidoglycan layer to which proteins can be covalently anchored via Sortase proteins (Figure 1-3).

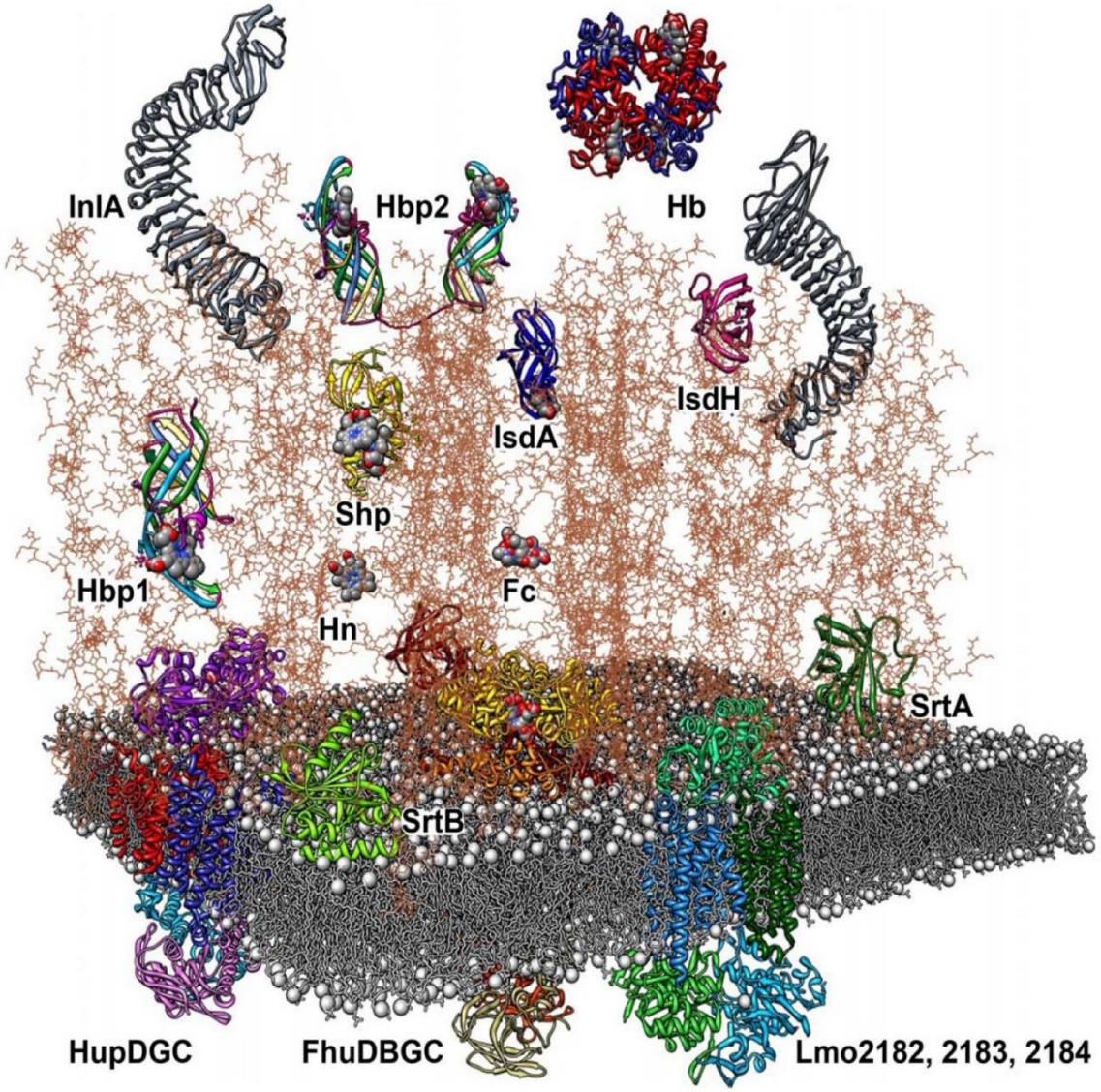

Figure 1-3: A model of the Gram-positive cell wall with NEAT-domain based heme uptake (Xiao et al, 2011. Reprinted with permission from John Wiley and Sons. License Number 4230991495410).

In iron-deficient conditions, Gram-positive bacteria produce heme binding proteins with a common structural feature called a NEAT (**NEA**r iron **T**ransporter) domain. NEAT-domains share an immunoglobulin-like beta-sandwich fold with 7 beta strands in two sheets and a single 3^{10} helix (Figure 1-4). NEAT-domains have a conserved YXXY (Y132 and Y136 in Figure 1-3) motif within the heme binding pocket which coordinates the heme

group during binding. Additionally, the 3_{10} helix region is responsible for coordinating the heme during binding and mediating protein-protein interactions during heme transfer between NEAT-domain containing proteins. Proteins containing NEAT domains can bind free heme or extract heme from hemoglobin. Proteins containing NEAT domains can be attached covalently to the peptidoglycan via C-terminal Sortase sequences. Sortase A utilizes a consensus LPXTG sequence and Sortase B utilizes a consensus NPXTN sequence, and genes encoding the Sortase proteins are commonly found within the same operon as NEAT-domain containing proteins (Mazmanian et al, 2003; Xiao et al, 2011). NEAT-domain containing proteins can also be secreted into the extra-cellular milieu where they function as hemophores (Maresso et al, 2008; Malmirchegini et al, 2014). Multi-NEAT domain proteins extract heme from hemoglobin and transfer heme to single-NEAT domain containing proteins, with the heme subsequently transferred to ATP-permeases (Pishchany et al, 2014; Fonner et al, 2014; Dickson et al, 2015). The heme can then directly be used by bacteria, or can be cleaved by heme dioxygenases to liberate iron.

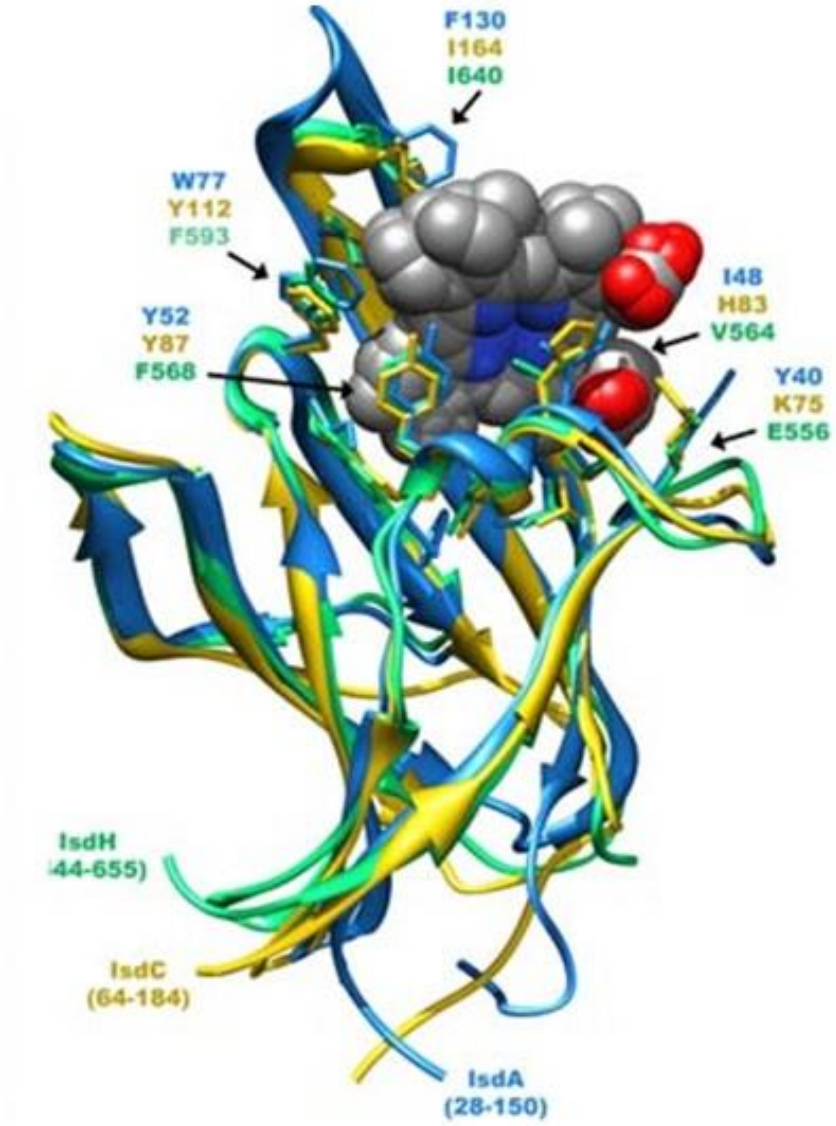

Figure 1-4: Alignment of Crystal Structures of NEAT-domains from *S. aureus* (Klebba et al, 2012. Reprinted with permission from Taylor & Francis).

Overall, NEAT-domains function as modular units which can be strung together to allow free heme binding or heme extraction. NEAT-domain containing proteins have been found to contain between one NEAT-domain (as seen in Hbp1, IsdC or IsdX1) up to five NEAT-domains (as seen in IsdX2) on a single polypeptide. Areas outside of NEAT-domains can contain Sortase sequences, allowing many of these proteins to be covalently attached to the peptidoglycan. In *Listeria monocytogenes*, NEAT-domain containing proteins are

attached to the peptidoglycan by Sortase B. Alternatively, NEAT-domain containing proteins can contain transmembrane domains, allowing the proteins to be internalized into membranes, as seen with Shr and Shp in Streptococcus pyogenes. Furthermore, Shp contains two NEAT-domains in addition to two protein domains of unidentified function along with a Leucine Rich Repeat (LRR), for interaction with an unknown protein. Other NEAT-domain containing proteins are noncovalently anchored to the bacterial S-layer via S-layer homology (SLH) domains, as seen in the NEAT-domain containing S-layer protein of *Bacillus subtilis*.

1.4 NEAT-domain Dependent Iron Uptake in *Listeria monocytogenes*.

L. monocytogenes is an infectious organism that can also be free-living. The organism is a common cause of food poisoning and has been recently implicated in food recalls for ice cream, cheese and cantaloupes. *L. monocytogenes* is implicated in the disease listeriosis, and is particularly dangerous in pregnant women, the elderly and other immunocompromised individuals. Listeria heme uptake proteins, are termed **H**eme **B**inding **P**rotein (Hbp) and **H**eme/Hemoglobin **Up**take protein (Hup). *Listeria monocytogenes* contains two NEAT-domain containing proteins. Hbp1(*lmo2186*), containing one NEAT-domain and Hbp2(*lmo2185*), containing three NEAT-domains (Figure 1-5). Hbp2 is thought to remove heme from hemoglobin and transfer it to Hbp1. The Hbp1 protein shuttles the heme to the bilobate lipoprotein HupD, which contains no NEAT-domain. HupD interacts with the ATP-permease components HupG/HupC, to

transport heme into the cytoplasm (Xiao et al, 2011; Fonner et al, 2014). The three NEAT domains in Hbp2 are capable of binding heme with different affinities, Hbp1 and Hbp2 NEAT1 and NEAT3 have been shown to bind hemoglobin to extract heme (Xiao et al, 2011; Malmirchegini et al, 2014).

Hbp1 is attached to peptidoglycan through its NKVTN or the overlapping NPKSS motif by Sortase B. Hbp2 can be attached by Sortase B through its NAKTN motif. The Sortase B protein cleaves the polypeptide sequence after the threonine or serine in the fourth position of the NXXTN motif, and forms a covalent bond between alpha-carboxyl of the Threonine (or serine) to the lysine of the peptidoglycan pentapeptide (Xiao et al, 2011) Despite the presence of the Sortase B sequence a large portion of Hbp2, and possibly Hbp1 is secreted into the host where they function as hemophores.

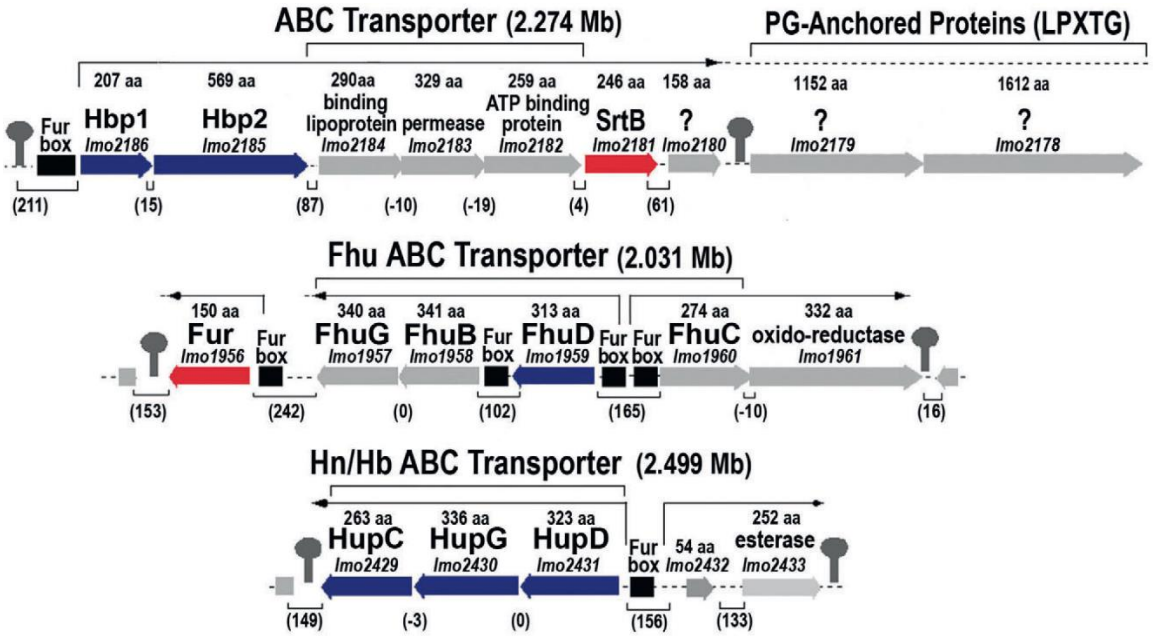

Figure 1-5: Chromosomal map of *Listeria monocytogenes* genes responsible for heme uptake (Xiao et al, 2011. Reprinted with permission from John Wiley and Sons. License Number 4230991495410).

1.5 NEAT-domain Dependent Iron Uptake in *Staphylococcus aureus*.

S. aureus is a common infectious agent with a high degree of resistance to antibiotics. *Staphylococcus* is one of the ESKAPE pathogens, which are associated with nosocomial infections. Methicillin-resistant *S. aureus* (MRSA) and Vancomycin-resistant *S. aureus* (VRSA) are growing problems throughout the world and are driving the need for new antibiotic discovery (Wencewicz et al, 2016). *In S. aureus* heme uptake proteins are known as the **I**ron-regulated **S**urface **D**eterminant (Isd) system. The Isd system is regulated by the Fur repressor and is composed of IsdA, IsdB, IsdC and IsdH as the NEAT-domain containing heme scavengers (Figure 1-6). IsdH contains three NEAT-domains and is anchored to the peptidoglycan via its LPXTG motif (Pilpa et al, 2008; Sjodt et al, 2016). IsdB and IsdA also have a LPXTG sequences, suggesting that IsdA, IsdB and IsdH are anchored by Sortase A to peptidoglycan (Pishchany et al, 2014). IsdC is anchored to the peptidoglycan by Sortase B via its NPQTN motif and the operon encoding IsdC also codes for Sortase B (Villareal et al, 2011). IsdH is thought to liberate heme from haptoglobin-bound hemoglobin in addition to binding heme from free hemoglobin (Sæderup et al, 2016; Zhu et al, 2014). IsdB contains two NEAT-domains and has been shown to liberate heme from free hemoglobin (Torres et al, 2006; Pishchany et al, 2014). IsdC and IsdA have a single NEAT-domain and are thought to shuttle heme to IsdE (Mazmanian et al, 2003). IsdE is the bilobate lipoprotein that interacts with permease components IsdD and IsdF, to transport heme into the cytoplasm (Mazmanian et al, 2003). Once inside the cytoplasm

iron is liberated from the heme porphyrin ring by monooxygenases IsdG and IsdI (Skaar et al, 2004).

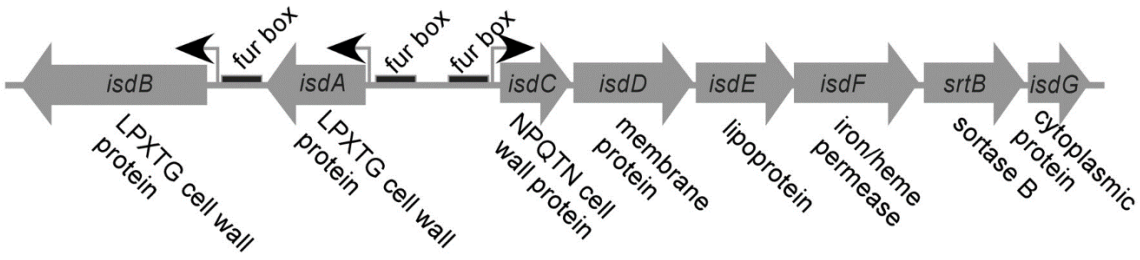

Figure 1-6: Heme Acquisition Operon of *S. aureus* (Mazmanian et al, 2003. Reused with permission from The American Association for the Advancement of Science. License Number 4231010417396).

1.6 NEAT-domain Dependent Iron Uptake in *Bacillus anthracis*.

Bacillus anthracis is a spore forming bacteria and the causative agent of the disease anthrax. The spores of *B. anthracis* are capable of germinating in phagosomes of macrophages, and spread as vegetative cells upon phagosome lysis (Balderas et al, 2012; Honsa et al, 2011; Maresso et al, 2006). The organism can grow intracellularly and extracellularly and faces different iron levels in these environments. *B. anthracis* has a heme acquisition operon, under the control of a Fur repressor, with Isd genes homologous to the ones found in *S. aureus* (Figure 1-6, Figure 1-7). The *B. anthracis* IsdC has 36% identity to *S. aureus* IsdC and both have an Sortase B anchoring signal (Maresso et al, 2008). IsdE/IsdE2/IsdF make up the ABC-transporter responsible for transferring heme across the inner membrane. As with the *S. aureus* Isd operon, the last two genes encoded by the *B. anthracis* operon include a gene coding for Sortase B and the

monooxygenase IsdG (Maresso et al, 2006). One notable difference between the heme-uptake operons of *S. aureus* and *B. anthracis* is the presence of two secreted NEAT-domain containing proteins IsdX1 and IsdX2. Both IsdX1 and IsdX2 lack a discernible Sortase signal and have been shown to be secreted into the extracellular milieu, and so are called hemophores (Honsa et al, 2011). IsdX1 contains a single NEAT-domain and has been demonstrated to bind heme and extract heme from hemoglobin (Maresso et al, 2008). IsdX1 contains 31% identity with IsdC from *S. aureus* and 40% identity with Hbp1 from *L. monocytogenes*. IsdX2 contains five NEAT-domains, NEAT-domain 1, 3, 4 and 5 have been shown to bind heme. NEAT domains 1 and 5, in addition to binding heme, can also extract heme from hemoglobin (Honsa et al, 2011). IsdX2 NEAT domains 1, 3 and 4 can transfer heme to IsdC, and NEAT domain 2 can neither bind, extract nor transfer heme.

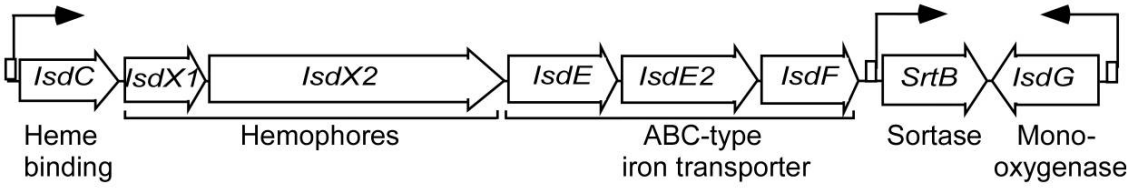

Figure 1-7: Heme Acquisition Operon of *B. anthracis*. Boxes with black arrows represent the Fur box and its orientation (Maresso et al, 2008. Reprinted with open-access article permission).

Outside of its heme acquisition operon, *B. anthracis* contains two more proteins which contain NEAT-domains, Hal and BslK. Hal (Heme-Acquisition Leucine-rich repeat protein) was first identified in a search of Sortase anchored proteins, and was found to encode a NEAT-domain (Gaspar et al, 2005). This protein contains two Leucine-rich-repeat (LRR) regions, which presumably assist in protein-protein interactions with

unknown proteins. This protein has been shown to bind heme and extract heme from hemoglobin (Balderas et al, 2012). Deletion of Hal has been shown to decrease *B. anthracis* growth in minimal media supplemented with heme or hemoglobin (Balderas et al, 2012). Hal is presumably anchored by Sortase A through its LGATG sequence (Gaspar et al, 2005). The other NEAT-domain containing protein outside of the heme acquisition operon is BslK (*B. anthracis* S-Layer protein K). As indicated by the name, BslK is attached to the S-layer of *B. anthracis* via three C-terminal S-layer homology (SLH) domains, which attach non-covalently to the S-layer (Mesnage et al, 2000; Tarlovsky et al, 2010). The S-layer is found in some Gram-positive bacteria and consists of a crystalline array of proteins outside of the peptidoglycan which is thought to protect the organism from the immune system of the host, among other functions. BslK has been shown to bind heme and transfer it to peptidoglycan anchored IsdC (Tarlovsky et al, 2010).

1.7 NEAT-domain Dependent Iron Uptake in *Streptococcus pyogenes*.

Streptococcus pyogenes is Gram-positive extracellular infectious organism that is a part of the skin microbiome. *S. pyogenes* often causes a variety of epidermal and mucosal infections that sometimes spreads to sepsis or toxic shock syndrome (Lu et al, 2012; Bates et al, 2003). This organism has two NEAT-domain containing proteins called Streptococcal hemoprotein receptor (Shr) and Streptococcal heme-associated protein (Shp). Shp contains a single NEAT-domain and is found as a part of an operon (Figure 1-8) reminiscent of the heme acquisition operons in *L. monocytogenes*, *S. aureus* and *B.*

anthracis (Bates et al, 2003). The Streptococcal heme acquisition operon contains nine open reading frames and no discernable Fur box, the operon is reportedly under the control of the MtsR repressor (Toukoki et al, 2010; Schmitt and Holmes, 1994). MtsR is a member of the DtxR/MntR repressor family, and negatively regulates virulence genes in the presence of iron, like the Fur repressor (Schmitt and Holmes, 1993; Bates et al, 2003). Following Shp is an ABC-type transporter HtsABC (also known as SiaABC), which is analogous to the ABC transporters of heme in the other Gram-positive organisms. HtsA is a heme binding lipoprotein, HtsB is a permease and HtsC is the ATPase that powers heme transport across the membrane (Nygaard et al, 2006). Proteins encoded by genes 1791 to 1787 have not yet been elucidated, but have inferred ABC-transport functions based on their sequences (Lei et al, 2003).

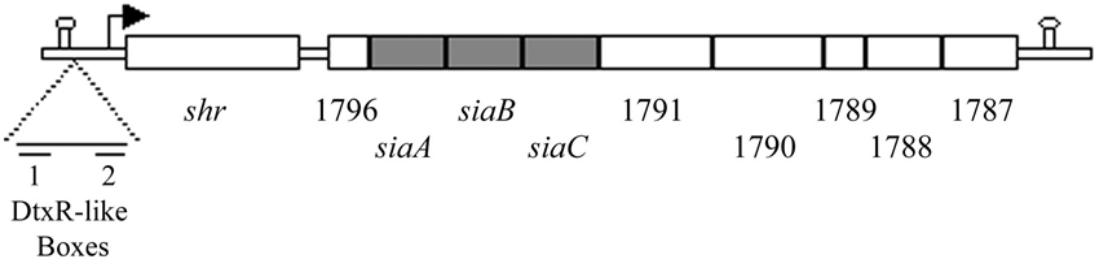

Figure 1-8: Heme Acquisition Operon of *S. pyogenes* (Bates et al, 2003. Reprinted with permission from the American Society for Microbiology).

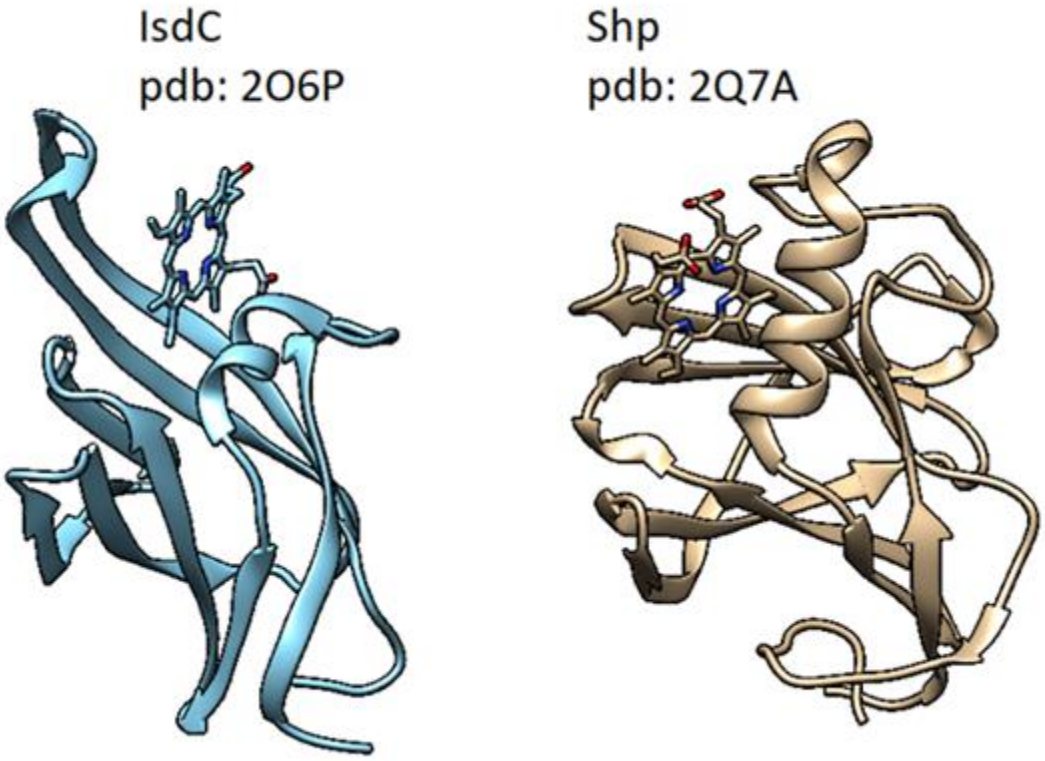

Figure 1-9: Comparison of *S. aureus* IsdC and *S. pyogenes* Shp crystal structures.

Shr is found upstream of the Streptococcal heme acquisition operon and contains two NEAT-domains, in addition to two domains of unknown function (DUF1533) and a LRR. Both Shr and Shp are unique among NEAT-domain containing proteins in they lack Sortase signals but have a transmembrane domain towards their C-terminus and localize to the cellular membrane instead of being anchored to the cell wall using the Sortase system, eliminating the need for a Sortase gene in their heme acquisition operon (Lei et al, 2002; Ouattara et al, 2013). Another notable difference is the lack of a monooxygenase as part of the operon. Despite being localized to the membrane Shr has been shown to extract heme from hemoglobin and transfer it to Shp (Zhu et al, 2008; Lu et al, 2012). Shp binds heme directly or receives it from Shr, and can subsequently transfer it to HtsA,

which internalizes the heme into the cytoplasm using the HtsB permease and HtsC ATPase (Lu et al, 2012). HtsA can also bind heme by itself, but with a relatively high K_d of 120µM (Nygaard et al, 2006). NEAT1 of Shr has been shown to acquire heme from hemoglobin and transfer it to Shp or NEAT2 of Shr, which under iron-rich conditions. (Ouattara et al, 2013). The conserved YXXXY motif in the seventh beta-strand is only found in NEAT2 of Shp, but both Shp and Shr can bind heme through an alternative bis-methionine coordination (Figure 1-10) according to a crystal structure (Aranda IV et al, 2008).

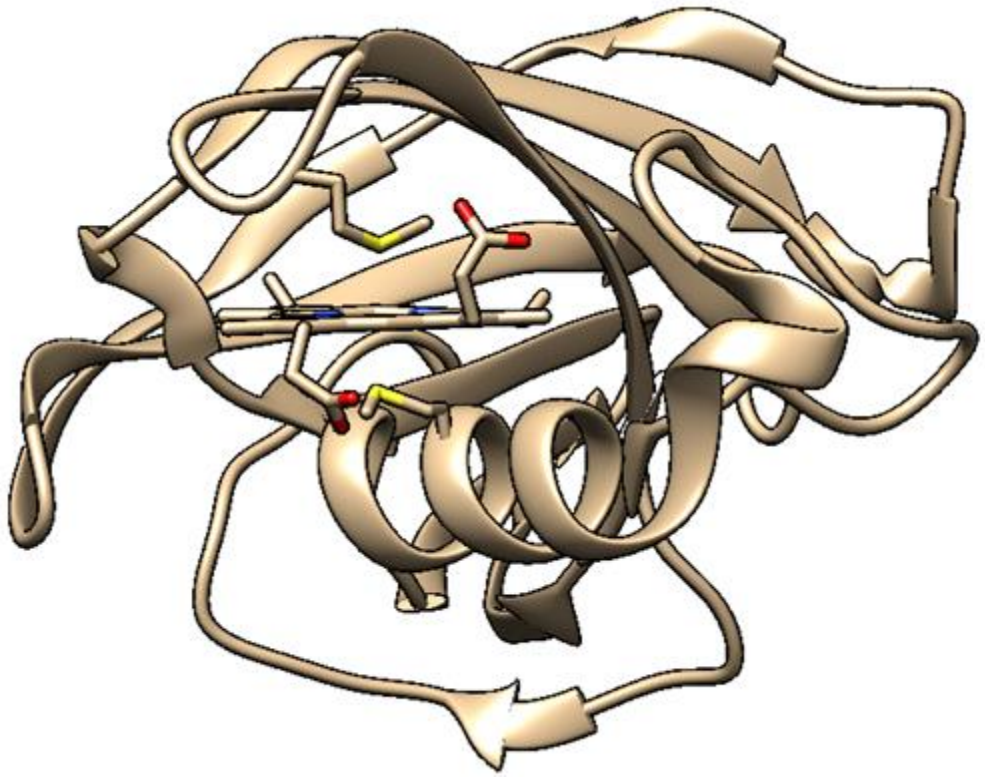

Figure 1-10: Coordination of Heme by *S. pyogenes* Shp residues M66 and M153.

1.8 NEAT-domain Independent Iron Uptake in Gram-positive Bacteria.

Like the Gram-negative organisms, Gram-positives produce and secrete siderophores, which allow for a key NEAT-domain independent source of iron uptake. In fact, Gram-positive bacteria do not need to transfer siderophores across an outer membrane, and take them up directly through their ABC-transporters (Xiao et al, 2011). Siderophores bind iron with high affinity, and are subsequently bound by membrane anchored Gram-positive lipoproteins and transported into the cytoplasm via a permease and ATPase (Jin et al, 2006). The ABC transporter components FhuD and FhuBCG in *L. monocytogenes* allow for the transport of ferrichrome and ferrioxamine B. *L. monocytogenes* can additionally acquire the siderophore corynebactin (Jin et al, 2006; Xiao et al 2011). *S. aureus* produces two siderophores Staphyloferrin A and B, which are transported by ABC transporters HtsABC and SirABC respectively (Grigg et al 2010). *B. subtilis* produces the siderophore bacillibactin which it internalizes using the ABC transporter FeuABC. This transporter can additionally import enterobactin, which is not produced in the *B. subtilis* (Grandchamp et al, 2017). *B. anthracis* produces two siderophores, bacillibactin and petrobactin (Lee et al, 2011). Bacillibactin is a catecholate type siderophore with three 2,3-dihydroxybenzoic acid groups, whereas petrobactin has two atypical 3,4-dihydroxybenzoic acid groups, with an additional carboxyl group for binding iron. *B. anthracis* additionally codes for seven different iron-siderophore permeases, two of which FpuABCD and FatBCDE are implicated in the transport of petrobactin (Dixon et al, 2012). *S. pyogenes* has an ABC transporter called HtsABCD/SiuADBG which can bind and transport ferrichrome, although whether the

species synthesizes ferrichrome is not indicated (Montañez et al, 2005; Hanks et al, 2005). The hijacking of siderophores is a recognized phenomenon, where organisms scavenge iron-siderophore complex produced by other bacteria without secreting that siderophore (Grandchamp et al, 2017). This works demonstrates for this first time that NEAT-domain containing proteins can be scavenged by other organisms to acquire heme, as is seen in siderophores.

Gram-positive bacteria have alternative systems for acquiring iron aside from heme-scavenging NEAT-domain containing proteins. Iron or heme can be directly taken up by ABC transporters in the inner membrane (Janulczyk et al, 2003; Xiao et al, 2011). *S. pyogenes* has a divalent metal cation ABC transporter MtsABC which can directly transport iron, manganese and zinc (Janulczyk et al, 2003). In *L. monocytogenes* the ABC-transporter HupDGC, which normally functions in coordination with NEAT-domain containing proteins, was found to transport heme independently at concentrations higher than 50nM (Xiao et al, 2011). Whether all heme-internalizing ABC transporters are capable of transporting heme independently has not been verified, but these proteins can function in coordination with other heme-binding domains to transport heme (Allen and Schmitt, 2011). Notably, *Corynebacterium diphtheriae* produces proteins with an alternative domain for binding heme called the **C**onserved **R**egion (CR) domain. The Gram-positive organism has a heme acquisition operon that includes the heme binding protein HtaA followed by the heme uptake ABC transporter HmuTUV. In HmuTUV, HmuT is a heme binding lipoprotein, HmuU is a heme permease and HmuV is an ATPase that powers heme uptake across the membrane (Drazek et al, 2000). HtaA can bind

hemoglobin and extract heme from it, then transfers the heme to Hta, which is downstream of the ABC-transporter. HtaA contains two CR domains and HtaB contains a single CR domain (Uluisik et al, 2017). These CR domains are distinct from NEAT-domains, but they coordinate heme through two conserved tyrosines and a histidine, which is similar in NEAT-domains (Allen and Schmitt, 2011). Like *S. pyogenes* Shp and Shr, HtaA and HtaB are membrane localized through a predicted transmembrane domain in their C-terminus, but HtaA is found secreted extracellularly under iron-rich conditions (Drazek et al, 2000; Allen and Schmitt, 2011). On a genetic level, as with Shr and Shp, HtaA and HtaB are controlled by the DtxR repressor, which is functionally analogous to the Fur repressor (Drazek et al, 2000). Once internalized, iron is liberated from the heme porphyrin ring by monooxygenase HmuO, analogous to IsdE in *S. aureus*.

1.9 Genetic Regulation of Iron Uptake.

For both Gram-negative and Gram-positive organisms, the expression of proteins and siderophores responsible for the acquisition of iron is regulated on a genetic level by metalloregulators (da Silva Neto et al, 2009; Newton et al, 2005). These proteins sense the presence of iron, heme, other metals or hydrogen peroxide and alter the global expression of genes through both positive and negative regulatory functions. Fur and DtxR are two such metalloregulators that are expressed in bacteria, and are functionally analogous, despite having little sequence similarity. Ferric uptake repressor (Fur) is a prototypical metalloregulator first identified in *E. coli*, but is present in both Gram-

positive and Gram-negative species. Fur is a member of a family of transcription regulators that includes other metal binding proteins Zur, Mur and Nur, which repress zinc, manganese and nickel uptake, respectively (Lee and Helmann, 2007). Additionally, the Fur family of proteins contains hydrogen peroxide sensing protein PerR and heme binding Irr which senses heme and regulates genes accordingly (Faulkner et al, 2012; Caux-Thang et al, 2014; Kim et al, 2011). In heme acquisition operons, Fur dimerizes upon iron binding and negatively controls the expression of heme uptake genes by binding to a sequence, known as a "Fur box", upstream of the start codon and repressing transcription (Baichoo and Helmann, 2002). The Fur box was originally identified in *E. coli* as a 9-1-9 palindromic sequence GATAATGATWATCATTATC, but subsequent analysis has suggested that the fur box consists of a head-head-tail orientation of the GATAAT motif (Escolar et al, 1998). In *B. subtilis* the fur box is identified as a 7-1-7 palindromic motif of TGATAATNATTATCA, with small modifications in this sequence being recognized as a PerR box TTATAATNATTATAA (Caux-Thang et al, 2014). In the presence of iron, Fur dimerizes and takes on a conformation that allows it to bind to Fur box, preventing binding by a promoter. In the absence of iron, Fur is unable to bind to the Fur box and the expression of iron acquisition proteins is de-repressed (Newton et al 2005, Ledala et al 2007, da Silva Neto 2009). Fur-based regulation of heme acquisition operons is observed in *L. monocytogenes*, *B. anthracis* and *S. aureus* species. In *S. pyogenes* however, the heme acquisition operon is repressed by the MtsR metalloregulator, which is a member of the DtxR/MntR family. MtsR is functionally analogous to Fur in that this protein represses transcription under high iron levels and de-represses transcription under low iron levels

(Toukoki et al, 2010). Both DtxR and Fur family proteins are helix-turn-helix containing DNA binding dimeric proteins that sense metals and modify global expression accordingly (Drazek et al, 2000; Lee and Helman, 2007; Merchant and Spatafora, 2014).

1.10 Development of the Universal Assay.

Labeled Hbp2 expressing *L. monocytogenes* produces minimal if any fluorescence change upon exposure to heme, and due to the large amount of Hbp2 secreted by the bacteria, we decided to evaluate heme uptake by mixing purified protein with iron-starved bacteria (This work). Previous experiments in our lab with heme/iron uptake have focused on direct fluorescent labeling of cells and tracking their iron uptake capacity. This approach proved ineffective in the Gram-positive heme uptake system, and using purified protein would allow for fluorescent detection of nutrient uptake in general. Any nutrient-binding secreted protein lacking cysteines (as is the case with Hbp2, and many other NEAT-domain containing proteins) can theoretically be cysteine modified and fluorescently labeled to generate a "protein-sensor." This sensor could track binding of the nutrient and subsequent dissociation during uptake, or a lack of binding could be detected in the presence of inhibitors. For Gram-negative organisms, where nutrient binding occurs at the outer membrane, a TonB-deficient mutant with a fluorescently labeled cysteine modification could be used as the equivalent of a protein sensor. In both the Gram-negative and the Gram-positive cases, once a protein sensor is established, mixing in WT cells would allow for quantification of nutrient uptake in general. The broad

applicability of this protein-sensor approach led us to call this method the “Universal Assay”.

1.11 Clinical Relevance of Iron Uptake by Pathogenic Bacteria.

Despite the rise of antibiotic resistance and superbugs, metal uptake mechanisms in bacteria present novel opportunities for therapeutic development. Currently there are five bacterial targets for antibiotic action: (1) Peptidoglycan synthesis, inhibited by bacitracin and β-lactams like penicillin. (2) cell membrane disruption, targeted by polymyxin B and the bacteriocin nisin. (3) DNA function and replication disruption, caused by quinolones and nitroimidazoles. (4) Protein synthesis disruption, caused by tetracyclines and aminoglycosides. (5) Folic acid synthesis inhibition, driven by sulfonamides and trimethoprim. The development of metal acquisition as a target for antibiotic action would be an exciting step forward for combating antibiotic resistance (Wencewicz, 2016). Characterizing metal uptake allows for development of new assays to screen for inhibitors of bacterial nutrient uptake (Nairn et al, 2017; Hanson et al, 2016; Yep et al, 2014) The presence of metal uptake proteins in extracellularly accessible sites allows for their targeting with vaccines and monoclonal antibodies (Mike et al, 2016; Proctor, 2012; Harro et al, 2010). Recent developments in understanding metal uptake in bacteria are sure to drive advances in combating microbial infections. Furthermore, the active transport of nutrients necessary for bacterial survival presents new mechanisms for enhancing the efficacy of current antibiotic classes, and in fact is exploited by bacteria

themselves for inter and intraspecies competition (Braun et al, 2009; Page et al, 2010; Thomas et al, 2004).

High-throughput screens (HTS) for new inhibitors of TonB action have yielded promising candidates for bacterial growth inhibition (Yep et al, 2014; Nairn et al, 2017). In Yep et al, 2014, 16 compounds were confirmed to inhibit bacterial growth and two were identified as specific inhibitors of TonB in a screen utilizing OD600 as a measure of UPEC growth. Nairn et al, 2017, utilized a fluorescently modified *E. coli* FepA to detect compound binding in a search for TonB inhibitors that yielded 44 potential candidates. While these HTS searches were specific to *E. coli*, the development of the Universal Assay expands our potential to search for inhibitors of metal uptake in other organisms. Compounds identified by HTS as inhibitory of metal uptake have the added benefit of not needing to cross membranes to achieve their inhibitory potential, since metal uptake systems are extracellularly exposed.

The availability of metal uptake systems for extracellular interaction has made these systems attractive as vaccine targets. Animal models show protection against UPEC using siderophores conjugated to bovine serum albumin, and targeting antibodies against siderophores or TonB-dependent receptors is a viable target for vaccines (Mike et al, 2016; Marsay et al, 2015). Clinical trials in humans have been performed using *S. aureus* IsdB as an antigen in a vaccine, the Merck V710 (Harro et al, 2010). Different amounts (5 μg, 30 μg and 90 μg) of IsdB were conjugated to the Merck aluminum adjuvant and showed increased anti-IsdB antibody titters. However, subsequent human trials failed to show an inhibition in *S. aureus* infections for patients undergoing cardiac surgery (Proctor,

2012). A report indicated that receipt of the V710 vaccine dramatically increased mortality rates in patients experiencing *S. aureus* infections compared to the placebo group, a concerning and unexpected finding (McNeely et al, 2014). The authors could not identify a causal relationship between the vaccine and mortality in *S. aureus* infections, but hypothesized that cell mediated immunity might have been activated in an aberrant way that increased the likelihood of mortality. However, as indicated by Proctor, 2012 and McNeely et al, 2014, the activation of alternative arms of adaptive immunity might provide protection against *S. aureus* infection. Additionally, an IsdB specific monoclonal antibody CS-D7 was found to mediate the killing of *S. aureus* and provide protection in an animal model, but the antibody did not inhibit heme binding to IsdB (Pancari et al, 2012). Using combinations of Isd antigens, or developing antibodies capable of inhibiting heme binding, might offer better protection against *S. aureus*, but a proper adjuvant must be determined for stimulating a protective type of humoral or cell mediated immunity (Proctor, 2012; Pancari et al, 2012; McNeely et al, 2014; Joshi et al, 2012).

The active import mechanisms associated with metal uptake systems allows for more effective targeting of antibiotics. Bacteria have already evolved ways to utilize iron uptake systems for targeting rival bacteria, as indicated in the vast array of bacteriocins (Thomas et al, 2004; White et al, 2017). Bacteriocins are protein-like toxins produced by bacteria to kill other bacteria. They are divided into Gram-positive sourced bacteriocins and Gram-negative sourced bacteriocins. The Gram-positive group includes lantibiotics like nisin, the only commercially used bacteriocin, with application in the food industry since the 1950's (Ruhr and Sahl, 1985). Gram-negative sourced bacteriocins include

microcins (<20kDa), colicins (20-90kDa) and tailocins (>90kDa). Colicins have three characteristic domains and utilize TonB-dependent transporters for binding and translocation via the first two domains, with a third cytotoxic domain mediating cell killing (White et al, 2017). Microcins have been reported to also have siderophore-type modifications, which allow these cytotoxic molecules to be taken up by TonB-dependent transporters (Thomas et al, 2004). Sideromycins are antibiotics that are covalently linked to siderophores and occur naturally (Braun et al, 2009; Page et al, 2010). Coupling known antibiotics to siderophores may enhance their effectiveness (van Delden et al, 2013). Colicins, microcins and sideromycins compete with siderophores for TonB-dependent transporters, and they have additional cytotoxic effects, increasing their potential for bacterial inhibition (Braun et al, 2009).

Chapter 2 – Materials and Methods

2.1 Bacterial Strains and Plasmids.

E. *coli* strain DH5α was used for genetic manipulation of plasmids, strain BL21 for expression of Staphylococcal proteins and strain SM10 for bacterial conjugation with genetic transfer to Listeria. OKN3 was used as a background strain lacking expression of FepA and OKN13 was used as a background strain lacking expression of both FepA and TonB. Listeria *monocytogenes* strain EGD-e with wild type heme binding protein expression was used to derive deletion mutants and for Listerial protein expression from genetic constructs. WT EGD-e and its deletion strains, along with *Bacillus subtilis* strain ATCC 21332 and *Staphylococcus aureus* Newman strain were used to test heme uptake in the fluorescent assay. *Caulobacter crescentus* strain NA1000 was used for expression of Caulobacter proteins. Plasmids pET28 was used for expressing His-tagged Staphylococcal and Listerial heme proteins, the low copy number plasmid pPL2 was used for chromosomal integration of Listerial genes, and the high copy number plasmid pAT28 was used for large scale listerial protein expression. pITS23/pITS47 were used to test the activity of FepA mutants in strains lacking chromosomal FepA expression. The tables below summarize the strains, their derivatives, primers and plasmids used.

Table 2-1: Bacterial Strains.

Strain	Genotype	Reference
Escherichia *coli*		
DH5α	*supE44 ΔlacU169(Φ80lacZ ΔM15) hsdR17 recA1 endA1 gyra96 thi-1 relA1*	Hanahan, 1983
BL21	*F⁻ dcm ompT hsdS*(rB⁻ mB⁻) *gal*	Stratagene
SM10	*F⁻ thi-1 thr-1 leuB6 recA tonA21 lacY1 supE44* (MuC⁺) *λ⁻ Km^R Tra⁺*	Lauer et al, 2002
BN1071	*F pro, trp, B1 entA*	Klebba et al, 1982
OKN3	BN1071 *ΔfepA*	Ma et al, 2007
OKN13	BN1071 *ΔfepA, ΔtonB*	Ma et al 2007
AN102	*Thi trp fep proC leu tonA*	Yeowell and White 1982
Listeria *monocytogenes*		
EGD-e	Sm^R	Bierne et al, 2004
EGD-e *ΔhupD*	*Δlmo2431*	Xiao et al, 2011
EGD-e *Δhbp1*	*Δlmo2186 Sm^R*	Xiao et al, 2011
EGD-e *Δhbp2*	*Δlmo2185 Sm^R*	Xiao et al, 2011
Bacillus *subtilis*		
ATCC 21332	WT	Annamalai et al, 2004

Staphylococcus *aureus*		
Newman strain	Clinical isolate used in animal models of infection	Baba et al, 2008
Caulobacter *crescentus*		
NA1000	Laboratory derivative of CB15 WT strain	Evinger & Agabian, 1977
MM90	NA1000 Δ02277	Balhesteros et al, 2016

Table 2-2: Plasmids.

Plasmid	Description	Reference
pET28	His-tag protein fusion vector	Novagen
pAT28	High copy shuttle vector	Trieu-Cuot et al, 1990
pPL2	Site specific Integrative shuttle vector	Lauer et al, 2002
pITS23/pITS47	FepA+ plasmid	Smallwood et al, 2009

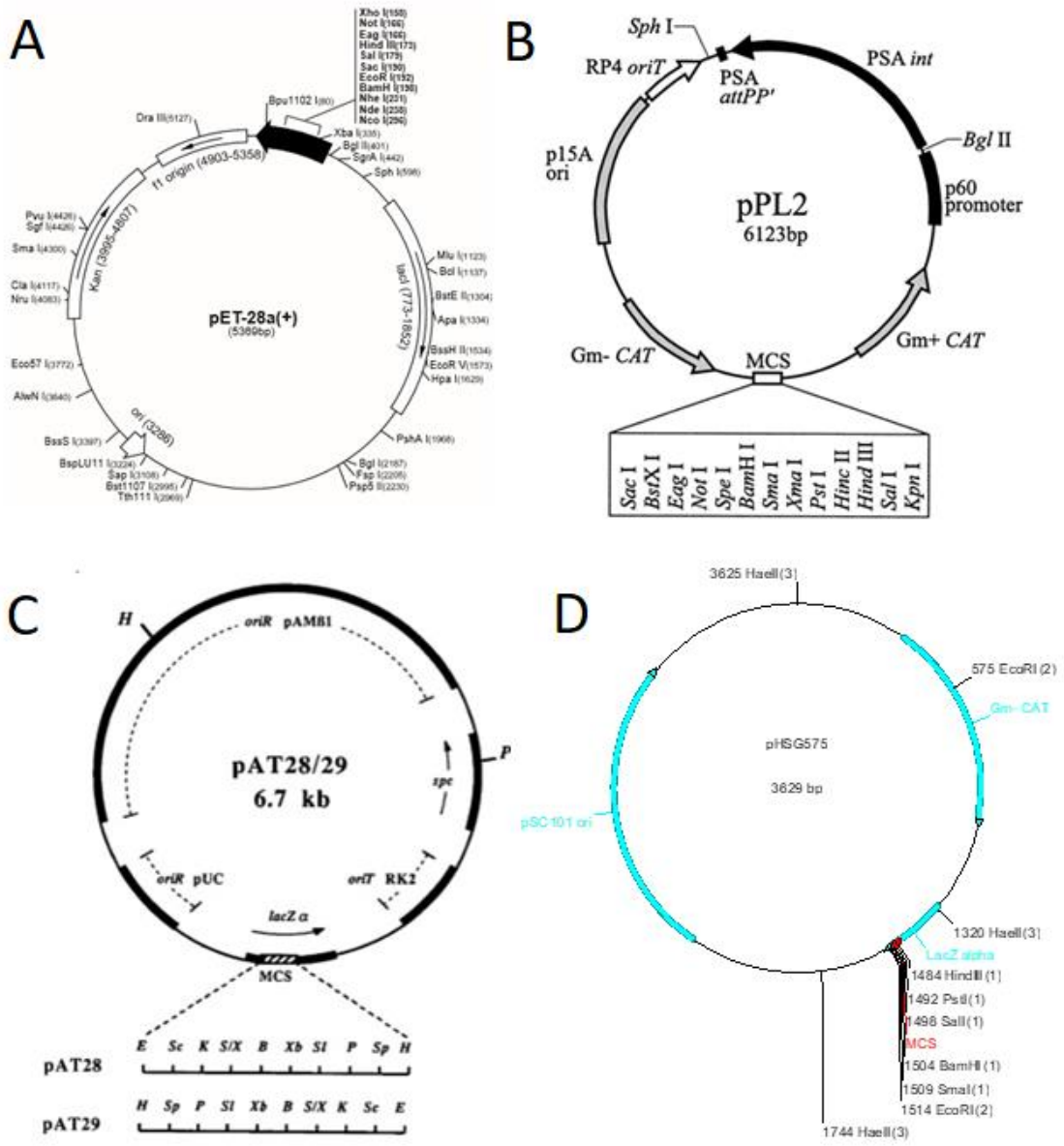

Figure 2-1: Plasmid Maps of His-tag expression vector pET28a (A), the integration-shuttle vector pPL2 (B), shuttle vector pAT28 (C), and *E. coli* expression vector pHSG575 (D).

2.2 Growth Media.

Luria-Bertani (LB) broth was used for growing Gram-negative bacteria. Super optimal broth with catabolite repression (SOC) was used for growing cells following electrotransformation or heat shock. Brain Heart Infusion (BHI) was purchased from Becton, Dickinson and Company (BD) and was used as iron-rich media for growing Gram-positive bacteria. Gram-positive MOPS minimal media (G+MMM) derived from KRM media by Dr. Xiaoxu Jiang (Jiang's dissertation, 2009) was used as iron-deficient media for inducing expression of fur regulated proteins. MOPS minimal media was used for growing Gram-negative organisms in iron limiting conditions (Neidhardt et al, 1974).

Table 2-3: Media.

Media	Reference
LB broth	Miller, 1972
SOC broth	Hanahan, 1983
Nutrient Broth	Becton, Dickinson and Co.
BHI Broth	Becton, Dickinson and Co.
MOPS Minimal Media (G-MMM)	Neidhardt et al, 1974
MOPS-L medium (G+MMM)	Jiang's Ph.D. dissertation, 2009
T-media	Klebba et al, 1982
PYE	Sigma-Aldrich Co.
M2 Minimal media	Neidhardt et al, 1974

2.3 Oligonucleotides

Oligonucleotides were procured from Integrated DNA technologies (IDT). Plasmid purification kits for mini-DNA preparations were obtained from QIAGEN. Zymoclean™ Kits for purifying DNA from agarose gels were obtained Zymo research. Taq DNA polymerase kits, restriction enzymes and ligases were obtained from New England Biolabs. Pfu Polymerase was obtained from Agilent.

Table 2-4: Oligonucleotides.

Oligonucleotide	Sequence
Listeria verification primers	
LLO forward	ATGAAAAAAATAATGCTAGTTTTT
LLO reverse	ACGGCCATACGCCACACTTGAGAT
pPL2 verification primers	
100bp upstream of MCS	TCGAAAGCAAATTCGACCCGG
100bp downstream of MCS	CGTCATCACCGAAACGCGCGA
pAT28 Verification primers	
100bp upstream of MCS	GTGAGTTAGCTCACTCATTAGGCACCCC
100bp downstream of MCS	GCCTCTTCGCTATTACGCCAGCTG
hbp1 and hbp2 primers	
hbp1 gene insertion forward	CCCCCCCTGCAGATGAAGAAAGTTTTAGTT TTTGCTGCTTTT
hbp1 gene insertion reverse	CCCCCCGGTACCTTATTTAAAAATCGCACG TCTTTTAAGTAA
hbp2 gene insertion forward	CCCCCCCTGCAGATGAAGAAATTATGGAA AAAAGGCTTAGTA

hbp2 gene insertion reverse	CCCCCCGGTACCTTAACTCAATCTTTTACGT TTTAATCGATA
pET28 100bp upstream	TGTTTAACTTTAAGAAGGAGA
pET28 100bp down-reverse	TGGGGAACCCCGGAGATTTGC
hbp1 sequencing primer	ATGAAGAAAGTTTTAGTT
hbp2 sequencing 1	ATGAAGAAATTATGGAAA
hbp2 sequencing 601	GATAGCAATTCAAGCATG
hbp2 sequencing 1201	GTTTATTTAACTTTAACA
hbp2 100bp-rev	CAGACGAGAATCAGCCGCGCTGGC
hbp1 D124C forward	AATGCGAAAATTAAAGTGGATATTTGTGA TGACGACTTGAATTATCATCAT
hbp1 D124C reverse	ATGATGATAATTCAAGTCGTCATCACAAAT ATCCACTTTAATTTTCGCATT
hbp2 K62C forward	ACGAAAGAATCTTCAGAAGCAGATTGTTA TATTGACCATACAGCAACGATT
hbp2 K62C reverse	AATCGTTGCTGTATGGTCAATATAACAATC TGCTTCTGAAGATTCTTTCGT
hbp2 D151C forward	TTCTCCTATATGCATATTAAGGTATGTGCA ATTAGTTATGATCACTGGTAT
hbp2 D151C reverse	ATACCAGTGATCATAACTAATTGCACATAC CTTAATATGCATATAGGAGAA
hbp2 S154C forward	ATGCATATTAAGGTAGATGCAATTTGTTAT GATCACTGGTATCAAGTGGAT

hbp2 S154C reverse	ATCCACTTGATACCAGTGATCATAACAAAT TGCATCTACCTTAATATGCAT

2.4 Genetic Constructs.

The gene for Hbp1 was amplified with its natural promoter and inserted into pPL2 and pAT28 using PstI and KpnI restriction sites. The gene for Hbp2 was amplified from a *Δlmo2185* chromosomal background, which contained a BamHI site in the middle of a small *hbp1* genetic artifact, under the normal Fur promoter (Figure 2-5, Figure 2-6). pET28-Δ30Hbp2 was used for expressing and purifying His-tagged Hbp2 protein (Figure 2-1). pPL2-Hbp2 was generated and integrated into an *L. monocytogenes* ΔHbp2 strain, but failed to produce detectable Hbp2 protein, leading to the utilization of pET28-Hbp2 for expressing His-tagged Hbp2 in *E. coli* and pAT28-hbp2 for expression of WT and mutant Hbp2 and *L. monocytogenes*.

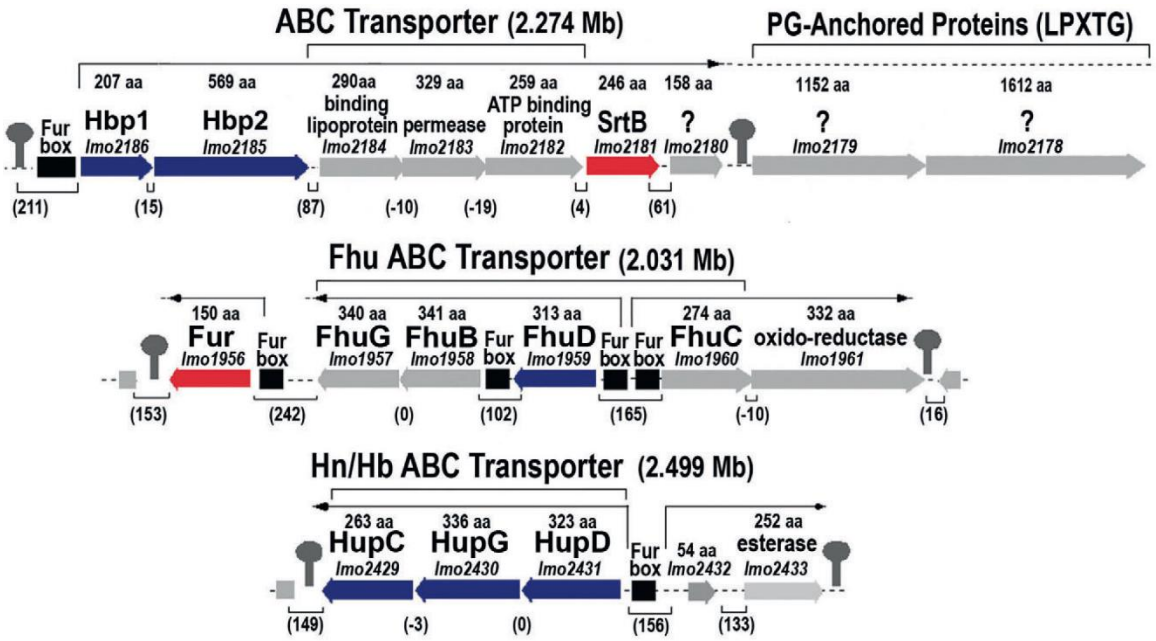

Figure 2-2: Chromosomal annotation of genes vital for the transport of heme and ferrichrome in the *L. monocytogenes* genome (Xiao et al, 2011. Reprinted with permission from John Wiley and Sons. License Number 4230991495410).

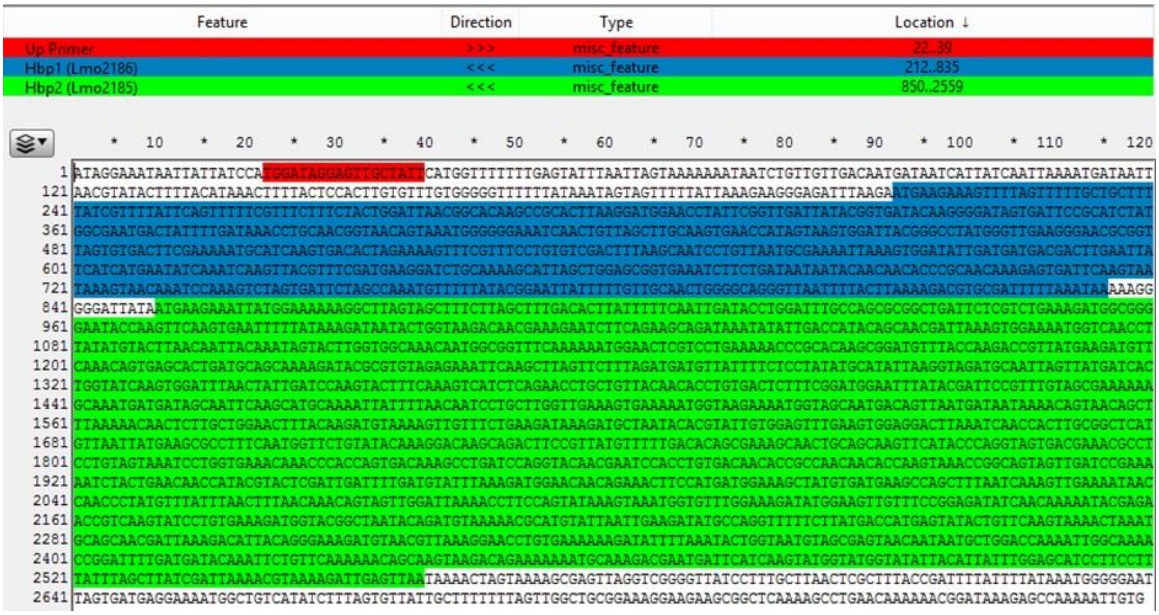

Figure 2-3: Chromosomal sequence of *hbp1* (blue) and *hbp2* (green), with the upstream primer (red). The fur box, identified via the GATAAT consensus sequence is at residues 92-97 and 114-119.

Figure 2-4: pET28a-Hbp2Δ30(S154C) Sequencing Confirmation. pET28a plasmid is in light blue. The BamHI restriction site in red. hbp2Δ30 is in green with the S154C mutation in red lower case.

2.5 Verification of *hbp1* Deletion from *L. monocytogenes* Strain EGD-e.

The deletion of *hbp1* from L. monocytogenes *Δhbp1* strain was verified via sequencing (Figure 2-6). A 79bp stretch of Hbp1 was present in the chromosome of the *Δhbp1* strain, with a BamHI site in the middle of the stretch, hence the *Δhbp1* strain expresses a truncated, non-functional version of Hbp1 (Figure 2-5). This construct was used to amplify genomic DNA for insertion into the pAT28 or pPL2 plasmids, allowing for expression of Hbp2 using the natural fur promoter as part of the polycistronic construct.

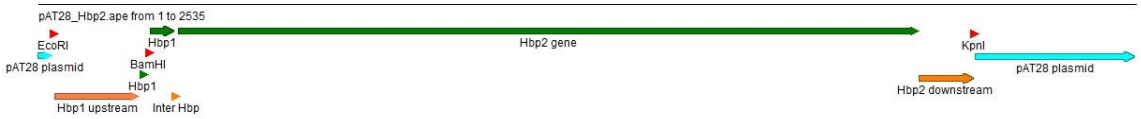

Figure 2-5: Map of WT *hbp2* Inserted into pAT28.

Figure 2-6: Sequence of *hbp2* in pAT28 Plasmid.

2.6 Verification of *hbp2* Deletion from *L. monocytogenes* Strain EGD-e.

The absence of *hbp2* was verified via western blotting. WT EGD-e was lysed on a French press and Hbp2 protein was detected in the cytoplasmic and membrane fractions, but the *Δhbp2* strain failed to express Hbp2 in either fraction (Figure 3-1). Transforming *Δhbp2* strains with pPL2 plasmid harboring *hbp2* clones failed to produce detectable Hbp2, despite an endogenous Listerial fur promotor. The high-copy number vector pAT28 (Figure 2-1) was used subsequently to express Hbp2 in listerial *Δhbp2* strains, and a significant amount of Hbp2 was found secreted into extracellular media upon iron starvation, although membrane fractions still had significant amounts of Hbp2 (Figure 3-2).

2.7 Preparation of Competent *E. coli* and *L. monocytogenes* Competent Cells.

For electrocompetent *L. monocytogenes* cells, EGD-e was inoculated into 25mL of BHI and grown overnight at 37°C with shaking, then subcultured 1:50 into 500mL fresh BHI and incubated at 37°C with shaking. Penicillin G with was added to a final concentration of 0.12 µg/mL at OD600 = 0.3. Cells were grown to an OD600 = 0.8~0.9 (roughly 2 h after the addition of penicillin G). The cells were spun down and the pellet was washed once with 100ml electroporation buffer (1mM Hepes + 500mM sucrose), once with 66ml of electroporation buffer and three times with 50 ml of electroporation buffer. Then the pellet was resuspended in 500 µL electroporation buffer with 15% glycerol and pipetted into microtubes (100ul each) and stored at -80 °C.

For electrocompetent E. coli cells, DH5a was inoculated into 10mL of LB and grown overnight at 37°C with shaking, then subcultured 1:100 into 100mL of LB and incubated at 37°C with shaking. The culture was placed on ice for 15 minutes, then it was spun down and resuspended in 50mL of ice cold H_2O. The competent cells were resuspended in 25mL of cold H_2O and spun down again. Then the culture was gently resuspended in 10mL of H_2O with 10% glycerol, and spun down again. After the last spin, the cells were resuspended in 200µL H_2O with 10% glycerol and 50µL aliquots were stored at -80°C.

2.8 Transformation of *E. coli* and *L. monocytogenes* Competent Cells.

Electrotransformation of *L. monocytogenes* was accomplished by taking 50uL of electrocompetent cells and mixing with 5µL of DNA, the cells were then electroporated at 2.4kV. The electroshocked cells were transferred to 950µL of warm BHI and incubated for three hours with gentle agitation at 37°C. 100-200µL were plated on BHI agar plates with appropriate antibiotics.

For heat shock, 50µL of competent cells were mixed with up to 5µL of DNA and kept on ice for five minutes. The cells and DNA were subsequently incubated in a 42°C water bath for one minute, before placing them back on ice for five minutes. Afterwards, 950µL of SOC media was added to the Eppendorf tubes and allowed to incubate for one hour with agitation. 100µL pf the cells were plated on LB plates with appropriate antibiotics. The remainder of the cells were spun down and resuspended in 100uL of fresh SOC media before plating on LB plates with appropriate antibiotics to get a 9X concentrated plate.

2.9 Verification of Plasmid Uptake.

Cells surviving on antibiotic containing plates were restreaked on new plates with appropriate antibiotics and grown overnight. Liquid cultures (10mL) were set up from the restreaked plates and grown overnight then mini-prepped using Qiagen kits. For Gram-positive plasmid isolation, spun down cells were resuspended in STET buffer with lysozyme (10mM Tris-HCl, pH 8.0, 100mM NaCl, 1mM EDTA, 5% Triton-X100 and 10mg/mL lysozyme), then incubated for 1 hour at 37°C. The Gram-positive cells were spun down and the STET buffer was aspirated prior to proceeding with QIAGEN mini-prep kit as with Gram-negative cells. Double digestions were set up to verify insert and vector of appropriate size (Figure 2-7) before submitting for sequencing via MCLab or Genewiz commercial sequencing (Figures 2-4, 2-6, 2-8). Alternatively, the presence of inserted genes in vectors was determined by PCR amplifying the insert with plasmid specific primers upstream and downstream of the MCS.

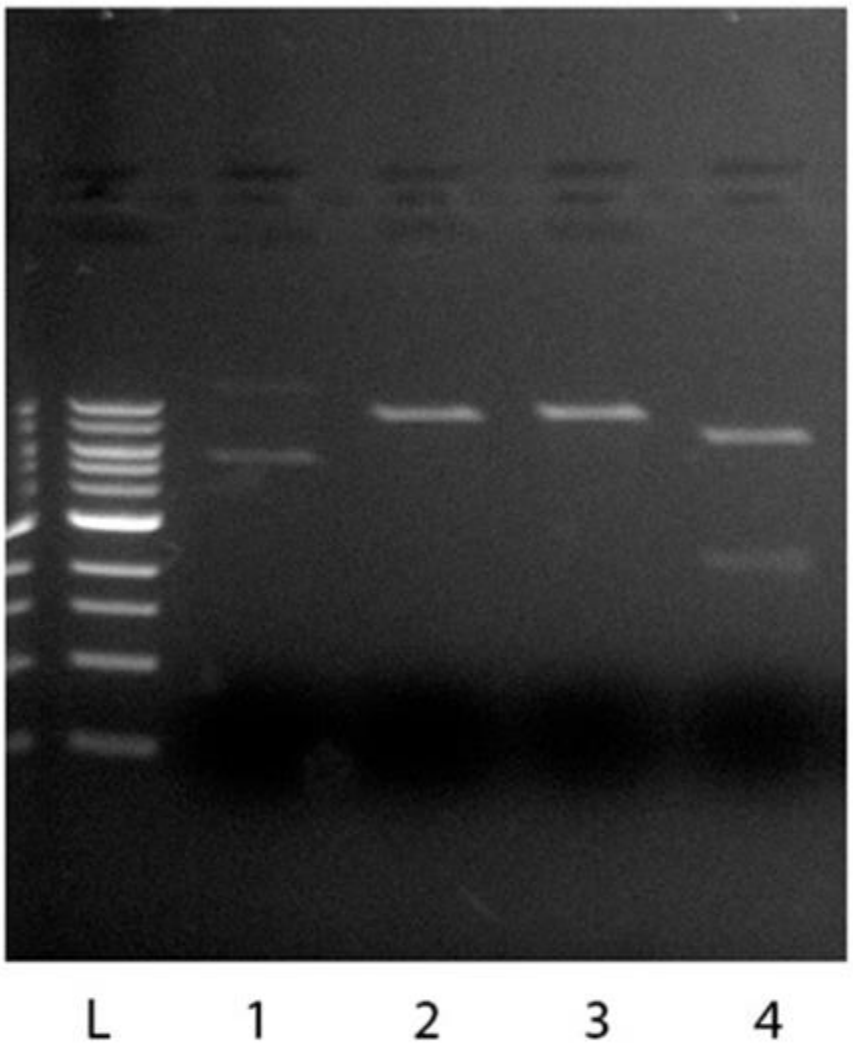

Figure 2-7: Double Digest of pAT28:Hbp2(K62C).

Figure 2-8: Alignment of pAT28-hbp2 to pAT28-hbp2(K62C).

2.10 Selection of Sites in Hbp2 for Mutation.

Criteria for selection of sites in Hbp2 included locations that were close to the heme binding site that would not sterically hinder heme binding. I chose three residues that fit this criteria in the first NEAT domain of Hbp2 (Figure 2-10). Since there is no structure available for the first NEAT-domain of Hbp2, I aligned the available structures with NEAT1 of Hbp2 in Clustal Omega (Figure 2-9). Of all the available structures of NEAT domains, IsdC matches most closely with Hbp1 NEAT1. The residues that were selected

for cysteine modification included K62, D151 and S154 (Figure 2-10). When *L.* pAT28-hbp2 bearing different mutations was transformed into *L. monocytogenes*, they were all overexpressed compared to WT Hbp2, in particular S154C was the most expressed. This mutant was further investigated since the high level of expression made it easier to purify mutated Hbp2. Furthermore, K62C would generate a cysteine mutation in the 3^{10} helix region. This region is predicted to be important for NEAT-NEAT interaction, which made K62C less optimal than the S154C mutant for evaluating heme uptake.

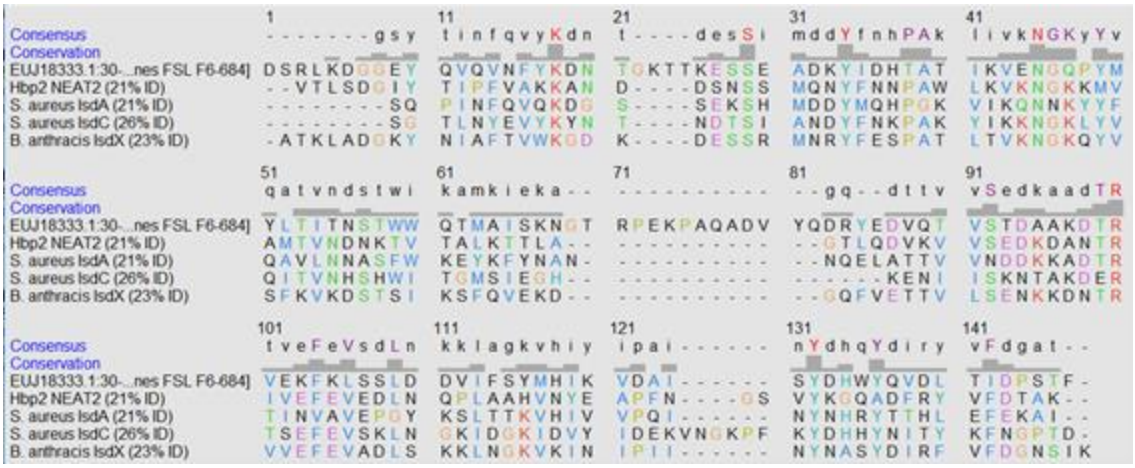

Figure 2-9: Clustal Omega Alignment of NEAT-domains with Available Structures to *L. monocytogenes* Hbp2 NEAT-domain 1.

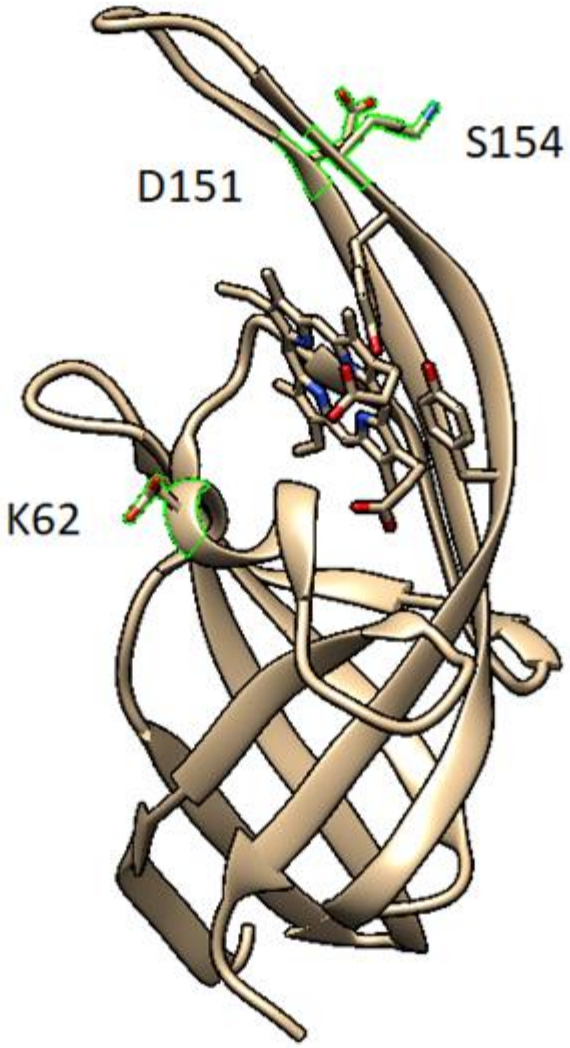

Figure 2-10: Location of Cysteine Mutants in Hbp2 NEAT1 Mapped on the IsdC Structure.

2.11 Expression and Purification of His-tagged Heme Uptake Proteins.

This approach was used for purifying his-tagged *L. monocytogenes* proteins HupD, Hbp1, Hbp2 and *S. aureus* proteins IsdB, IsdC and IsdH. A 10mL overnight culture of *E. coli* BL21 with pET28a-Δ30Hbp2(S154C) was set up in LB with kanamycin (50ug/mL) and grown at 37°C with shaking. The cells were subcultured into one liter of fresh LB with kanamycin and grown to an OD_{600} = 0.5, at which point 1mM IPTG was added to the subculture and incubated for an additional three hours. The cells were pelleted at 10000g for 10 min and the supernatant was decanted. The cells were resuspended in 20mL of lysis buffer (PBS pH 7.4 with DNase, RNase, 2mM DTT and 5mM Imidazole). The cells were lysed using three passes through a French Press with a pressure of 14,000 lb/in^2. The lysate was centrifuged at 5000g for 10 minutes to remove unbroken cells and the resulting supernatant was further spun down at 18000g for one hour to pellet the membranes, the cytoplasmic fraction remained in the supernatant. The cytoplasmic fraction was passed three times over a column of Talon Superflow Cobalt-resin to bind the His-tag containing proteins. The loaded column was subsequently washed with two column volumes of PBS pH7.4 with 5mM imidazole, then five column volumes of PBS pH7.4 with 20mM imidazole, and a final wash step of five column volumes of PBS pH7.4 with 40mM imidazole. The His-tagged Hbp2 was eluted using PBS pH7.4 with 250mM imidazole. Forty fractions (one mL each) were collected and evaluated via SDS-PAGE stained with Coomassie dye. (Figure 3-4). A significant amount of protein was observed in the 40mM imidazole wash fraction and the His-tag purified protein retained a significant amount of heme when coming off the column and post-dialysis into PBS pH7.4 buffer (Figures 3-5, 3-6). To remove the heme

from the His-tagged Hbp2, an acid-acetone wash method was utilized for generating apo-Hbp2 (Ascoli et al, 1981). The apo-Hbp2Δ30(S154C) was subsequently labeled with coumarin maleimide (Section 2.13).

2.12 Expression and Purification of Hbp2 from *L. monocytogenes*.

An overnight culture of EGD-e *Δhbp2* containing pAT28-Hbp2 was set up in 10mL BHI with streptomycin (120 μg/mL) and spectinomycin (100 μg/mL). The overnight culture was subcultured 1:100 into 20mL G+MMM with antibiotics and grown overnight for primary iron starvation. The overnight primary iron starved cells in G+MMM were subcultured again into a one liter of G+MMM with antibiotics to further iron starve the cells in a large volume to increase yield. The cells were spun out at 10,000xg for 10 minutes, and the supernatant (secreted fraction) was put on ice, the pellet with the cells was discarded. Subsequent steps were performed on ice or with chilled buffers. TCA (6N) was added to the secreted fraction to a final concentration of 0.86M TCA and was refrigerated for an hour to precipitate Hbp2, then spun down at 13,000xg for one hour. The supernatant was discarded and the pellet was resuspended in 20mL PBS, then 80mL acetone was added to perform an 80% acetone wash step. The Hbp2 protein was spun down at 13,000xg for one hour and the supernatant was carefully decanted. The acetone was evaporated by keeping the centrifugal tube open in a fume hood overnight. The pellet was resuspended in PBS and Ammonium sulfate was added to 40%, incubated at 4°C for an hour, then spun down at 13,000xg for one hour. The pellet was discarded and the supernatant was transferred to a new container, more ammonium sulfate was added to

a concentration of 60% and the solution was incubated at 4°C for an hour before spinning down at 13,000xg for an hour. The supernatant was discarded, and the pellet containing the 40-60% fraction was resuspended in PBS. Following resuspension the Abs_{280} was measured and the concentration of Hbp2 was determined using an extinction coefficient of 68.76/(mM*cm), so an Abs_{280} = 1.0 indicated 14.5 µM of Hbp2. The extinction coefficient was determined using the sequence of processed Hbp2 in the ExPASy protein parameters tool.

2.13 Preparation and Quantification of Fluorescein Maleimide, Coumarin Maleimide, Heme and FeEnt.

Fluorescein maleimide was purchased from AnaSpec Inc. and was resuspended in DMF. This stock was diluted into 10mM Tris, pH 8.0 and analyzed on a spectrophotometer. The absorbance peak at 493nm was used to determine the concentration using the Beer-Lambert law with a molar extinction coefficient at 493nm of $81 mM^{-1} cm^{-1}$.

Coumarin maleimide was purchased from Setareh Biotech LLC and was resuspended in DMSO. This stock was diluted into methanol and analyzed on a spectrophotometer. The absorbance peak at 393nm was used to determine the concentration using the Beer-Lambert law, with a molar extinction coefficient at 383nm of $33.5 mM^{-1} cm^{-1}$.

Bovine hemin chloride was purchased from Sigma and was resuspended into DMSO. This stock was diluted into 40% DMSO and analyzed on a spectrophotometer. The

absorbance peak at 400nm was used to determine the concentration using the Beer-Lambert law, with a molar extinction coefficient at 400nm of 180$mM^{-1}cm^{-1}$. Working solutions of hemin were diluted into PBS and utilized the same day.

Ferric Enterobactin was prepared using the AN102 strain. An overnight culture of AN102 was grown up in LB with streptomycin (100ug/mL) and subculture 1:50 into 150mL of LB and grown to late log phase. The 150mL subculture was transferred to 15L of T-media and grown until the OD_{600} stopped increasing. The cells were spun out and the supernatant was kept on ice for the rest of the purification. The Enterobactin was extracted into the organic phase by treating a liter of the supernatant with 150mL of ethyl acetate once and 100mL of ethyl acetate twice. The organic extracts were combined and the Enterobactin was concentrated using a rotary evaporator to a final volume of 100mL ethyl acetate. The concentrated Enterobactin was washed with 10mL of 100mM citrate, pH 5.5 and then with 10mL of distilled water. 10 grams of anhydrous $MgSO_4$ was added to dehydrate the ethyl acetate. The $MgSO_4$ was subsequently filtered out and the sample was again concentrated using rotary evaporation to a final volume of 10mL. Hexane was added dropwise to the ethyl acetate until Enterobactin started precipitating, at which point the Enterobactin was pelleted by spinning at 1000g for 10 minutes and the supernatant was decanted and the enterobactin was allowed to dry. To generate ferric Enterobactin, Enterobactin was dissolved in methanol and $FeSO_4$ was dissolved in water. An equimolar amount of Enterobactin was added to $FeSO_4$ and the mixture was incubated for one hour at room temperature, then Na_2HPO_4, pH 6.5 was added to a final concentration 100mM.

2.14 Labeling Cysteine Locations in Hbp2.

For labeling cysteine containing Hbp2 mutants, the protein was resuspended in PBS pH 6.7, following TCA/acetone precipitation, to make the buffer suitable for maleimide labeling (a pH value closer to the pKa of lysine results in maleimide labeling of lysine residues). The protein was diluted to 5 μM and treated with 5 μM of TCEP for ten minutes to reduce disulfide bonds and make the cysteine mutations available for reaction with fluorescein or coumarin maleimide. The fluorophore was added to a final concentration of 5 μM and the reaction mixture was incubated at 37°C for thirty minutes. The insoluble proteins following labeling were spun down before the 40-60% ammonium sulfate fraction. Not spinning down the insoluble fraction prior to harvesting the 40-60% ammonium sulfate precipitated fraction resulted in protein aggregates during subsequent size-exclusion chromatography. The 40-60% fraction of labeled protein resuspended in PBS pH7.4 and subsequently separated on a Sephacryl-300 High Resolution column to remove any residual TCEP, ammonium sulfate and coumarin maleimide and to isolate pure samples of fluorescently labeled Hbp2. Fractions 41-45 were subsequently used for heme uptake experiments.

2.15 Fluorometric Analysis of Heme Binding to Hbp2.

Fluorometric analysis was performed on an SLM OLIS Fluorimeter using an excitation wavelength of 390nm and an emission wavelength of 480nm. At first buffer was added to the cuvette and the background fluorescence was monitored. Purified Hbp2(S154C) labeled with coumarin was added to a final concentration of 30nM, resulting

in fluorescence of approximately 1.0, and the signal was allowed to stabilize, which took roughly ten minutes, with minimal fluorescent fluctuation in the subsequent 20 minutes. Afterwards, heme was added to a final concentration at 100nM, resulting in a 75-80% quenching of the fluorescent signal. Subsequently a titration was performed with increasing amounts of heme added to 30nM of labeled Hbp2 and the fluorescent quenching was tracked up to 255nM, since half the signal quenching occurred at 15nM, this concentration was chosen as optimal for tracking heme uptake by bacteria.

2.16 Iron Starvation of Gram-positive Cells and *In vivo* Heme Uptake Experiments.

Cells were grown in BHI overnight with appropriate antibiotics. The iron-rich bacteria at stationary phase were subcultured 1:500 into MOPS-L medium with appropriate antibiotics and grown overnight. A secondary subculture of 1:500 into MOPS-L medium with appropriate antibiotics containing 200µM bipyridyl and 10nM heme was used to starve the cells of iron and induce heme uptake proteins respectively. Heme uptake was evaluated in the OLIS SLM using MOPS-L medium lacking riboflavin and casamino acids (as both ingredients produced a fluorescent signal when using excitation of 390nm and emission of 480nm). Prior to adding cells to the fluorometer, their concentration was evaluated based on the culture's absorbance at 600nm, and cells were added to a final concentration of $5 \cdot 10^7$ cells/mL or a final OD_{600} of 0.25. Furthermore, once determining the volume of culture to be added, the cells were spun down and 90% of the supernatant was aspirated. The pellet was resuspended in residual supernatant and added to the cuvette. The removal of 90% of the media eliminated any dilution effects

observed due to the cultures being at different stages of growth, also a large jump in fluorescence upon addition of the cells was mitigated. The jump was attributed to fluorescent metabolites or secreted heme binding protein being present in the supernatant. Completely aspirating the supernatant and resuspending the cells in fresh media depressed heme recovery, suggesting that secreted proteins assisted the live cells in heme uptake.

Modifications in growth to achieve optimal growth or heme uptake in the different bacteria were as follows. *Serratia marcescens* (Gram-negative organism) was grown in MOPS minimal medium instead of MOPS-L medium and uptake was tested in PBS pH7.4 with 0.4% glucose. *S. aureus* failed to grow in MOPS-L medium, and this minimal medium was supplemented with 2% BHI for the primary and secondary subculture. *L. monocytogenes* grew in MOPS-L medium, but bipyridyl had to be added to 100µM instead of 200µM to allow growth.

2.17 Fluorophore Labeling and Analysis of FeEnt Uptake in *E. coli*.

An overnight culture of *E coli* OKN3 containing pITS23(S271C) was set up in 10mL LB with streptomycin (100 µg/mL) and chloramphenicol (20 µg/mL). The overnight culture was subcultured 1:100 into 20mL G-MMM with antibiotics and grown for 5.5 hours to iron starve the cells. The cells were spun down at 7,000g for 10 minutes, and resuspended in 20mL of 50mM Na_2HPO_4, pH6.7 to wash the cells. The cells were pelleted again and resuspended in 20mL of the same buffer as the wash step. Fluorescein maleimide was added to the resuspended cells to a final concentration of 5uM and incubated for 15

minutes at 37°C. The reaction was quenching by adding BME to a final concentration of 1.3mM, and the cells were spun down at 7000g for 10 minutes. The cells were subsequently resuspended in 20mL of 1XPBS as a wash step, then spun down again. Following the wash, the cells were resuspended in 20mL of 1X PBS with 0.4% glucose. For SLM analysis, cells were added to a final concentration of 0.1OD_{600} in 1X PBS with 0.4% glucose, FeEnt was added to a final concentration of 10nM. Excitation wavelength of 490nm and emission of 520nm was used for fluorescein labeled cells. For experiments utilizing energy poisons, after the cells were resuspended in PBS with 0.4% glucose, the energy poisons were added to the appropriate concentration and incubated with the cells for 30 minutes at 37°C prior to analysis on the SLM (Figure 2-11).

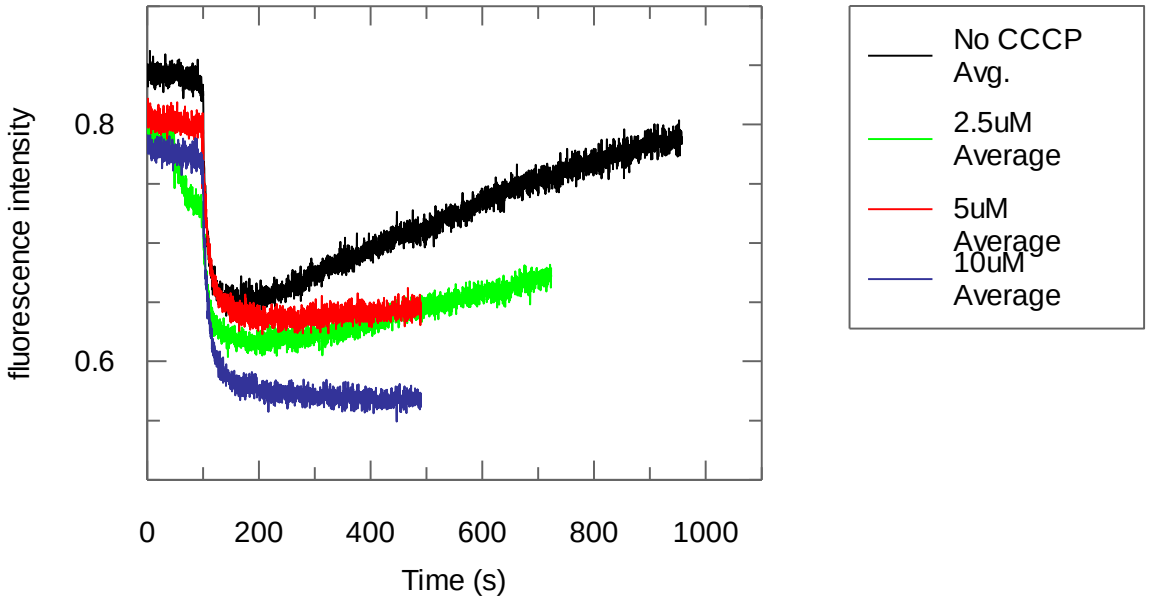

Figure 2-11: Inhibition of *E. coli* FeEnt Uptake by Different Concentrations of the Energy Poison CCCP.

2.18 Fractionation of the *Caulobacter crescentus* Inner and Outer Membranes.

Cells were grown overnight in NB and resuspended 1:100 into NB containing 50uM $FeSO_4$ or NB containing 100uM Enterobactin to stimulate growth in iron rich and iron poor conditions respectively. The cells were pelleted at 10,000g for 10 min and resuspended in lysis buffer (50mM Tris-Cl, pH 7.4 with DNase and RNase). The cells were lysed using three passes through a French Press with a pressure of 14,000 lb/in^2. The lysate was centrifuged at 5000g for 10 minutes to remove unbroken cells and the resulting supernatant was further spun down at 18000g for one hour. The supernatant contained the cytoplasmic fraction and the pellet contained the inner and outer membranes. The pellet was resuspended in PBS pH7.4 with 0.1% Sarkosyl and subsequently spun down at 18000g for one hour. The cytoplasm contained the inner membranes and the pellet contained the outer membranes. The fractions were subsequently analyzed using SDS-PAGE and coomassie staining (Figures 6-5, 6-6). Attempts to fractionate the membranes using sucrose gradients, Triton X-100 and 0.5% Sarkosyl produced poor results with known outer membrane proteins contaminating the inner membrane fractions.

Chapter 3: Expression of NEAT-domain Containing Proteins, their Interactions and *in vivo* Heme Uptake by Gram-positive Cells.

3.1 Expression of Hbp2 Using the pPL2 Plasmid in *L. monocytogenes*.

Development of a fluorescent assay in *E. coli* indicated that expression of surface exposed protein labeled with fluorescein is appropriate for detection of nutrient uptake. To test this approach in *L. monocytogenes* EGD-e, I transformed *Δhbp2* strains using pPL2-Hbp2, coding for a WT version of Hbp2 under the natural Fur repressor sequence and pPL2-Hbp2(D151C), coding for a cysteine mutant in a spot chosen to avoid interference with heme binding. Since pPL2 is an integration plasmid in *L. monocytogenes*, the rescue expression of Hbp2 was supposed to occur at a WT chromosomal level. The plasmid construct inserts were evaluated by PCR amplification and sequencing using *hbp2* specific primers. WT EGD-e, EGD-e *Δhbp2*, *Δhbp2* with pPL2-Hbp2 and *Δhbp2* with pPL2-Hbp2(D151C) were expressed under low iron conditions. After reaching mid-log phase, the cells were harvested and lysed via French press. Cytoplasmic and membrane fractions were prepared using differential centrifugation and 50μg of total protein (determined via UV280 absorbance) of each fraction were loaded onto an SDS-PAGE gel. The presence of Hbp2 was detected using mouse α-Hbp2 and alkaline phosphatase conjugated goat α-mouse secondary antibodies (Figure 3-1).

Expression of Hbp2 was detected in the cytoplasmic and membrane fractions of WT EGD-e strain (Figure 3-1**,** Lanes 2 and 6). A positive control with his-Hbp2 (expressed in *E. coli*) was overloaded into Lane 10, and verified the effectiveness of the Western blot. No noticeable Hbp2 bands were identified in the EGD-e *Δhbp2* strain, as expected.

However, attempted rescue with plasmid bearing the WT or mutant version of Hbp2 failed to show any detectable Hbp2 bands. Therefore, the chromosome integrated pPL2 constructs were not able to express any detectable amounts of Hbp2, possibly because the integration vector provides the cell with fewer copies of the Hbp2 gene compared to expression from a high-copy vector.

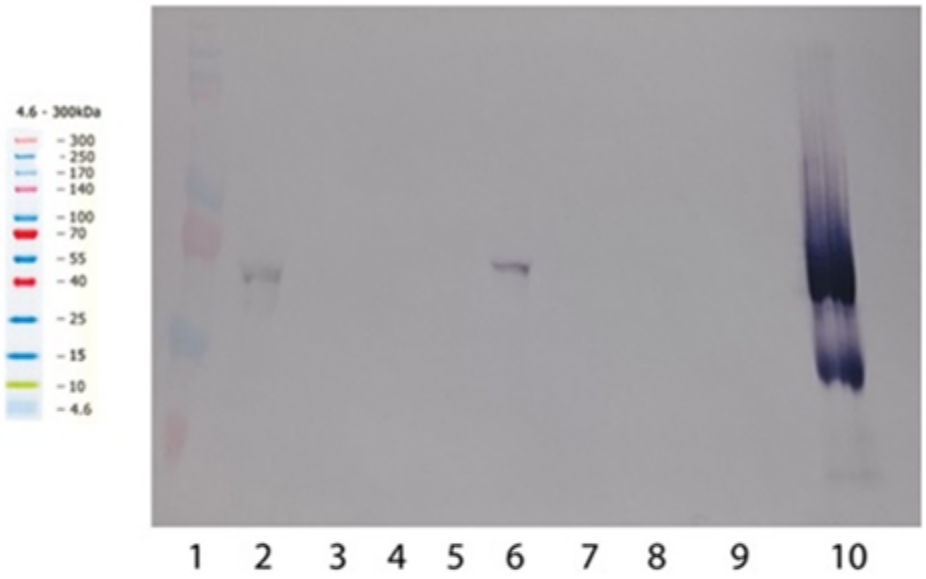

1. Protein Ladder
2. WT EGD-e, cytoplasmic fraction
3. EGD-e *Δhbp2*, cytoplasmic fraction
4. EGD-e *Δhbp2*, WT *hbp2* integrant, cytoplasmic fraction
5. EGD-e *Δhbp2*, *hbp2*(D151C) integrant, cytoplasmic fraction
6. WT EGD-e, membrane fraction
7. EGD-e *Δhbp2*, membrane fraction
8. EGD-e *Δhbp2*, WT *hbp2* integrant, membrane fraction
9. EGD-e *Δhbp2*, *hbp2*(D151C) integrant, membrane fraction
10. Hbp2 positive control

Figure 3-1: Expression of Hbp2 from WT EGD-e. Lack of Expression from ΔHbp2 Strain and Integrated pPL2-Hbp2 Plasmids.

3.2 Expression of Hbp2 Using the pAT28 Plasmid in *L. monocytogenes*.

To overcome the lack of expression issue observed in the EGD-e *Δhbp2* strain, I attempted to express Hbp2 in the high-copy shuttle vector pAT28. The pAT28-Hbp2 construct was verified using colony PCR and sequencing. WT EGD-e, EGD-e *Δhbp2*, along with *Δhbp2* strains bearing an empty pAT28 plasmid, pAT28-Hbp2 and pAT28-Hbp2(S154C) and pAT28-Hbp2(K62C) strains were grown under iron-poor conditions in Gram-positive MOPS minimal media. Cells were harvested and the secreted fraction was collected and precipitated using TCA precipitation. The cells were subject to lysis using a French press and the membrane fractions were separated from the cytoplasm using differential centrifugation. A total of 50 μg of protein were loaded (determined via UV280 absorbance) of the secreted and membrane fractions for each strain. The secreted fraction of the WT EGD-e strain showed detectable, but small amounts of Hbp2 (Figure 3-2**,** Lane 1). The ΔHbp2 strain showed no detectable expression of Hbp2, as expected (Lane 2). The ΔHbp2 strain expressing the empty pAT28 plasmid also showed a lack of detectable Hbp2 expression (Lane 3). The *Δhbp2* strain transformed with pAT28-Hbp2, expressed secreted Hbp2 in far greater amounts than the WT strain (Lane 4). The *Δhbp2* strain transformed with pAT28-Hbp2(K62C) coding for cysteine containing mutant Hbp2 expressed secreted protein at a level similar to pAT28-Hbp2 (Lane 6). The *Δhbp2* strain transformed with pAT28-Hbp2(S154C) expressed secreted Hbp2 in levels even greater than the Hbp2(K62C) mutant (Lane 5). The membrane fractions (Lanes 7-12) mirrored the results observed in the secreted fractions, but at slightly lower levels of Hbp2 expression in the membrane fractions of the plasmid rescued deletion strains (data not shown).

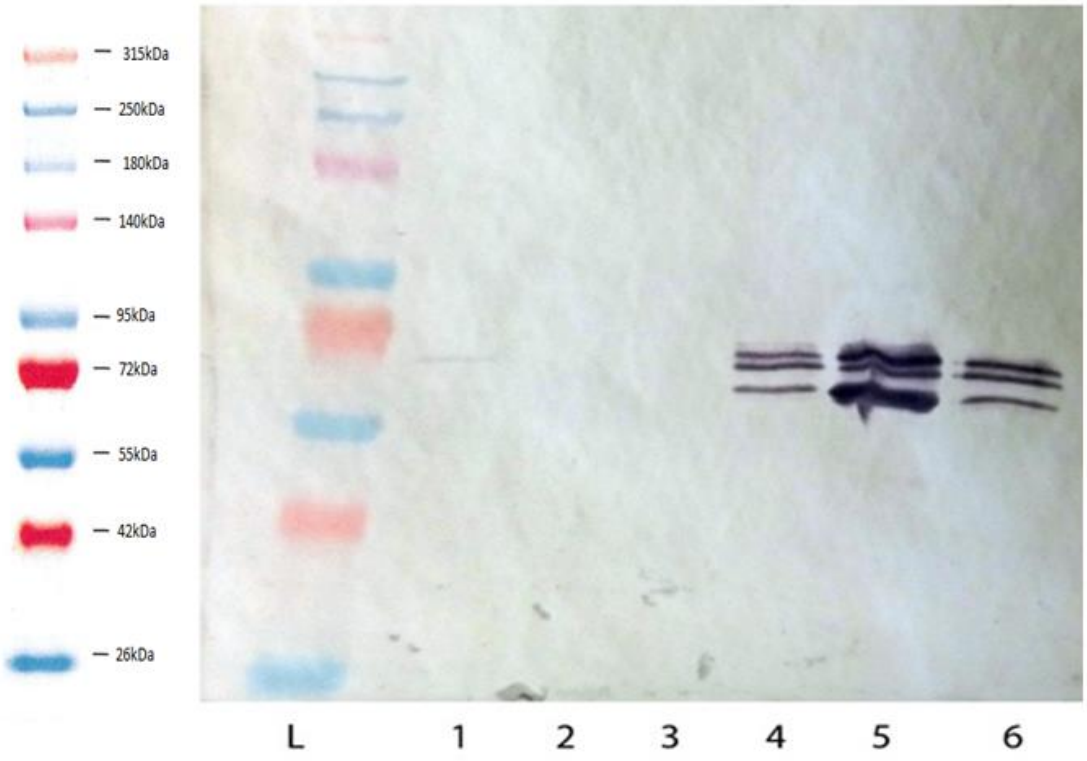

L. Protein Ladder
1. WT EGD-e – secreted fraction
2. EGD-e *Δhbp2* – secreted fraction
3. EGD-e *Δhbp2* with pAT28 – secreted fraction
4. EGD-e *Δhbp2* with pAT28-Hbp2 – secreted fraction
5. EGD-e *Δhbp2* with pAT28-Hbp2(S154C) – secreted fraction
6. EGD-e *Δhbp2* with pAT28-Hbp2(K62C) – secreted fraction

Figure 3-2: Western Blot Showing the Expression of WT Hbp2 and the K62C and S154C Mutants from the pAT28 Vector.

3.3 Labeling of *in vivo* Hbp2 in *L. monocytogenes*.

The significant levels of expression of mutant Hbp2 in *L. monocytogenes* cells suggested that it would be possible to reconstitute the Gram-negative approach to tracking iron uptake in live cells. Shortly, an extracellularly exposed protein would be mutated to generate a cysteine modification that could be labeled with fluorescein

maleimide. Upon addition of a ligand that bound to the labeled protein, the fluorescence level would drop, and would be followed by a recovery of fluorescence to the initial level seen before addition of the ligand as the cell transported the ligand into the cytoplasm.

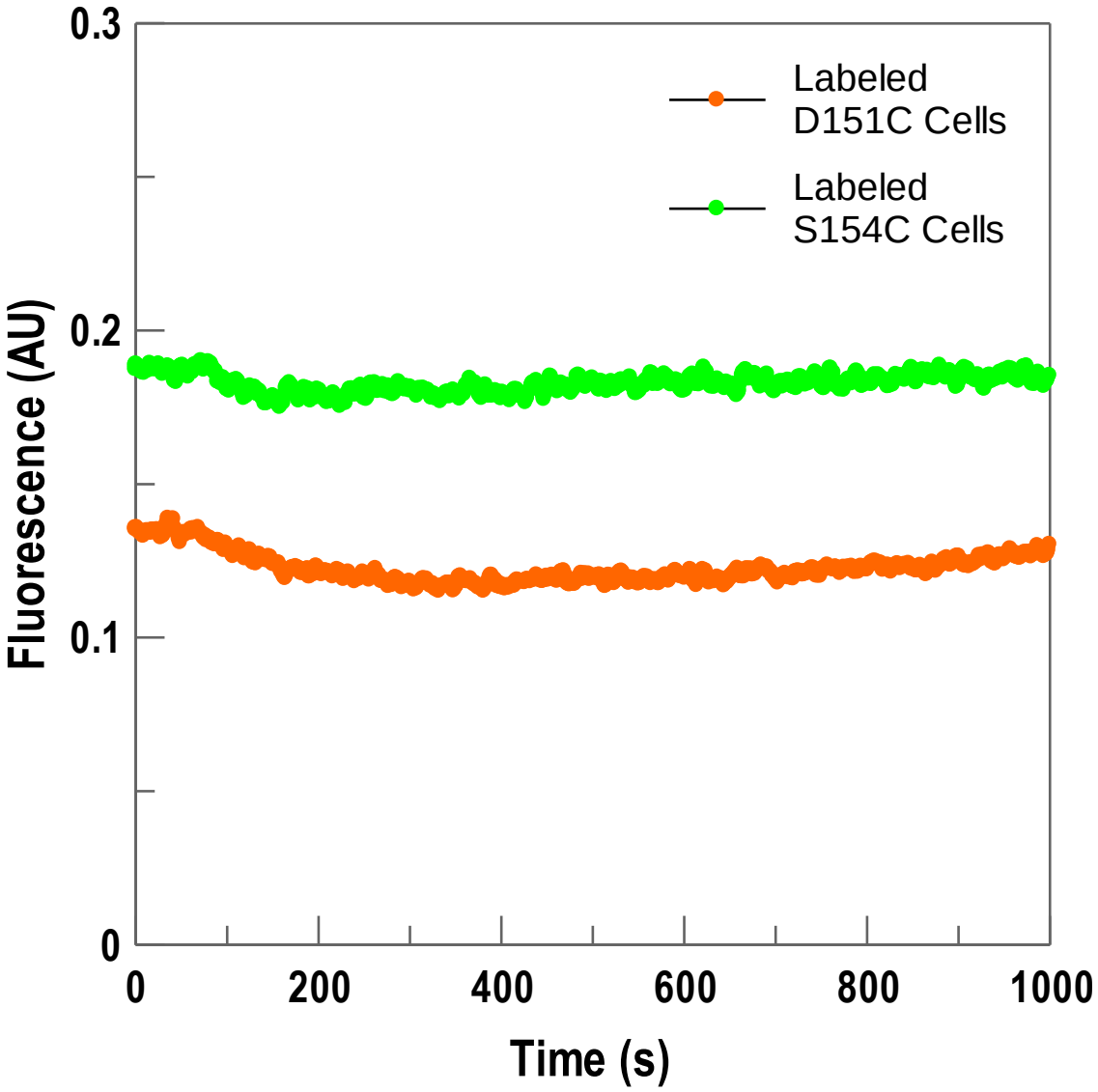

Figure 3-3 Fluorescent Labeling and Heme Response of *L. monocytogenes* Cells Expressing Cysteine containing Hbp2.

Cells expressing Hbp2(S154C) and Hbp2(D151C) were labeled with fluorescein maleimide using the Gram-negative labeling protocol established in Smallwood et al,

2014. Cells were grown under iron-poor conditions to stimulate expression of Hbp2 in EGD-e ΔHbp2 strain bearing pAT28-Hbp2(S154C) and pAT28-Hbp2(D151C). Cells were harvested during mid-log phase and resuspended in PBS pH6.7 to Abs_{600} = 1.0. Fluorescein maleimide was added to a final concentration of 5μM and incubated at 37°C for 5 minutes. After quenching with BME, the cells were spun down and washed with ice-cold PBS pH7.4 with 0.4% glucose. The labeled cells were diluted into PBS pH7.4 with 0.4% glucose to a final concentration $0.1OD_{600}$ and the fluorescence level was tracked in an OLIS SLM spectrofluorometer using an excitation wavelength of 490nm and an emission wavelength of 520nm (Figure 3-3). Fluorescence was tracked for 100 seconds, at which point heme was added to a final concentration of 100nM. The cells were labeled, but to a relatively low level, compared to the fluorescence levels observed at similar concentrations of labeled FepA in *E. coli* cells. Furthermore, the addition of heme generated little to no drop in the fluorescence level. Alternative concentrations of heme and labeled cells were tested, but did not result in appreciable differences in the results. The lack of observable quenching suggested that despite expression from a high-copy plasmid, the amount of Hbp2 present on the cell wall was not as great as the amount of FepA expressed in the outer membrane of *E. coli*. Alternatively, the presence of the thick peptidoglycan layer generated scattering that reduced the observed fluorescence signal from peptidoglycan-anchored Hbp2.

3.4 Expression and Purification of Hbp2 from *E. coli* Using pET28.

To express Hbp2 in *E. coli, Δ30hbp2* was inserted into the pET28 His-tag fusion vector. Cells were cultured in iron rich LB media and expression of His-Hbp2 was induced with IPTG. The cells were lysed using a French press and the cytoplasm was harvested for running on a Talon superflow affinity column. A SDS-Page gel was used to evaluate the effectiveness of the purification and the gel was coomassie stained (Figure 3-4). His-Δ30Hbp2 is present as the top band in Figure 3-4, and a significant amount of Hbp2 was present in the 40mM Imidazole wash. Fractions 5 and 6 contained relatively pure samples of Hbp2 compared to the other eluted proteins. The 40mM wash was combined with fractions 1 through 10 were pooled and purified using a 50kDa-cutoff centrifugal filter. The purified Hbp2 was evaluated spectroscopically and showed a significant amount of heme (roughly 1μM heme per 5μM Hbp2) present as judged by the Soret band around 400nm (Figure 3-5). Despite the presence of heme in the purified fraction, the protein was still able to bind 5μM heme as judged by the increase in the Soret band and the redshift of the absorption maxima from around 383nm to 400nm (Figure 3-5). Attempts to extract heme from Hbp2 using dialysis showed a decrease in the Abs_{280} and the Abs_{400} maxima, but this drop was mostly due to a dilution effect rather than heme loss by the protein (Figure 3-6). An acid-acetone wash was subsequently utilized to fully remove heme from Hbp2.

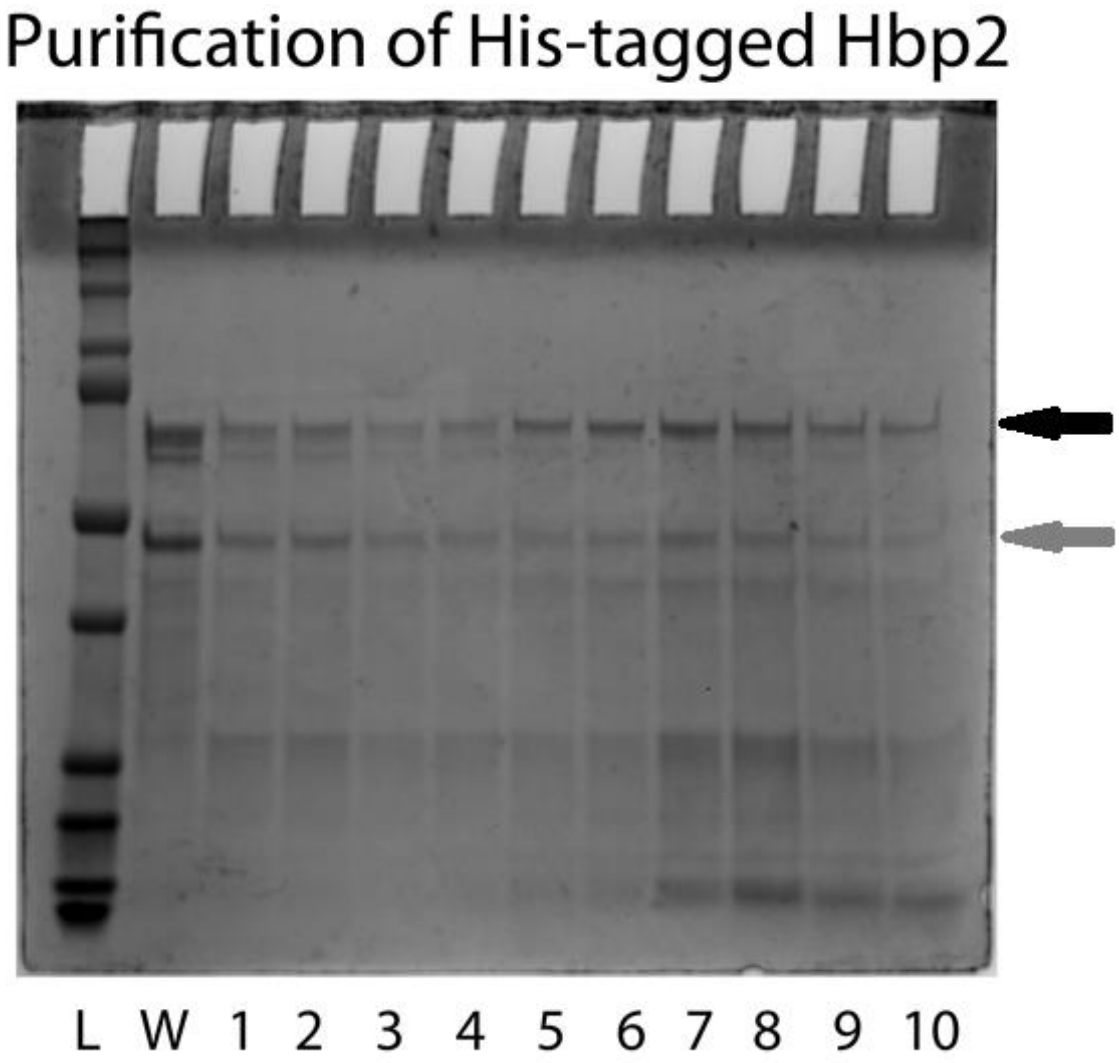

Figure 3-4: Coomassie Stained Gel of 40mM imidazole Wash and Eluted Fractions of His-tagged Hbp2Δ30(S154C). The black arrow denotes His-Hbp2 and the gray arrow denotes a degradation product of His-Hbp2.

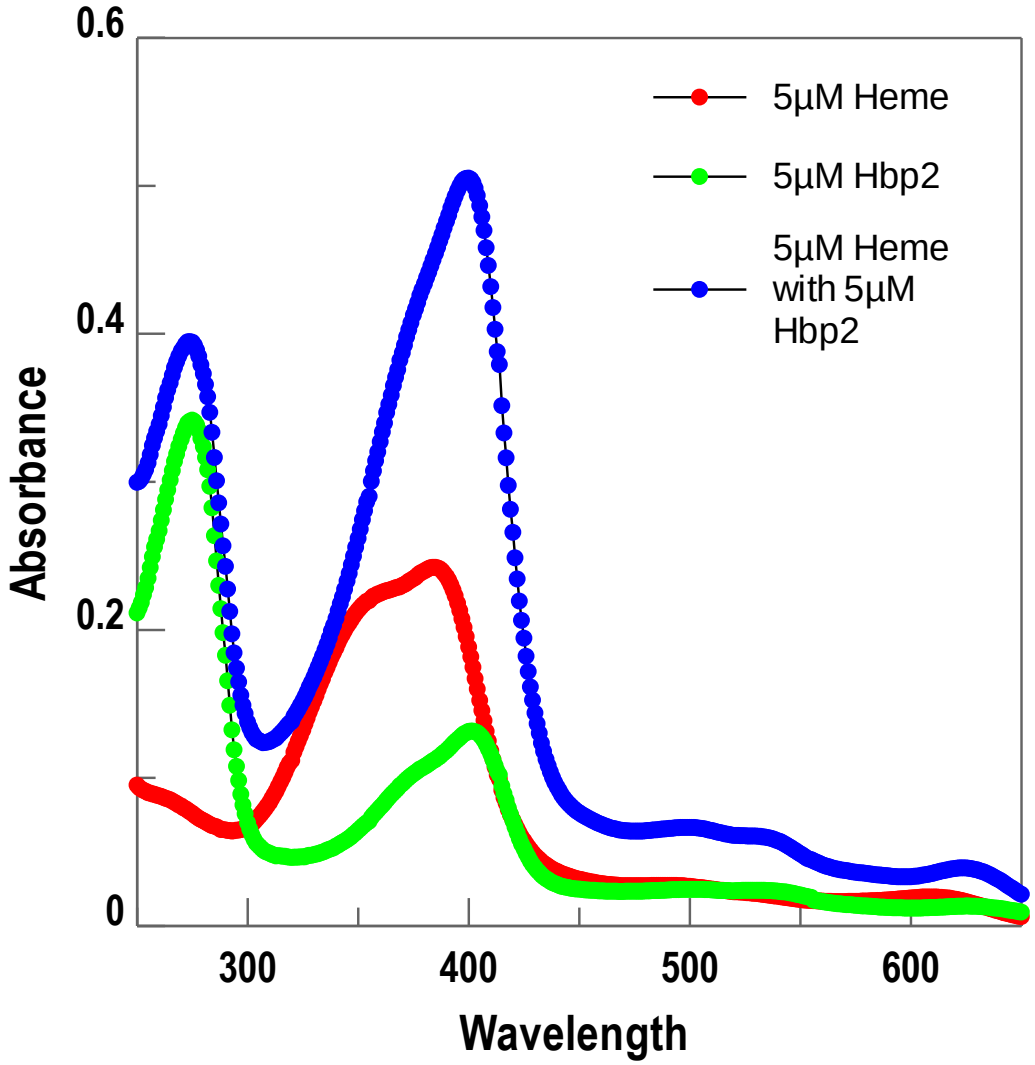

Figure 3-5: Spectroscopic Analysis of Heme Binding to His-Hbp2(S154C).

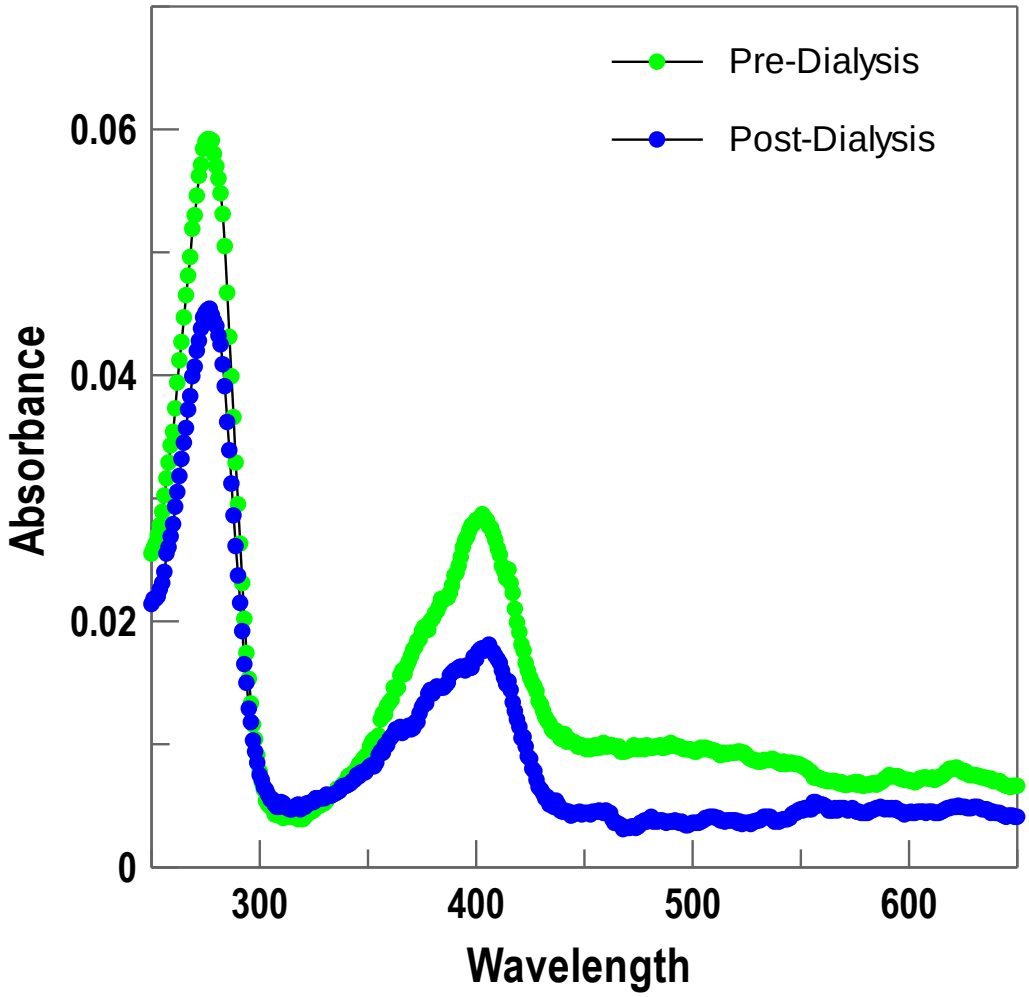

Figure 3-6: Dialysis of His-Tagged Hbp2Δ30(S154C).

3.5 Expression and Purification of Hbp2(S154C) from *L. monocytogenes*.

Due to the high level of heme contamination in Hbp2 during His-tagged Hbp2 purification in *E. coli* and because the presence of the His-tag might affect heme binding to Hbp2, I expressed Hbp2 in *L. monocytogenes.* Purifying Hbp2 from its native organism was also made easier by the presence of Hbp2 expressing cells secreting a significant amount of protein into the extracellular media when expressed from the pAT28 vector. The secreted fraction was harvested, purified and labeled as explained in Chapters 2.12-

2.14. The protein of interest eluted around fraction 42-45, and fractions 39-49 were analyzed by fluorescent gel and coomassie staining (Figure 3-7). The fluorescent gel was imaged in a UVP Biospectrum imaging system using an excitation of 365nm and a coumarin emission filter. Fractions 42-45 had a large amount of Hbp2 with minimal contamination from other proteins and were subsequently used during heme binding and uptake experiments.

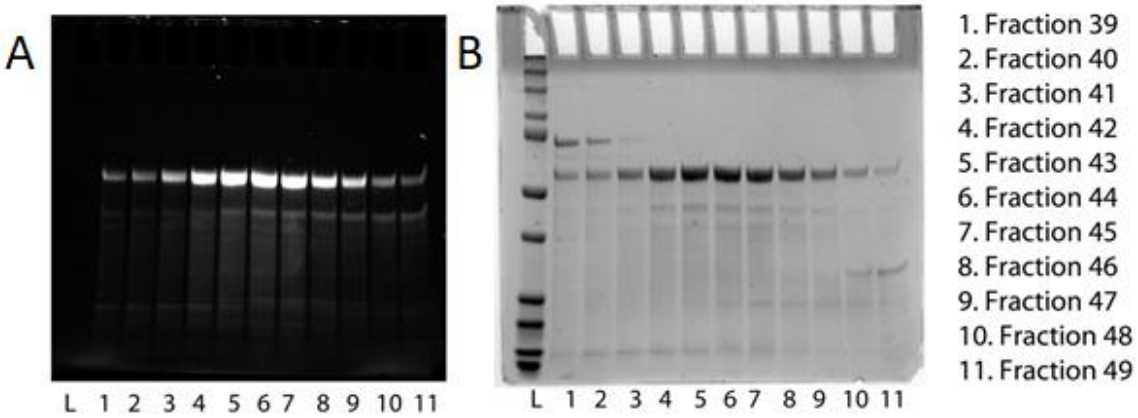

Figure 3-7: Fluorescent Gel (A) and Coomassie Stain (B) of S300HR-purified Hbp2.

3.6 Spectroscopic Analysis of Coumarin-Labeled Hbp2(S154C).

I took an absorbance spectrum of coumarin maleimide labeled Hbp2(S154C), diluted in PBS pH7.4 to determine the concentration of coumarin and protein in the sample (Figure 3-8). This task was complicated by the fact that coumarin has some absorbance at UV280, the wavelength which was used to track protein concentration, and that the spectra of coumarin shift based on the solvent and the reaction state of coumarin (Figure 3-9). In methanol coumarin maleimide has an extinction coefficient of $33.5 mM^{-1}cm^{-1}$ at 383nm, and this value was used to determine the concentration of

coumarin added during labeling. However, once the proteins are labeled with coumarin, they are present in a PBS buffer, which alters coumarin's absorbance spectrum, depressing and redshifting the absorbance around the 383nm maxima to 391nm, and increasing the absorbance around 280nm. Additionally, it's important to separate the contribution of coumarin and protein to the wavelengths at 280nm and 390nm. To account for these contributions and accurately calculate the concentrations of Hbp2(S154C) and coumarin in the absorbance spectrum of Fraction 43 (Figures 3-8 and 3-9). Furthermore, the absorbance maxima around 390nm rather than 400nm (Figure 3-5, 3-6) verified that the peak was due to coumarin and not heme.

The Abs_{280} of fraction 43 was determined to be 0.039, and adjusted to 0.0361 to account for background scattering extrapolated from the background scattering between 450nm-650nm. After factoring in the 50x dilution, the absorbance at 280nm of the initial sample was calculated at 1.805. The absorbance at 390nm of fraction 43 was measured at 0.0141, and adjusted to 0.01158 by subtracting the background scattering. When accounting for dilution, the adjusted absorbance at 390nm of the initial sample was calculated at 0.5792 (Figure 3-8). Since coumarin maleimide binding to cysteine increases the absorbance at 390nm, I incubated the fluorophore with free cysteine and determined the extinction coefficient at 390nm of cysteine-bound coumarin in PBS to be 25.42 $mM^{-1}cm^{-1}$ (Figure 3-9). Using this extinction coefficient in the Beer-Lambert law ($A=l\varepsilon c$), the concentration of coumarin in fraction 43 was calculated to be 22.78 µM. To subtract the contribution of coumarin to the absorbance at 280nm, I took a reading of unbound coumarin in PBS. Unbound coumarin in PBS was chosen over cysteine-bound coumarin

because cysteine contributed slightly to the Abs_{280} reading, and the values at 280nm were very similar for unbound coumarin and cysteine-bound coumarin in PBS (Figure 3-9). For unbound coumarin in PBS, the extinction coefficient at 280nm was calculated to be $9.86 mM^{-1}cm^{-1}$. Using the Beer-Lambert law, the contribution of coumarin to the reading at 280nm was calculated to be 0.2246. Subtracting this value from the adjusted overall reading at 280nm gave a value of 1.5804. Using the extinction coefficient of 68.76 $mM^{-1}cm^{-1}$ for Hbp2 at 280nm, the concentration of Hbp2 in fraction 43 was calculated to be 22.98 µM. Therefore fraction 43 contained 22.98 µM of Hbp2(S154C) and 22.78 µM of coumarin maleimide, demonstrating a 99.1% labeling efficiency.

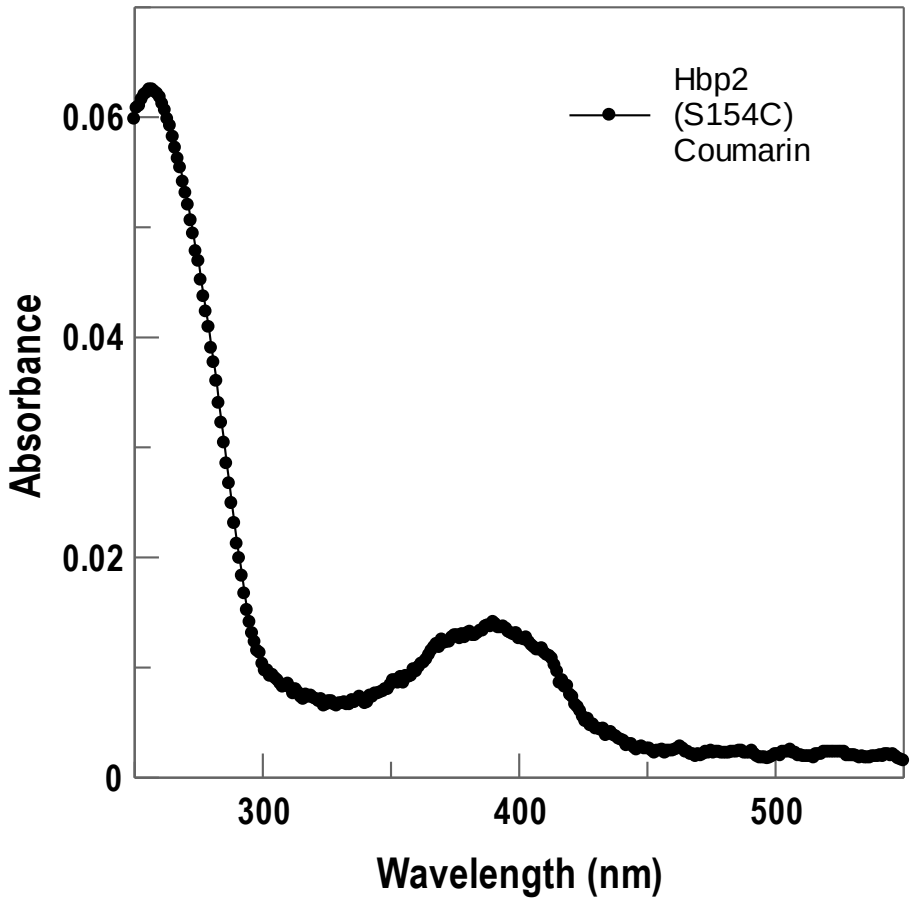

Figure 3-8: 50x Dilution of Coumarin Labeled Hbp2(S154C) from Fraction 43.

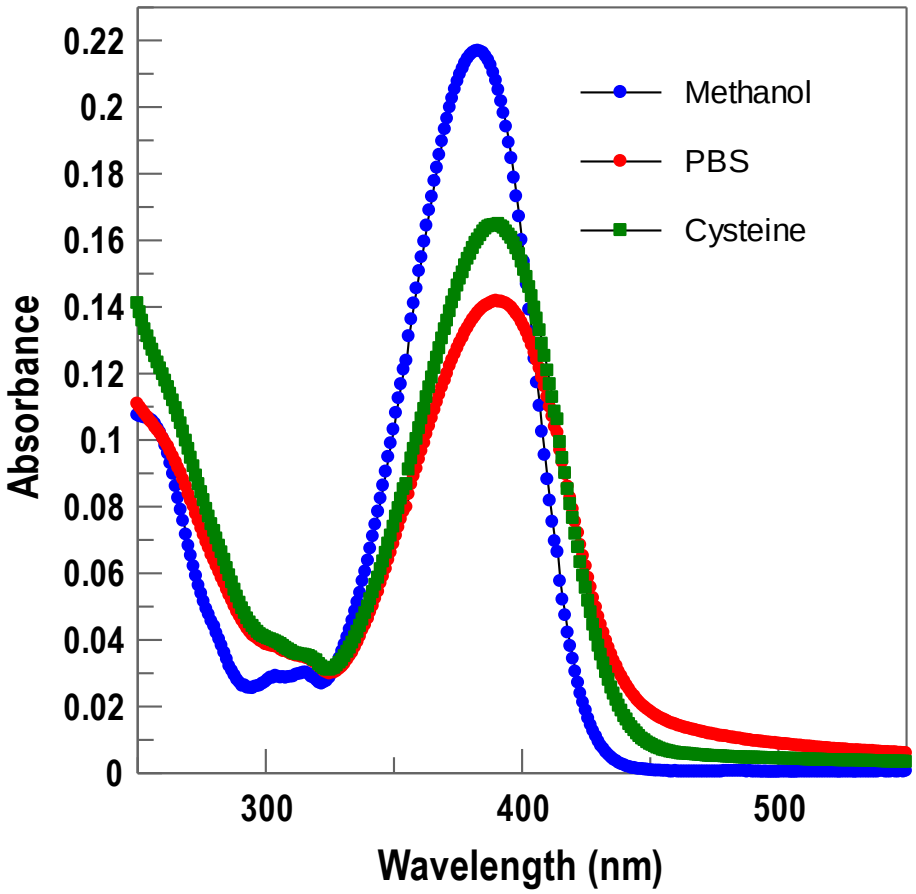

Figure 3-9: Absorbance of Free Coumarin-maleimide in Methanol and PBS, Compared to Coumarin Maleimide Reacted with Cysteine in PBS.

3.7 Analysis of Total Quenching During Heme Binding to Hbp2.

The fluorescent quenching associated with heme binding in coumarin labeled Hbp2(S154C) was evaluated using an OLIS SLM fluorometer (Figure 3-10). Using an excitation and emission scan, an optimal excitation wavelength of 390nm and an emission wavelength of 480nm were utilized. The background wavelength of the media was measured, and gave a reading of approximately 0.06 fluorescence-volts. At 600 seconds, protein was added to 30nM, producing a reading slightly above 1.0 and after a small drop of approximately 0.05 fluorescence volts over 100 seconds, remaining stable over the next 1800 seconds. Addition of heme to 100nM at approximately 2400 seconds resulted in a 75% fluorescence drop, a significant level of quenching (Figure 3-10).

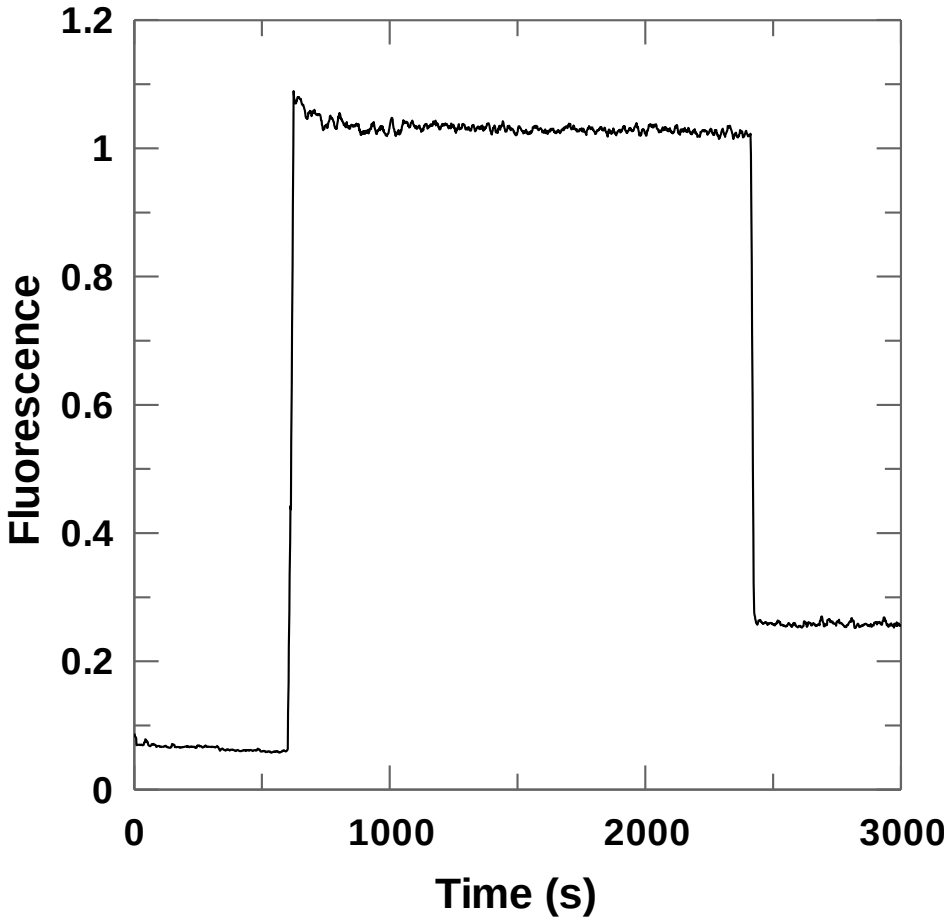

Figure 3-10: 30nM of Labeled Hbp2(S154C) with 100nM Heme.

3.8 Titration of Heme into Hbp2 to Determine K_d.

Heme was titrated into fluorescently labeled Hbp2 to determine the dissociation constant for heme interaction with coumarin labeled Hbp2(S154C). The fluorescence was evaluated using an excitation wavelength of 390nm and an emission wavelength at 480nm on an OLIS SLM. The background fluorescence of the PBS pH7.4 buffer was around 0.06 fluorescence-volts. Hbp2 was added to 30nM at 100 seconds and the fluorescence settled at 1.1 fluorescence-volts with 300 seconds. Heme was added to 1nM at 500 seconds, 3nM at 750 seconds, 7nM at 1100 seconds, 15nM at 1350 seconds, 31nM at 1700 seconds, 63nM at 2000 seconds, 127nM at 2300 seconds and 255nM at 2650 seconds (Figure 3-11). The drop in the fluorescence level associated with the total concentration of heme is summarized in Table 5. The values from table 3-1 were plotted in Grafit 6.0 software from Erithacus Software Ltd (Figure 3-12). The data was fitted using a one site ligand binding function and the fit gave a K_d = 15.7nM. Since around half the fluorescence signal from 30nM of Hbp2(S154C) was quenched by 15nM of heme, these concentrations of protein and ligand were chosen for subsequent experiments.

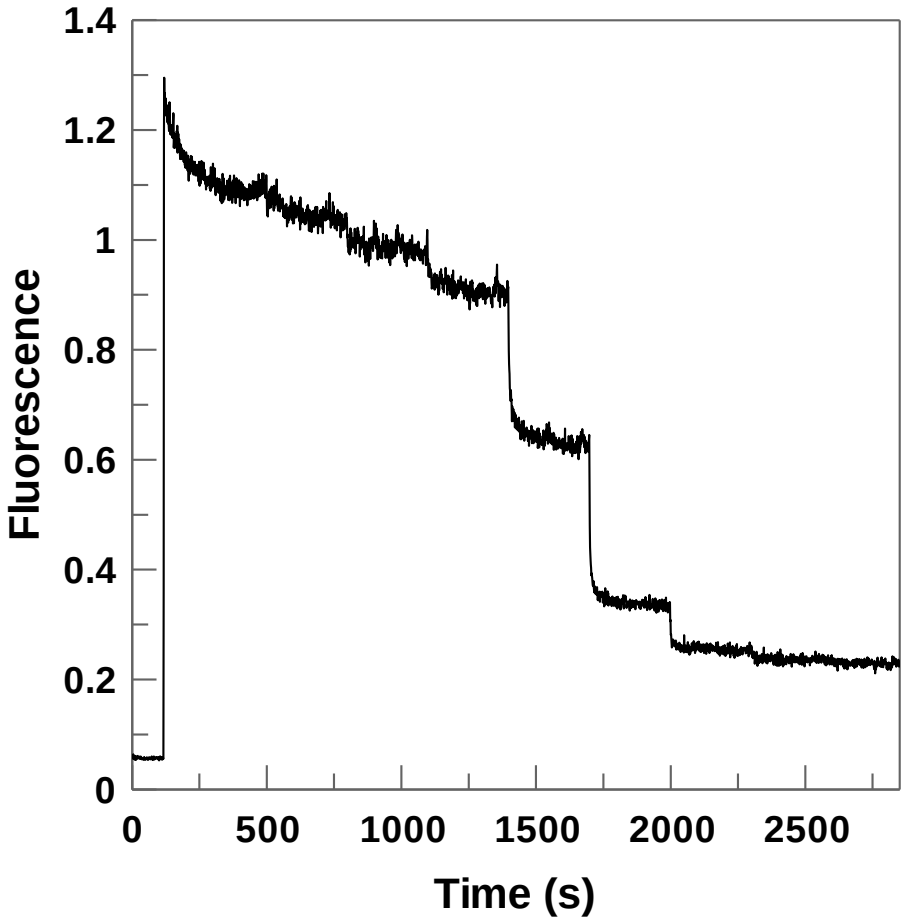

Figure 3-11: Titration of Heme into 30nM of Coumarin Labeled Hbp2(S154C).

Heme(nM)	Fluorescence Quenching
0	0
1	0.0531
3	0.1039
7	0.192
15	0.4647
31	0.7615
63	0.8399
127	0.8529
255	0.8624

Table 3-1: Fluorescence quenching from heme being added to purified Hbp2(S154C) labeled with coumarin.

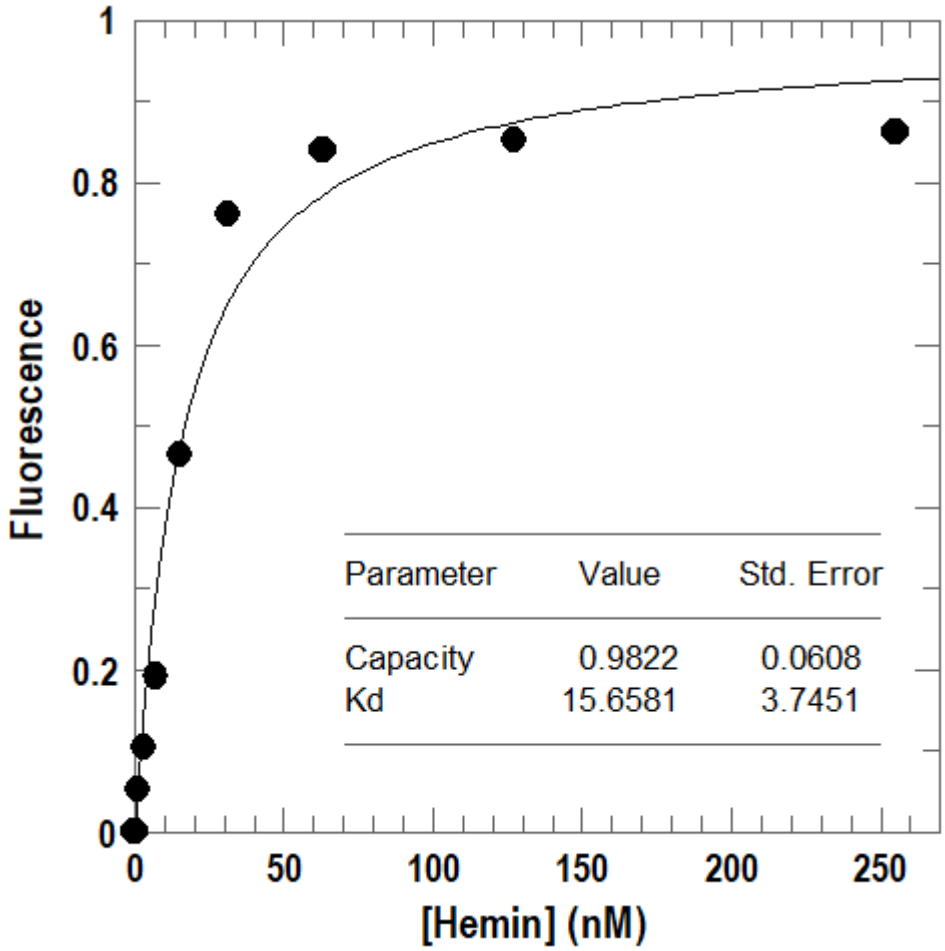

Figure 3-12: Fluorescence Drop from Heme Binding to Hbp2.

3.9 Heme Transfer from Hbp2 to Hbp1, HupD and IsdC, IsdB and IsdH.

Since heme transfer is proposed to occur between his-tagged Hbp2, Hbp1 and HupD as part of heme uptake in *L. monocytogenes*, I evaluated the ability of purified holo-Hbp2 to transfer heme to apo-Hbp1, apo-HupD, apo-IsdC, apo-IsdB and apo-IsdH. To generate holo-Hbp2, I diluted coumarin labeled Hbp2(S154C) to 30nM in PBS pH7.4, and allowed the fluorescence to stabilize, then at 300 seconds I added heme to 30nM. The quenching associated with heme addition was roughly 50% of the original fluorescent signal. Then at 600 seconds, I added (to 600nM, a 10-fold excess of) heme-free his-tagged proteins which are part of the proposed heme acquisition pathways in *L. monocytogenes* and *S. aureus*. Addition of apo-Hbp1 to holo-Hbp2 caused a rapid increase in fluorescence to around 80% of the original fluorescent signal, indicating that Hbp1 could remove heme from Hbp2. The fluorescent signal did not recover completely to the original level, despite the 10-fold excess of holo-Hbp1, suggesting that Hbp2 has a higher affinity for heme than Hbp1 (Figure 3-13). Hbp2 at 30nM was also mixed with HupD, and there was no associated unquenching of the fluorescent signal (Figure 3-14). I reasoned that Hbp1 was necessary to transfer heme from Hbp2 to HupD, but addition of Hbp1 followed by apo-HupD (added at 900 seconds, Figure 3-15) did not further increase the unquenching beyond the level provided by Hbp1, suggesting that perhaps the transfer reaction between Hbp2-Hbp1-HupD occurred on far longer time-scales than were measured or that HupD must be in contact with a heme-permease and ATPase in the membrane to acquire heme from Hbp2.

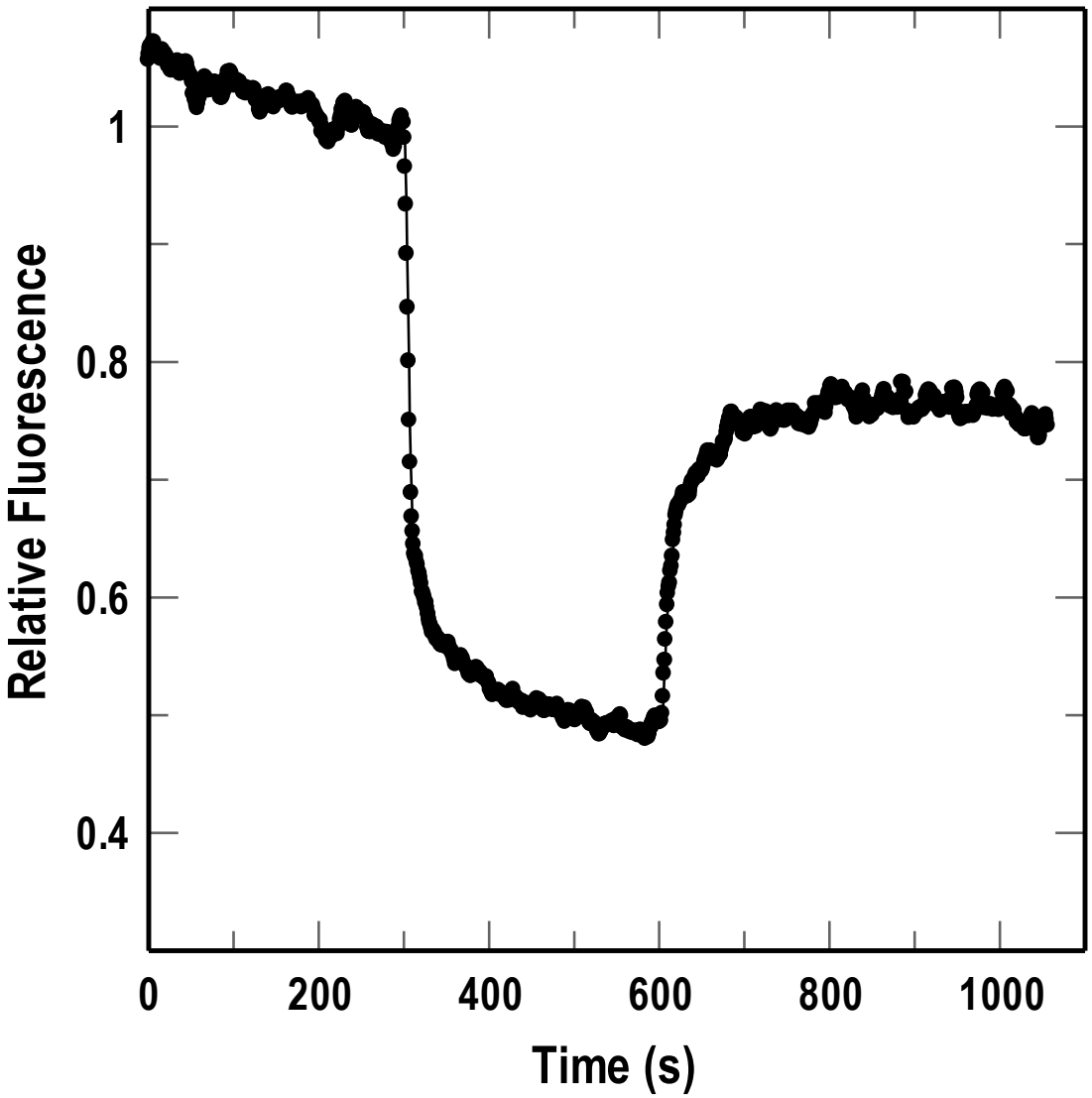

Figure 3-13: Heme Transfer from holo-Hbp2 to apo-Hbp1.

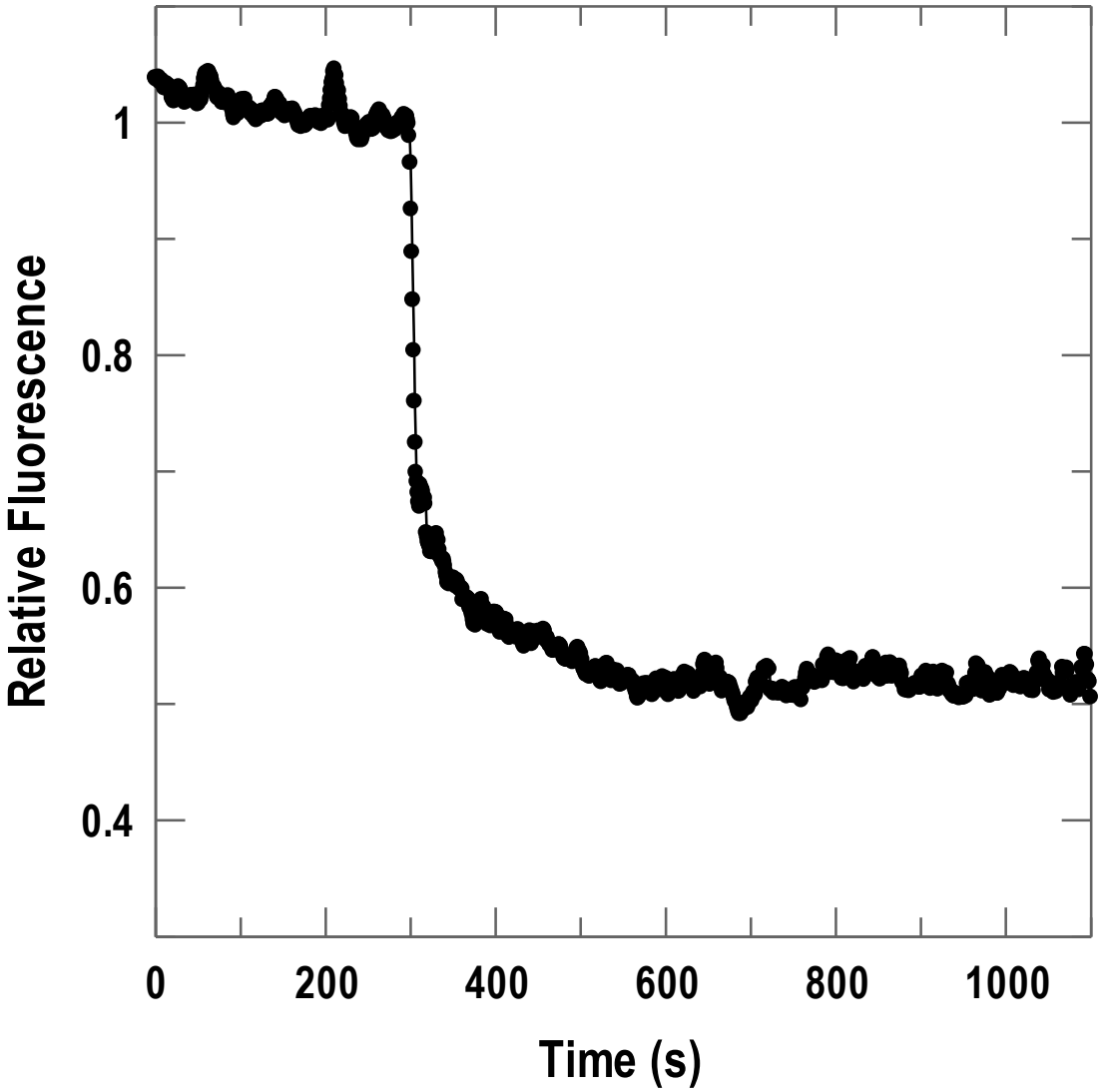

Figure 3-14: Heme Transfer from holo-Hbp2 to apo-HupD.

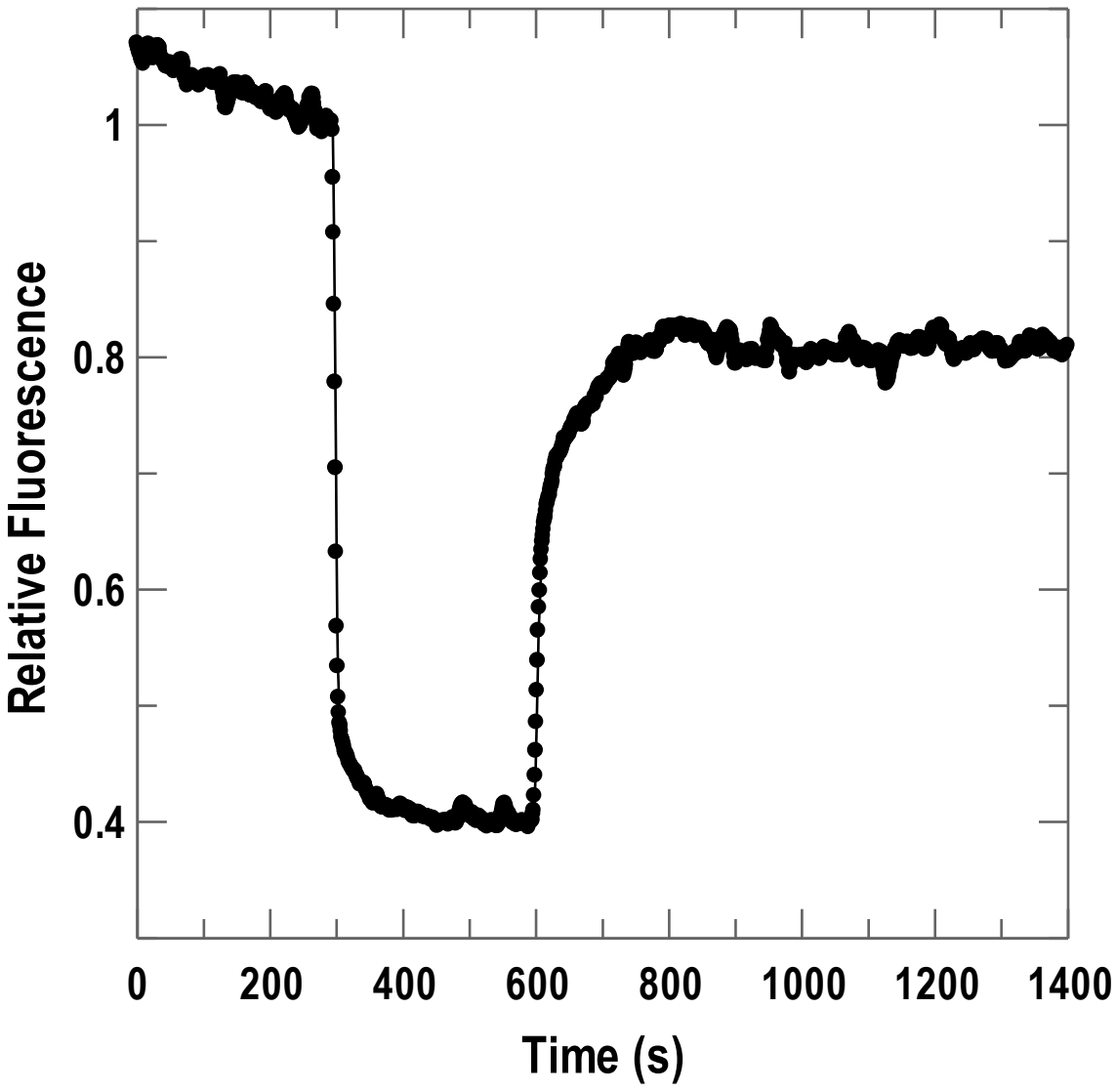

Figure 3-15: Heme Transfer from Holo-Hbp2 to apo-Hbp1 then apo-HupD.

NEAT-domain containing proteins from *S. aureus* were also tested for their ability to take up heme from Hbp2. As with the *L. monocytogenes* proteins, 30nM Hbp2 was added to PBS and allowed to equilibrate for 300 seconds, at which point heme was added to 30nM, and then the apo-protein was added at 600 seconds. Adding apo-IsdC to holo-Hbp2, resulted in significant unquenching of the fluorescent signal, more than the unquenching that was seen with Hbp1 (Figure 3-16). Addition of apo-IsdB to holo-Hbp2 had no effect on the fluorescence signal, similar to what was observed with apo-HupD (Figure 3-17). Addition of apo-IsdH to holo-Hbp2 resulted in a small drop in the fluorescent signal, but this was due to the low concentration of apo-IsdH that was available, which required a greater volume to get to 600nM, and so diluted the fluorescent signal (Figure 3-18). The finding that IsdC can acquire heme from a NEAT-domain containing protein from another organism is novel and shows that hemophores can be hijacked by different organisms to acquire heme in a similar manner to that observed with siderophore pirating by different organisms.

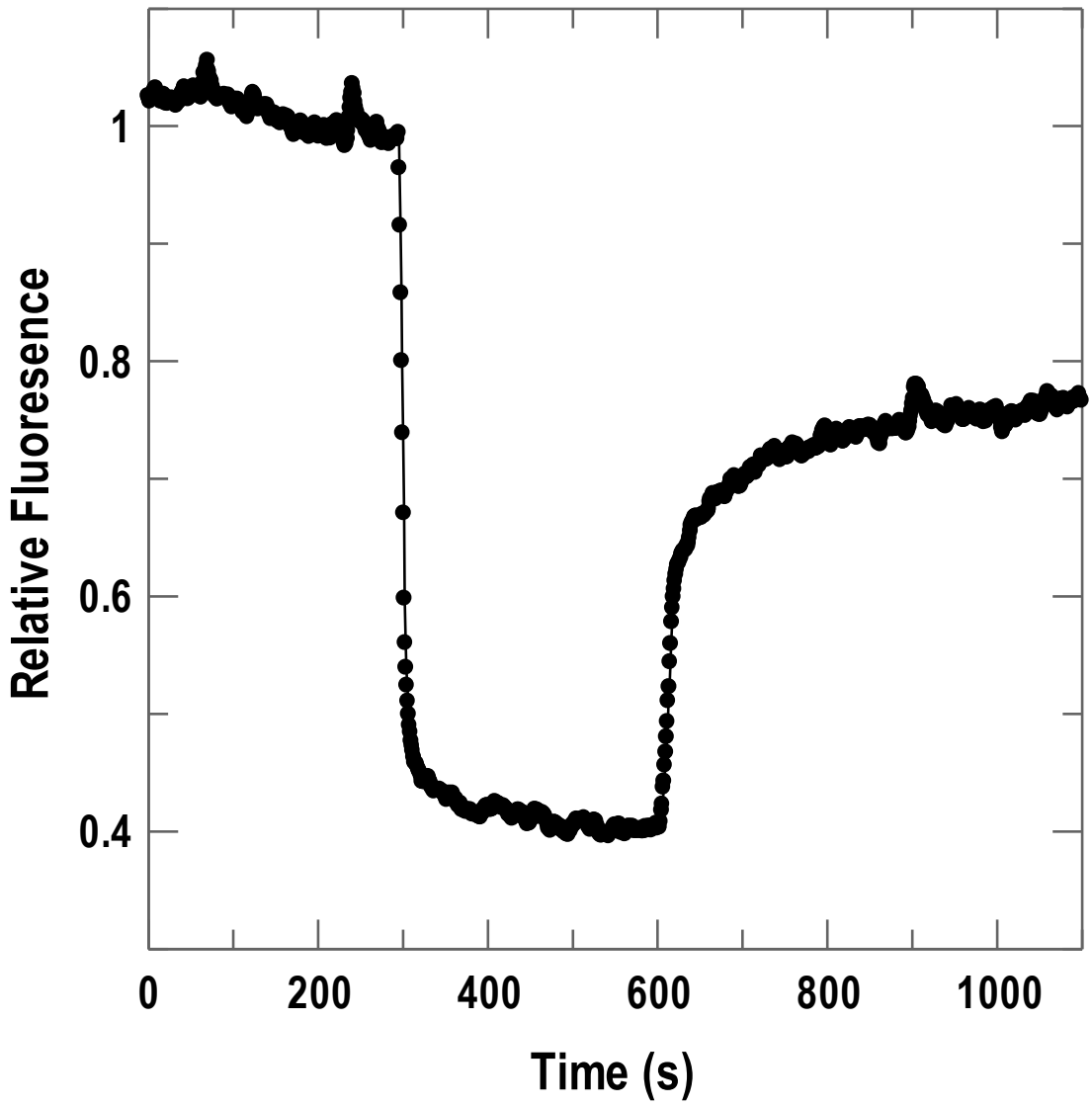

Figure 3-16: Heme Transfer from holo-Hbp2 to apo-IsdC.

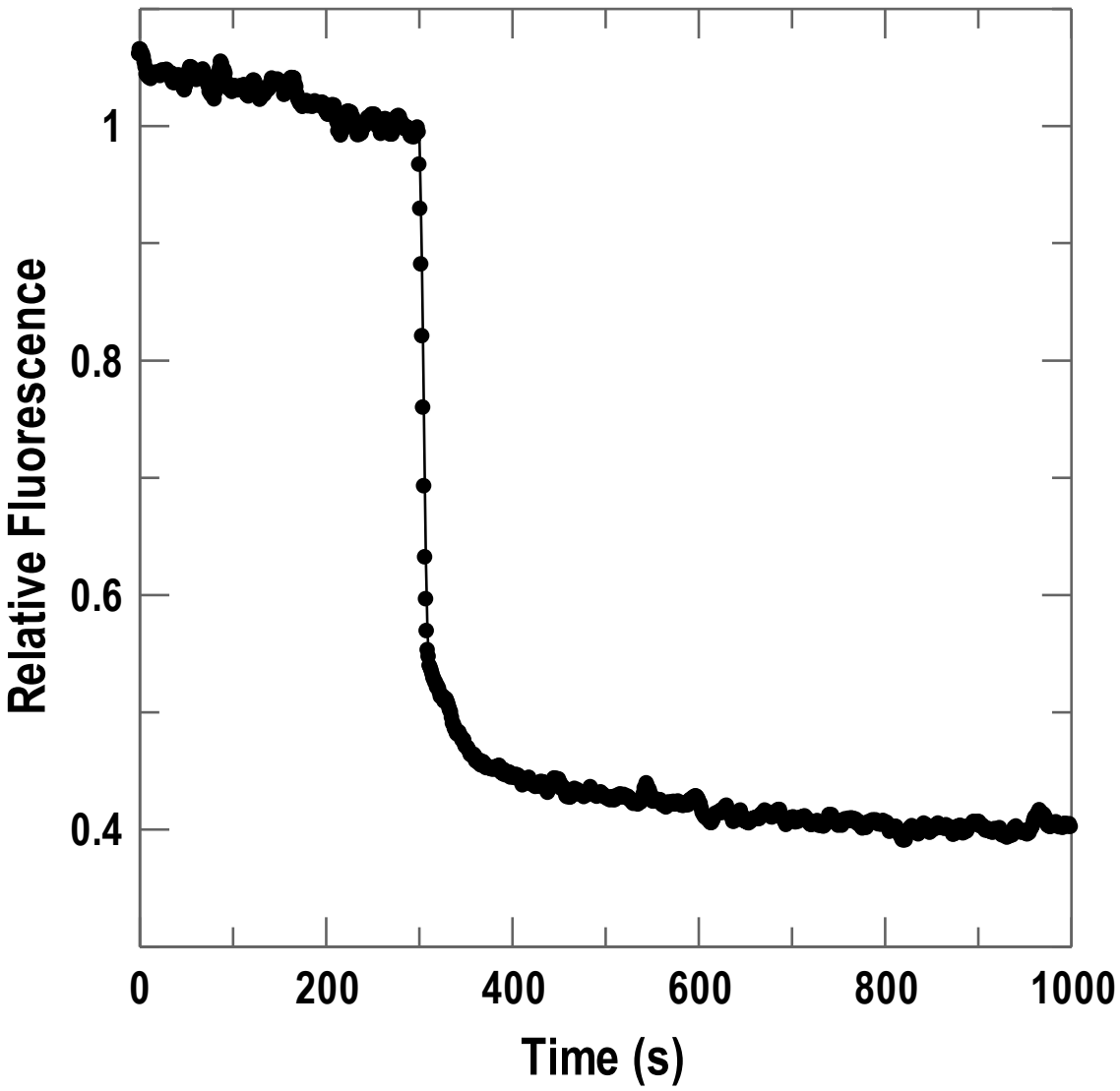

Figure 3-17: Heme Transfer from holo-Hbp2 to apo-IsdB

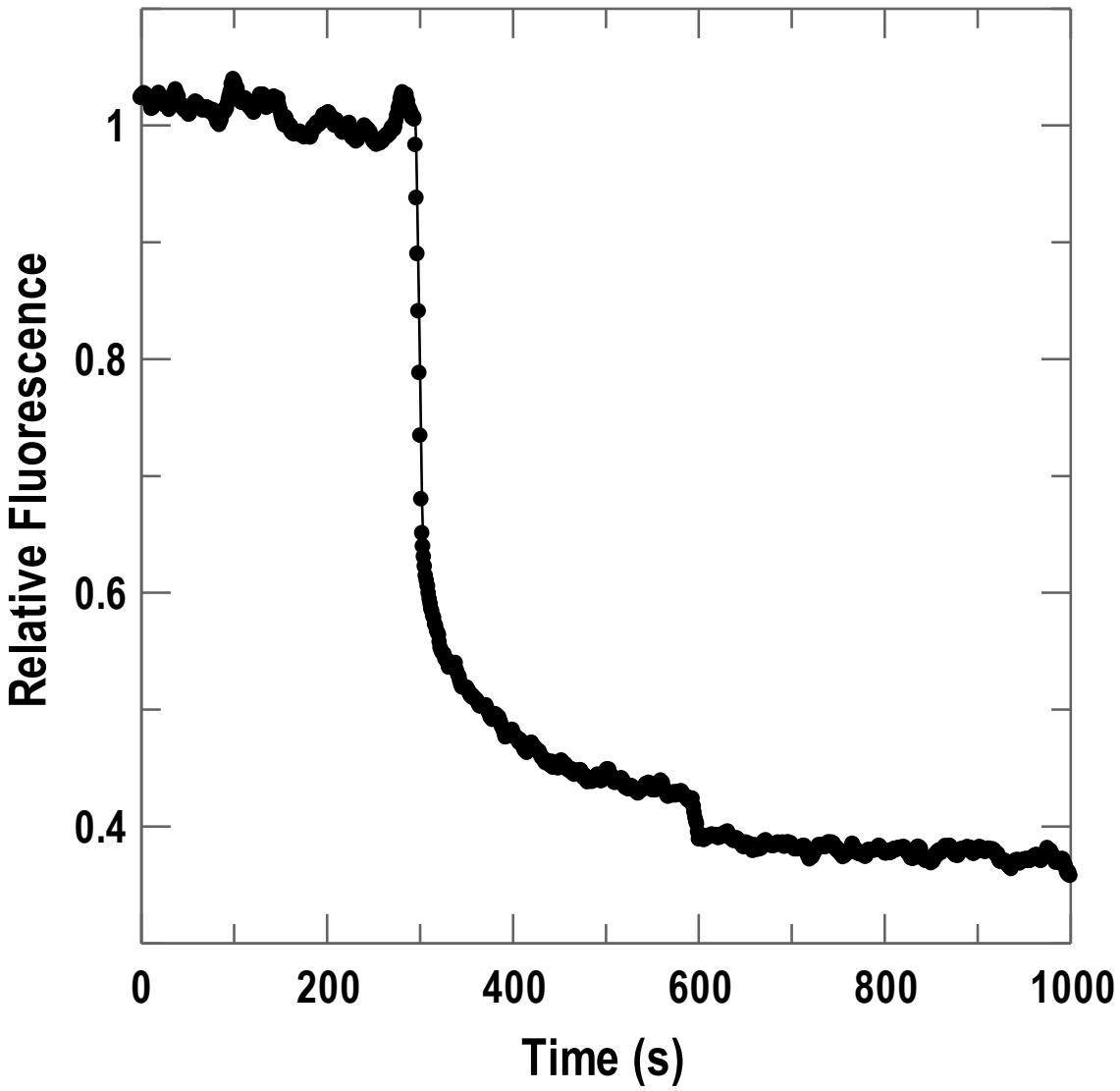

Figure 3-18: Heme Transfer from holo-Hbp2 to apo-IsdH.

3.10 Heme Uptake from Hbp2(S154C) by *B. subtilis*, *L. monocytogenes* and *S. aureus*.

The heme transfer assay was further modified in the pursuit of the development of the Universal Assay. The *L. monocytogenes* sourced coumarin labeled Hbp2(S154C) was used as a sensor protein for detecting heme uptake in *B. subtilis* strain ATCC21332, *L. monocytogenes* strain EGD-e and *S. aureus* Newman strain. An OLIS SLM with an excitation wavelength of 390nm and an emission wavelength of 480nm was used to track heme uptake. The Hbp2(S154C) sensor protein was added to 30nM, producing a fluorescence reading of around 1.0 fluorescence volts, and heme was added at 300 seconds to 15nM (Figure 3-19). Then at 600 seconds, iron starved bacterial cells were added to a final concentration of $0.25OD_{600}$, or $5 \cdot 10^7$ cells/mL. The cells were subsequently incubated for two hours as the fluorescence was tracked. *S. aureus* Newman strain was observed to take up heme at a rate of 0.5 pmoles/10^9 cells/min. *L. monocytogenes* strain EGD-e was observed to take up heme at a rate of 1.0 pmoles/10^9 cells/min. *B. subtilis* was observed to take up heme at a rate of 1.9 pmoles/10^9 cells/min (Figure 3-19). The rate of heme transport in *L. monocytogenes* strain EGD-e was about 20-fold lower than previously measured in Xiao et al, 2011. The discrepancy may be due to the presence of a mutation in the heme source, holo-Hbp2, in addition to a fluorescent tag near the heme binding site.

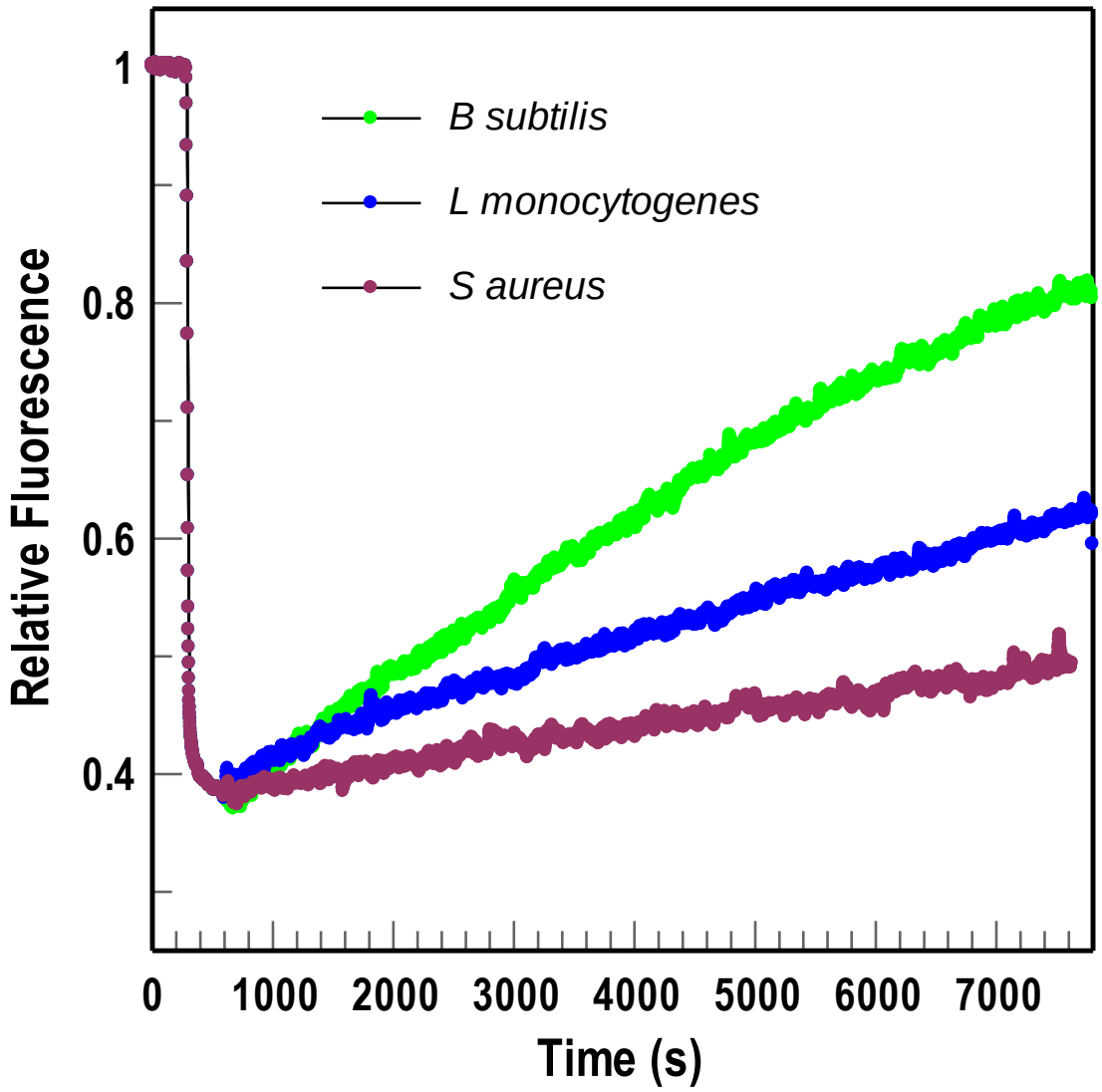

Figure 3-19: Fluorescence recovery during heme uptake in *B. subtilis*, *L. monocytogenes* and *S. aureus*.

Chapter 4 – Concerted Loop Motion Triggers Induced Fit of FepA to Ferric Enterobactin.

Smallwood CR, Jordan L, Trinh V, Schuerch DW, Gala A, Hanson M, Shipelskiy Y, Majumdar A, Newton SMC and Klebba PE. Journal of General Physiology. Volume 144. Issue 1. Pages 71-80. June 2014. Figures reprinted with permission from the Rockefeller University Press. Order License ID: 4230971472764.

4.1 Introduction.

Enzymes affect their catalytic activity by stabilizing a transition state intermediate on the pathway of substrate to product. The substrate and enzyme undergo induced fit, where initial weak interactions drive conformational changes in the enzyme that promote strong binding of the substrate transition state by the enzyme. The concept of induced fit also applies to receptor-ligand and transporter interactions, where conformational changes in the proteins are an inherent part of their function.

Nutrient transport in *E. coli* and other Gram-negative organisms requires passage through two membranes. The E. coli cell envelope consists of a porous outer membrane and an inner membrane separated from the outer membrane by the periplasmic space. The outer membrane contains Outer Membrane Porins (OMPs) which allow passive diffusion of substances smaller than 600Da. Molecules larger than 600Da, or those in concentrations that are too low for passive diffusion require active transport across the outer membrane. However, the outer membrane is incapable of supporting a proton motive force (PMF) due to the presence of OMPs, and high energy molecules are not

present in the periplasmic space, so active transport across the outer membrane is facilitated by an inner membrane complex consisting of the TonB/ExbB/ExbD complex. The TonB-complex transduces the energy of the PMF to the outer membrane. TonB's partners in the outer membrane are β-barrel transporters with an N-terminal plug that prevents passive diffusion, these transporters are called TonB-dependent transporters (TBDT). FepA is a prototypical TBDT which facilitates the uptake of ferric Enterobactin (FeEnt) across the outer membrane.

Transport of FeEnt occurs in two separate steps, the first involves high affinity interaction of FeEnt with the surface loops of FepA, locking FeEnt into a vestibule in the outer membrane protein with conformational changes that form a tight fit between FepA and FeEnt. FeEnt association is proposed to be driven initially by hydrophobic interactions between FeEnt and the aromatic residues in FepA, followed by electrostatic interactions with positively charged amino acids. This first step does not require TonB or a PMF. The second step in the transport process involves the PMF dependent interaction of TonB with FepA that makes an N-terminal portion of FepA called the TonB-box accessible for interaction with TonB and results in the translocation of FeEnt from a vestibule in FepA to the periplasmic space. This second step also includes conformational changes that must first expose the Ton-box and then either unravel or displace FepA's N-terminal plug from the barrel along with the release of FeEnt into the periplasmic space.

To evaluate the conformational changes involved in the outer loops of FepA during the initial step of FeEnt binding, we used site-directed mutagenesis to generate cysteine mutants in seven outer loops of FepA. We labeled these mutants with fluorophore

maleimides and evaluated their degree of labeling, their transport and binding rates and the drop in the fluorescence associated with binding by FeEnt, which we called quenching. The results showed that the different loops closed at different rates, indicating an induced fit model where the individual loops closed around FeEnt in a manner similar to fingers closing around a tennis ball.

4.2 Results

Site-directed Fluorescence Labeling of Cys Substitutions in the Surface Loops of FepA. *E. coli* strains lacking FepA (OKN3) or lacking both FepA and TonB (OKN13) were transformed with plasmids derivatives of pHSG575, which contains the *fepA* gene. Mutant versions of the *fepA* gene were generated with cysteine modifications in the outer loops of FepA, the TonB box, on the periplasmic end of FepA and in the interior of the protein. *E. coli* strains deficient in chromosomal FepA were grown in iron deficient media to express plasmid encoded mutant FepA protein. The cells were labeled with fluorescein maleimide (FM) or Alexa Fluor 546. For the external loops of FepA, 5μM FM at pH 6.7 was sufficient to effectively label these residues within 5 minutes (Figure 4-1). The periplasmic cysteines were unlabeled with Alexa Fluor 546 due to the size exclusion limit of the outer membrane. Additionally, larger concentrations (300 μM) of FM were required to effectively label the periplasmic loops, and residues in the interior of the protein were not labeled with either FM or Alexa Fluor 546. The modifications on the outer loops had identical expression to WT FepA, and bound and transported ferric Enterobactin at similar levels, with some exceptions. When the sites were unmodified with fluorophore, their

transport ability ranged from 40-100% compared to WT FepA, whereas fluorescent modification dropped their transport rates in most cases to 10-90% compared to WT. We evaluated residues in seven loops: L2 (S216C), L3 (S271C), L4 (S322C), L5 (S383C), L7 (S490C), L8 (T550C) and L11 (A698C) to study their motion upon binding and transport of FeEnt. Furthermore, S275C in loop 3 was chosen as a negative control since it labeled with fluorescein but didn't show quenching upon binding of FeEnt (Figure 4-2).

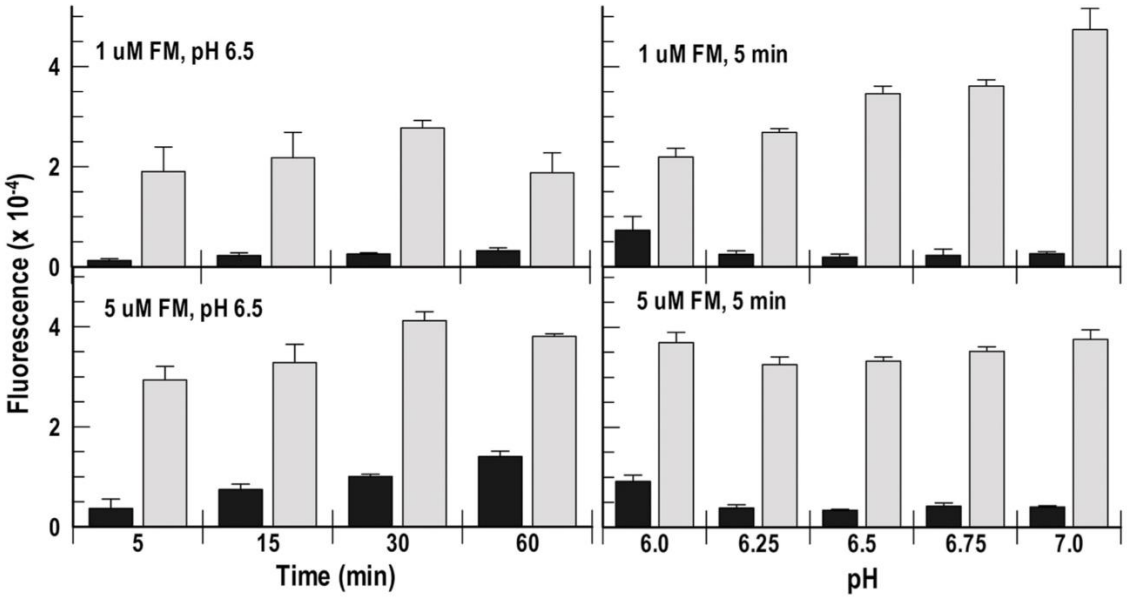

Figure 4-1: Labeling Efficiency of WT and S271C FepA Under Various Time, Concentration and pH Conditions (Smallwood et al, 2014. Figure S1).

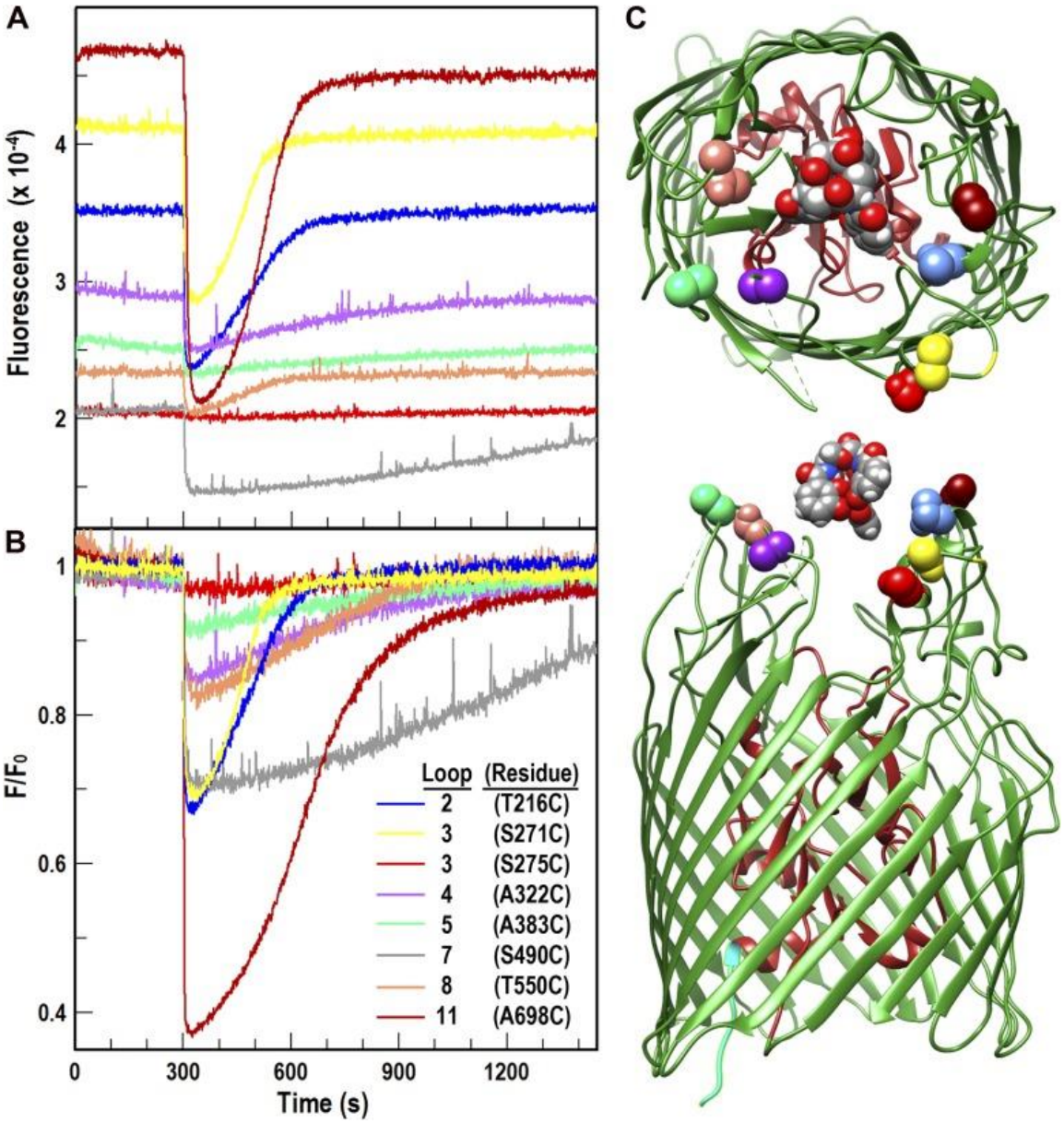

Figure 4-2: Fluorescence Response from FeEnt Binding to FepA with Different Cysteine Mutations (Smallwood et al, 2014. Figure 1).

Loop Motion During FeEnt Binding and Transport by FepA. Binding by FeEnt to fluorescein labeled loops caused a drop in the level of fluorescence. As the bacteria in the solution internalized the fluorescein, it's concentration in the media fell with a concurrent increase in fluorescence intensity. The fluorescence levels of the individual mutants varied based on the electrostatic environment differences corresponding to their location within the FepA protein. The drops in fluorescence associated with FeEnt binding also varied for the different mutants, ranging from 10-60% of the initial fluorescence level. Some of the mutated residues were not effectively labeled with fluorescein and were not further investigated. S275C in loop 3 was fluorescently labeled but did not show any quenching upon FeEnt binding, whereas S271C on the same loop showed quenching to 30% of the original fluorescence level (Figure 4-2). Just as the initial fluorescence levels and quenching upon ligand binding showed variation, the recovery of fluorescence associated with nutrient uptake also showed differences. The half-times for recovery varied from 70 to 700 seconds for the various mutants, with the fastest recovery being observed in S271C and the slowest in S490C. The time of recovery varied with different concentrations of FeEnt, and larger concentrations showed higher quenching with longer times for recovery, in this study 10nM FeEnt was chosen as a good concentration since most mutants could recover to their original fluorescence levels within 10 minutes (Figure 4-2). Recovery was also dependent on TonB as strains lacking this protein showed quenching with no recovery.

Correspondence Between Fluorescence Spectroscopic and Radioisotopic Measurements of FeEnt uptake. The rates of binding and transport for the unlabeled and labeled mutants was evaluated to compare the effects of these modifications. While transport rates can be determined from the fluorescein modified mutants, radioisotopic measurements are the standard approach for determining FeEnt uptake and binding rates, and can determine these parameters for WT FepA and mutated proteins without fluorescent levels. We used the uptake of ^{59}Fe-Ent to determine the effects of cysteine mutations in the different locations, and the effects of fluorescently labeling these mutations. The binding constant K_d remained the same for most mutants as WT (1-3nM) before fluorescein modification. The presence of fluorescein slightly increased the K_d to around 2-6nM, likely due to the inhibitory effect of a 400Da group in an environment important for transporter function. Transport for WT protein showed a rate of around 100pMol/10^9 cells/mL, and the mutations had little effect on transport rate, 10-50% at most for A383C. Treatment with fluorescein generally dropped the transport rate by 10-80% with most residues showing a drop of 70% in transport rate. The fluorometric data supported the radioisotopic findings, showing A383C with a ten-fold inhibition in the uptake rate. S271C and A698C were the fastest at transporting FeEnt according to fluorescent and radioisotopic measurements (Figure 26).

	N domain										C domain								
Location	**TonB-box**		**Periplasm**			**Interior**			**Loops**		**Loops**								**Periplasm**
Residue	**12**	**14**	**30**	**32**	**33**	**54**	**59**	**127**	**63**	**101**	**216**	**271**	**280**	**322**	**383**	**482**	**550**	**698**	**666**
Expression[1]	**100**	100	100	100	100	100	100	60	100	100	100	100	100	100	100	100	100	100	100
Functionality of Cys substitution mutants before fluoresceination																			
Binding[2]	25	100	100	100	100	60	40	25	40	30	47	88	100	59	82	10	48	100	100
Transport[3]	20	40	100	100	100	100	30	0	20	10	77	84	100	62	45	0	28	100	100
Susceptibility to fluoresceination at 0°C																			
5 μM[4]	50	25	52	44	38	63	45	13	25	100	125	100	35	50	75	38	13	100	50
300 μM[5]	75	ND	90	88	60	ND	ND	ND	ND	ND	ND	100	100	ND	ND	ND	ND	100	75
Susceptibility to fluoresceination at 37°C																			
5 μM[4]	30	10	60	52	20	20	15	20	120	90	80	100	45	120	100	65	70	80	20
300 μM[5]	90	ND	100	100	90	ND	ND	ND	ND	ND	ND	100	100	ND	ND	ND	ND	100	100
Functionality of Cys substitution mutants after fluoresceination																			
Binding[2]	17	83	100	90	83	33	40	7	13	13	43	81	100	21	19	10	67	87	90
Transport[3]	7	53	100	100	100	53	27	0	13	0	37	60	100	19	32	0	26	86	100

Table 4-1: Phenotypes of FepA cysteine mutants (Smallwood et al, 2014. Table S1).

Effects of *ΔtonB* on ligand adsorption to FepA *in vivo*. The fluorescent response from FeEnt binding was tested in *ΔtonB* strains. An initial result, supported by the literature showed a decrease in fluorescent quenching (James et al, 2008). This result suggested a decrease in binding ability in strains lacking the energy transduction ability of TonB. However, upon further investigation, we determined that there is a drop in FepA expression in *ΔtonB* strains, which resulted in greater background fluorescent labeling compared to FepA mutants. Therefore, the difference in labeling and quenching observed in the strains was due to decreased FepA expression (Table 4-2).

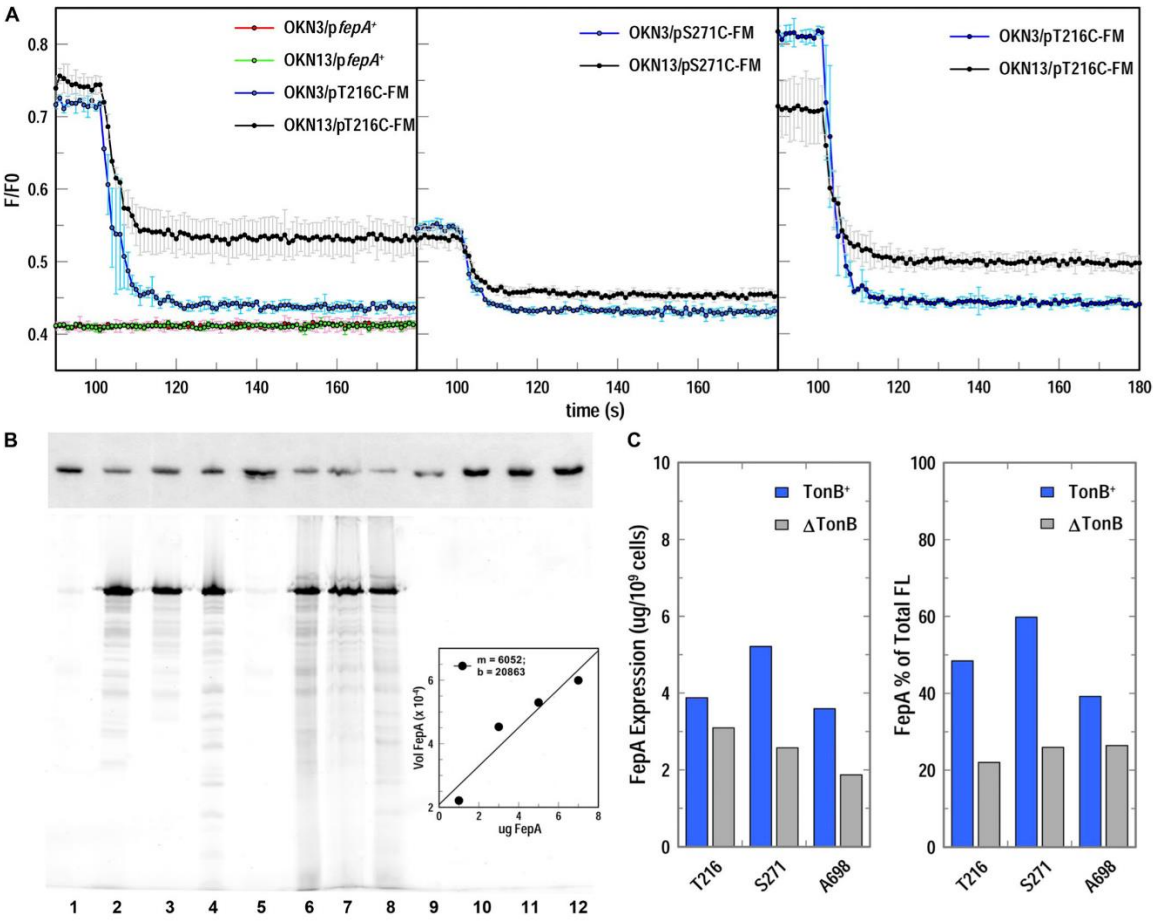

Figure 4-3: Evaluation of FepA Expression and Fluoresceination in Strains Expressing or Lacking TonB (Smallwood et al, 2014. Figure S5).

Rates of FM quenching in different loops of FepA. The rates of quenching were measured in live bacteria using a stopped-flow device. While the binding rate was determined for T216C in loop 2 using live cells, the level of fluorescent labeling was not enough to overcome the scattering from the cells. To overcome this problem, outer membrane fragments were generated by lysing the cells and removing unbroken cells and debris. Using the outer membrane fragments, we determined the kinetics of loop motion during FeEnt binding. Our results showed that FeEnt binding to FepA occurs within about

a second, and this rate is orders of magnitude faster than those previously published in the literature (Payne et al, 1997). Loop 3 (S271C) was found to have the fastest rate of closure, with a half-time of 0.12 seconds, it was also the only loop tested to exhibit a biphasic decay, with the second kinetic phase occurring with a half-time of 2.23 seconds (Table 4-2). The other loops had slower binding kinetics, with loop 11 closing the fastest and loop 4 closing the slowest with half-times of 0.14 seconds and 0.83 seconds respectively (Table 4-2).

Mutant	Loop	k (SE)	$t_{1/2}$	Rank
		s^{-1}	s	
T216[a]	2	1.08 (0.08)	0.64	7
T216	2	1.73 (0.04)	0.40	4
S271C[b]	3	5.72 (0.81); 0.31 (0.04)	0.12; 2.23	1
A322C	4	0.84 (0.05)	0.83	8
A383C	5	1.64 (0.15)	0.43	5
S490C	7	2.32 (0.13)	0.30	3
T550C	8	1.09 (0.06)	0.64	6
A698C	11	4.90 (0.18)	0.14	2

Table 4-2: Binding Kinetics During FeEnt Binding to Different Loops of FepA (Smallwood et al, 2014. Table 1).

Bulk observations of FeEnt transport in living cells. Previous results in the literature have indicated that FepA occurs in greater abundance than TonB in iron starved cells (Newton et al, 1999; Higgs et al, 2002). Furthermore, microscopic analysis of fluorescent FepA and TonB demonstrated that FepA is present throughout the outer membrane, whereas TonB appears to be absent from the poles at the inner membrane, showing unique localization for bacterial cells (Jordan et al, 2013). We used fluorescence microscopy to test if polar localized FepA could take up FeEnt. We transformed the OKN13 strain (lacking chromosomal FepA and TonB) with a GFP-TonB fusion and FepA(S271C) which we labeled with Alexa Fluor 546. As with our previous results, we found a lack of TonB fluorescent signal at the poles, and a lack of quenching of the GFP signal upon exposure to FeEnt, as expected. The fluorescent microscopy results showed quenching in the FepA Alexa Fluor 546 signal, followed by a recovery of fluorescence (Figure 4-3). The fluorescence recovered throughout the cell, even at the poles, posing a paradox, where TonB is absent at the poles, but the cells are still able to take up FeEnt bound to FepA in the polar regions.

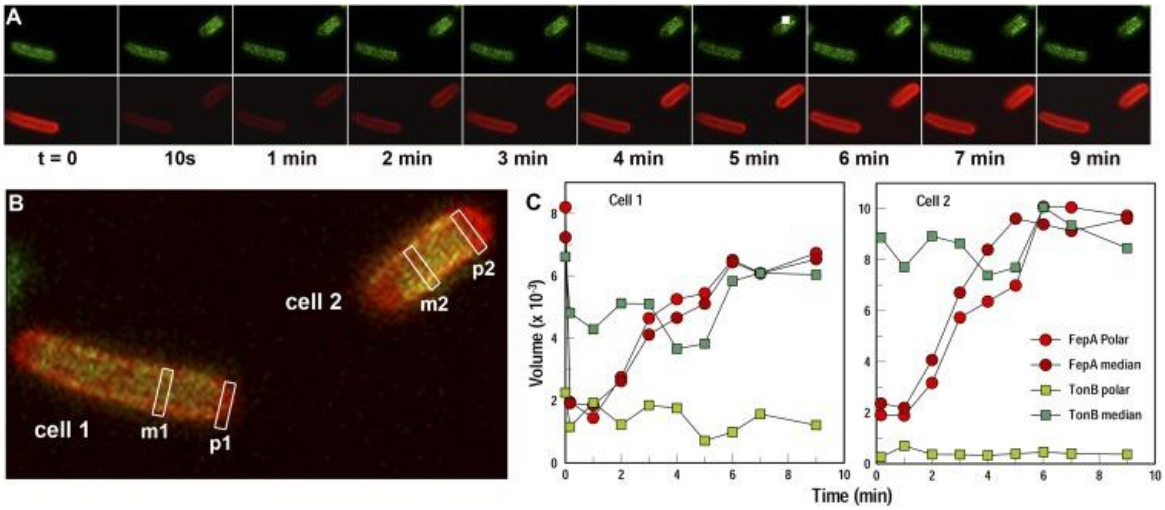

Figure 4-4: Fluorescent Microscopy of GFP-TonB and FepA(S271C) Labeled with Alexa Fluor 546 upon FeEnt Binding (Smallwood et al, 2014. Figure 3).

My personal contributions to Smallwood et al, 2014 include growing up cells expressing mutations in the loops of FepA, labeling those cells and determining the quenching and recovery associated with FeEnt binding in the different mutants (Figure 1 in Smallwood et al, 2014). I also tested the quenching and recovery levels under various concentrations of FeEnt, as seen in Figure S2.

Chapter 5 – High-Throughput Screening Assay for Inhibitors of TonB-Dependent Iron Transport.

Hanson M, Jordan LD, Shipelskiy Y, Newton SMC and Klebba PE. Journal of Biomolecular Screening (Renamed to SLAS Discovery). Volume 21. Issue 3. Pages 316-322. March 2016. Figures reprinted under cleared permission from SAGE Publishing.

5.1 Introduction

Iron is important for bacteria due to its role in the electron transport chain, metabolism and other processes. A common strategy for Gram-negative bacterial acquisition of iron involves active transport across the outer membrane using the TonB/ExbB/ExbD complex to transduce energy from the IM proton motive force. The outer membrane lacks its own PMF and ATP, NADH or other high energy compounds are not found in the periplasm of Gram-negative bacteria. To acquire iron, Gram-negative bacteria secrete siderophores, which bind iron with high affinity and allow the uptake of the iron-siderophore complex using outer membrane transporters called TonB-dependent transporters (TBDTs). FepA is a prototypical TBDT which can bind ferric Enterobactin (FeEnt), the siderophore with the highest known binding affinity for iron ($K = 10^{52}$ M^{-1}). Once FeEnt is bound to FepA, TonB interacts with FepA via a conserved portion of FepA's N-terminus called the TonB box, allowing FeEnt to enter the periplasm, where FeEnt is bound by FepB then subsequently transported into the cytoplasm using the ABC transporter FepCDG. If TonB is deleted or its function is inhibited through the

depletion of the PMF across the inner membrane, then FeEnt remains attached to FepA, but it can't be transported into the periplasm.

Utilizing this uptake system, we have devised a spectrofluorimetric approach for monitoring iron uptake by *E. coli in vivo*, that was optimized for high-throughput screening (HTS). This method involves modifying key residues in FepA to cysteines, and then labeling live cells with mutant FepA using fluorescein maleimide. The mutations must not inhibit function of the TBDT, and must show high levels of fluorescence drop (quenching) upon binding by FeEnt. A good mutant in this regard was determined to be FepA(S271C). After fluorescence quenching upon FeEnt binding to FepA(S271C), the iron-starved bacteria internalized the FeEnt and depleted it from the media, resulting in a fluorescence rebound that we called "recovery". Using this S271C mutant, we tested *E. coli* ability to take up FeEnt under various conditions and expanded this approach for use in a 96-well plate microtiter format. Additionally, we tested a few common energy poisons (CCCP, DNP, cyanide, azide and arsenate) to test the sensitivity of the *E. coli* TonB system, to collect Z-factors that indicated that the fluorescence responses and subsequent recovery were significant.

5.2 Results

Fluorescence Spectroscopic Measurement of TonB-Dependent Transport. The TonB dependent outer membrane transporter for ferric Enterobactin was mutated to allow conjugation to fluorescein maleimide, rendering the protein fluorescent. Upon binding FeEnt, the loops in FepA close around the siderophore and quench the fluorescent

signal observed in the unbound protein. When tested in a cuvette, live cells can consume the ferric Enterobactin substrate from the media, resulting in a recovery of fluorescence. Whereas inhibition of the TonB-process using energy poisons results in fluorescence quenching with no subsequent recovery of the signal, allowing this assay to function as a reporter of TonB activity (Figure 30-A). By taking fluorescent readings before FeEnt addition, immediately following FeEnt addition and after an incubation period, allows the assay to be used in a HTS assay for TonB inhibitors. The dose dependence of the fluorescent response to the addition of FeEnt was tested using 1, 2, 4, 8, 16 and 32nM FeEnt and both 16 and 32nM FeEnt showed maximum quenching of the fluorescent signal. Adding smaller amounts of FeEnt allowed visible recovery within eight minutes, with 16nM FeEnt just starting to show recovery by eight minutes, whereas recovery from 2 or 4nM was almost complete within four minutes (Figure 30-B).

Fluorescence Measurements in Microtiter Format. Using data obtained from cuvette based spectrofluorometric analysis, we set up a microtiter plate analysis of the FeEnt uptake assay. The microtiter assay utilized 200nM FeEnt in 200uL wells with reads taken over two hours. Different concentrations of cells ranging from 2.5 x 10^7 to 0.07 x 10^7 were tested for their ability to take up 200nM FeEnt over the time course. The fluorescence signal was lower when smaller concentrations of cells were used, as expected, and larger concentrations of cells recovered FeEnt quickly, within 50 minutes, whereas lower concentration of cells had minimal fluorescence recovery within the two-hour assay. (Figure 30-C).

Bacterial Viability, Reproducibility, and Optimization of Cell and FeEnt Concentration. Due to the time constraints, inherent in high throughput screening, we tested the bacteria for their ability to take up FeEnt after storage on ice. We resuspended bacteria to a final concentration of 1 x 10^7 cells/mL in PBS with glucose after storing them on ice for 0, 1, 3, 5, and 9 hours. After measuring initial fluorescence, FeEnt was added to a concentration of 20nM and fluorescence was tracked for eight minutes (Figure 31-A). The cells showed similar levels fluorescence levels after storage on ice, similar levels of quenching, about 40% of the initial fluorescent signal, and similar rates of FeEnt uptake, despite storage on ice for up to 9 hours, showing good cell durability and assay stability. Subsequently, the same cells were stored on ice for 11 hours and their fluorescence levels and their ability to take up FeEnt was tested in the presence and absence of the energy uncoupler carbonyl cyanide m-chlorophenylhydrazone (CCCP). When FeEnt was not added to the cells, there was a minimal drop in fluorescence, upon addition of 10nM FeEnt there was a significant drop in fluorescence with a subsequent recovery of the signal, and in the presence of CCCP, addition of FeEnt caused a drop in the fluorescence with no subsequent recovery (Figure 5-1B). The Z-factors were calculated using the conditions in Figure 5-1B as positive and negative controls and were found to be near 1, which suggested a good assay for HTS (Figure 5-2C). Z-factors were additionally above 0.5 for cell concentrations between 5 x 10^5 to 5 x 10^6 (Figure 5-2D).

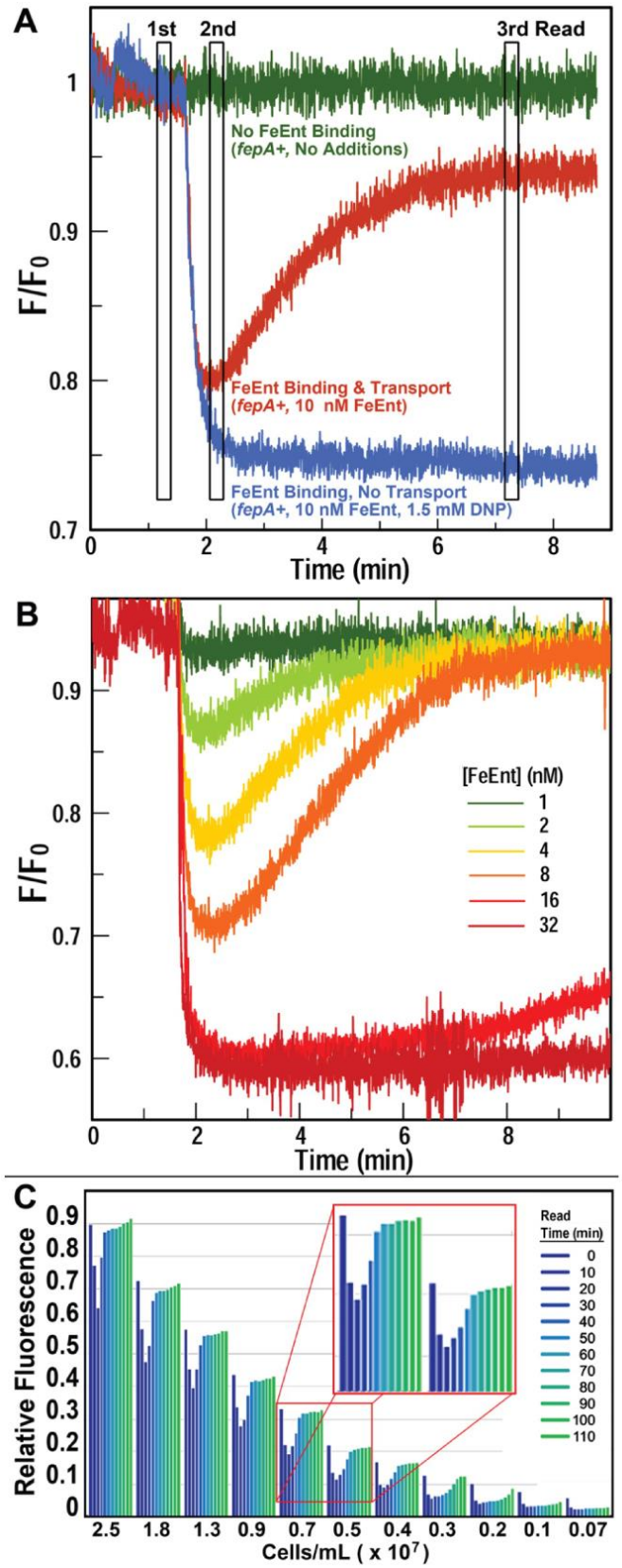

Figure 5-1: Fluorescence Quenching and Recovery from Ferric-enterobactin Binding to FepA (Hanson et al, 2016. Figure 1).

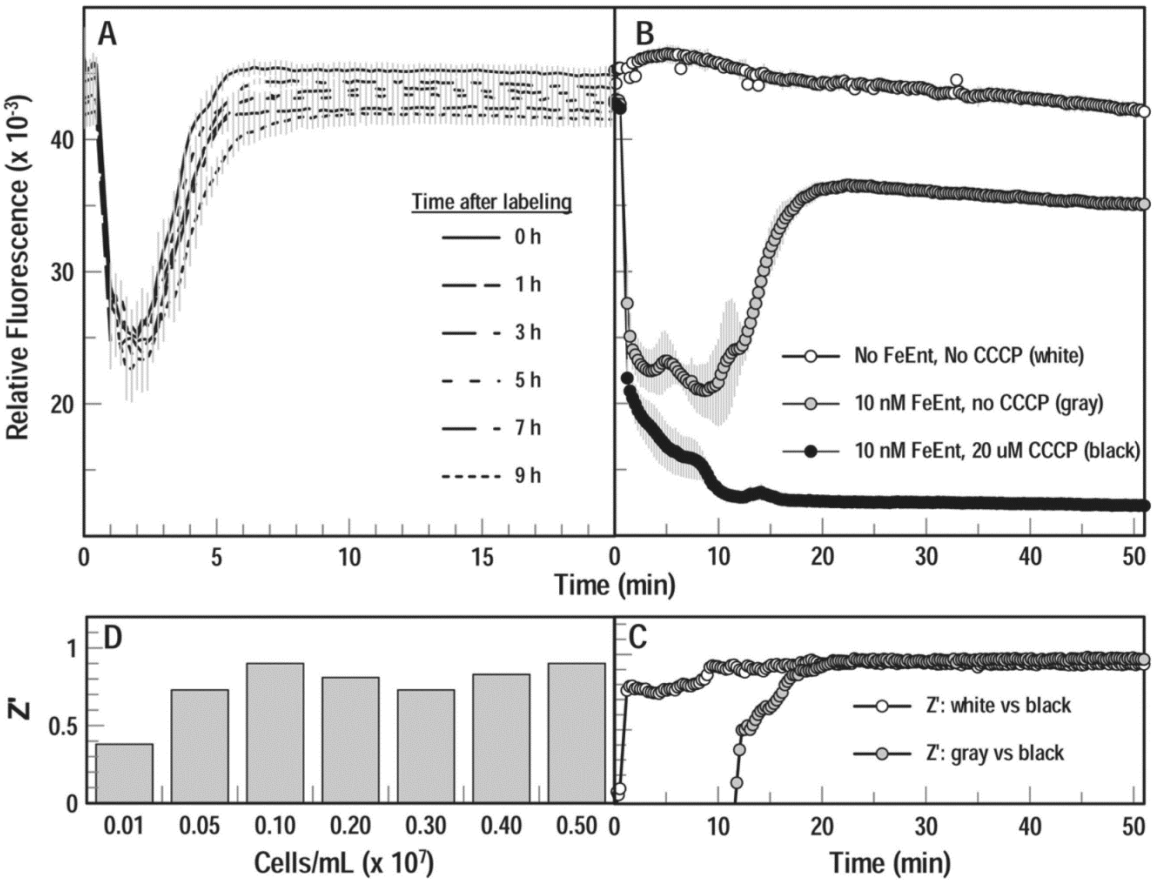

Figure 5-2: Evaluation of *E. coli* Ability to Take up FeEnt after Storage on Ice and Z-factor Analysis of the Microtiter Assay (Hanson et al, 2016. Figure 2).

Effects of Inhibitors. We studied the effects of various energy poisons on the ability of *E. coli* to take up FeEnt in our assay using cuvette-based spectrofluorimetric analysis. Different concentrations of inhibitors were tested for their ability to inhibit FeEnt uptake (Figure 2-11), and the concentrations resulting in 50% and 100% uptake inhibition over ten minutes were noted. Of the energy inhibitors tested, CCCP was the most effective at stopping fluorescence recovery, with a functional concentration of 5-10uM. DNP inhibited uptake at .75-1.5mM, cyanide was inhibitory at 3-9mM, azide at 9-18mM

and arsenate was the least effective, requiring final concentrations of 90-180mM to inhibit TonB-dependent FeEnt uptake (Table 5-1). CCCP and DNP are energy uncouplers, cyanide and azide are inhibitors of electron transport and arsenate is a phosphate analogue that inhibits ATP dependent processes. The effectiveness of the energy poisons at inhibiting TonB-dependent uptake was related to how effectively they could deplete the PMF across the inner membrane of the bacterial cells.

	Concentration (mM)	
Compound	50% Inhibition	100% Inhibition
CCCP	0.005	0.01
DNP	0.75	1.5
Cyanide	2–3	9
Azide	9	18
Arsenate	90	180

The 50% inhibitory values represent the final concentration of the test compound that allowed 50% recovery of fluorescence during the uptake time course; at the 100% inhibition level, we did not observe recovery of fluorescence.

Table 5-1: Inhibitory Concentrations of Various Energy Poisons for TonB-dependent Reactions (Hanson et al, 2016. Table 1).

My personal contributions to Hanson et al 2016 included the growth and fluorescent labeling of cells for subsequent experiments in cuvette based and microtiter assay based experiments. Additionally, I collected results for the IC_{50} and IC_{100} inhibition levels for the different energy poisons, contributing to the results shown in Table 5-1, or Table 1 in Hanson et al 2016.

Chapter 6 – TonB-Dependent Heme/Hemoglobin Utilization by *Caulobacter crescentus* HutA.

Balhesteros H, Shipelskiy Y, Long NJ, Majumdar A, Katz BB, Santos NM, Leaden L, Newton SMC, Marques MV and Klebba PE. Journal of Bacteriology. Volume 199. Issue 6. Page e00723-16. March 2017. Figures reprinted with permission from the American Society for Microbiology.

http://journals.asm.org/site/misc/ASM_Author_Statement.xhtml

6.1 Introduction

Caulobacter crescentus is a Gram-negative alphaproteobacterium commonly found in fresh water and streams. The organism is a model for cellular differentiation since it divides into a mobile flagellated cell and a stationary stalked cell, which is attached to a biofilm or other surface. We studied strain NA1000 a laboratory derivative of the CB15 WT strain (Evinger & Agabian, 1977). Because the organism is found in fresh-water aquatic environments, it encounters low concentrations of essential nutrients like iron and sugar, and must actively transport them.

C. crescentus requires iron for various proteins important to cellular metabolic processes, particularly oxidoreductases, cytochromes and other hemoproteins. However, iron is limited in water as it oxidizes to insoluble ferric iron and forms ferric hydroxide polymers. Bacteria in general commonly secrete small organic compounds, named siderophores, that can bind iron and make it available for bacterial uptake. Siderophores make a hexacoordinated complex with iron and are actively transported in Gram-negative

organisms across the outer membrane via TonB-dependent transporters. These siderophores are synthesized from amino acids using chromosomally encoded operons for nonribosomal peptide synthetases. Siderophores can be defined by the chemical groups that compose the three binding partners that form the hexacoordinated complex (Figure 1-2). The first such group is composed of the hydroxamates, like asperchromes, ferrichromes, ferrioxamine B and rhodotorulic acid, among others. The second group is composed of the catecholates and includes ferric Enterobactin, the compound with the highest known affinity for iron ($K_d = 10^{-52}$). The last group consists of "mixed" chelates, in which the three chemical groups forming the hexacoordinate are not the same and include combinations of hydroxamate, catecholate and carboxylate groups. This mixed group includes aerobactin, mycobactin and pseudobactin, among others.

While *C. crescentus* lacks recognizable operons for siderophore synthesis, and likely does not synthesize any siderophores, it does have 62 TBDT compared to *E. coli* which has a comparatively modest 8 TBDTs (Table 1). In *E. coli*, the TBDTs are mostly used for iron import, with BtuB facilitating Vitamin B_{12} uptake. Since some of the TBDTs in *C. crescentus* are iron-responsive, it seems that the TonB system is important for iron uptake as well. Indeed, the study found that four TBDT genes: Ccr00028, Ccr 00138, Ccr 02277 and Ccr 03023 are overexpressed in iron limited conditions, and two more: Ccr00210 and Ccr 01196 are overexpressed in iron replete conditions. Other authors have additionally found TonB-dependent uptake of carbohydrates in *C. crescentus* (Neugebauer et al, 2005). Showing that the types of nutrients available for uptake are apparently more diverse in *C. crescentus* than *E. coli*. Additionally, *C. crescentus* has two copies of the TonB

operon, but the functional implication of these separate TonB proteins has not been elucidated. A few possibilities for multiple TonBs with *C. crescentus* could be: (1) The different TonBs can interact with different sets of transporters, (2) both TonB's are synthesized and function to accommodate the large amount of TBDTs or (3) only one is synthesized or is functional.

6.2 Results

Siderophore Nutrition Tests. To analyze the ability of *C. crescentus* to utilize various iron sources, we performed Siderophore Nutrition Tests. The organism was grown in NB supplemented with iron chelators, then transferred to agar plates with iron chelators. Small paper discs were placed on the agar and different iron sources were pipetted onto the paper discs. If the bacteria could use the iron source on the paper disc, there would be a halo of growth around it, a lack of halo indicates that bacteria are unable to use the iron source on the paper disc. In addition to NB, the experiments were performed with PYE and M2 minimal media, but NB gave the best results. At first the iron chelator 2'2 bipyridyl (200uM) was used to make iron inaccessible, but bipyridyl has the drawback of chelating other cations like Calcium. After an initial round of screening, ferric Enterobactin was identified as a non-utilizable siderophore for *C. crescentus*, which allowed us to use it instead of bipyridyl, as ferric Enterobactin gave similar results as bipyridyl but more reproducible and with sharper halos. In addition to being more specific, Enterobactin has the strongest affinity for iron of any known substance ($K_d = 10^{-52}$), making it a good choice for iron-starving *C. crescentus*. Overall, the results showed

that *C. crescentus* can use a variety of hydroxamate-type siderophores, but not catecholate-type siderophores (Figure 6-1, Table 6-1).

Siderophore nutrition tests with *C. crescentus*. Strain NA1000 was grown in NB to mid-log phase, and 100 μl of the culture was plated on an NB plate in NB top agar containing enterobactin (100 μM). Paper discs were deposited on the surface of the agar, and 10 μl of 50 μM solutions of ferric siderophore complexes were applied to the discs: 1, asperchrome B1; 2, ferrichrome; 3, ferrichrome A; 4, malonichrome; 5, ferrioxamine B; 6, tetraglycyl ferrichrome; 7, rhodotorulate; 8, aerobactin; 9, $FeSO_4$; 10, hemin; 11, hemoglobin (15 μM); 12, dimerum acid; 13, mycobactin; 14, schizokinen; 15, coprogen; 16, vibriobactin; 17, corynebactin; and 18, agrobactin. See Table 1 for a compilation of siderophore nutrition results.

Figure 6-1: Siderophore Nutrition Tests for *C. crescentus* (Balhesteros et al, 2016. Figure 2).

Siderophore (reference[s])	Halo size (cm)
Hydroxamates	
Asperchromes[b] (39)	2.5
Ferrichromes[c] (37)	2.2
Malonichrome[d] (38)	2.3
Coprogen (39)	None
Ferrioxamine B (39)	1.4
Rhodotorulic acid (40)	None
Dimerum acid (52)	0.9
Fusarinines[d] (52)	None
Iron porphyrins	
Hemin	1.4
Hemoglobin	1.5
Catecholates	
Enterobactin (2)	None
Vibriobactin (42)	None
Corynebactin (43, 44)	None
Agrobactin (97)	None
Mixed chelates	
Aerobactin[e] (46)	0.9
Schizokinen (47)	None
Mycobactin (48, 49)	None
Pseudobactin (50)	None
Albomycin (4, 37)	R[f]

[a]Bacteria were grown in NB, and 10^8 cells were poured onto NB plates in NB top agar containing 100 μM enterobactin. Purified ferric complexes of the tabulated siderophores were dissolved or prepared in 10 mM $NaHPO_4$, pH 7. Aliquots of 10 μl of 50 μM solutions of the ferric siderophores (except hemoglobin, which was used at 15 μM) were deposited onto paper discs on the surface of media and the plates were incubated at 30°C overnight, after which we measured the growth halos (in centimeters).
[b]Asperchromes B1, B2, C, and D1 (51).
[c]Ferrichrome, ferrichrome A, ferrichrome C, ferrichrysin, ferricrocin, ferrirhodin, ferrirubin, and tetraglycine ferrichrome (37).
[d]Fusarinine and triacetylfusarinine (52).
[e]Growth halos formed around ferric aerobactin at higher concentrations (e.g., 200 μM).
[f]R, resistant.

Table 6-1: Summary and Quantification of Halos for Siderophore Nutrition Tests with *C. crescentus* (Balhesteros et al, 2016. Table 1).

Growth in Iron deficient media. Different concentrations of bipyridyl and Enterobactin were tested for their ability to inhibit *C. crescentus* growth in NB media. Maximal growth inhibition was achieved for bipyridyl and Enterobactin at concentrations of 200uM and 100uM respectively (Figure 6-2B). Growth in media made iron deficient

with 200uM bipyridyl was noticeably lower within two hours and fell by 70% over 18 hours (Figure 6-2A). Addition of 10uM ferrichrome, a utilizable iron source, to cells starved for iron in NB with Enterobactin showed a recovery in growth to the level of cells grown in regular NB media (Figure 6-2C). The addition of 10uM ferrichrome to NA1000 grown in NB with bipyridyl failed to show recovery as was observed with Enterobactin, indicating that the inhibitory effects of bipyridyl extend to the limitation of cations in the media apart from iron.

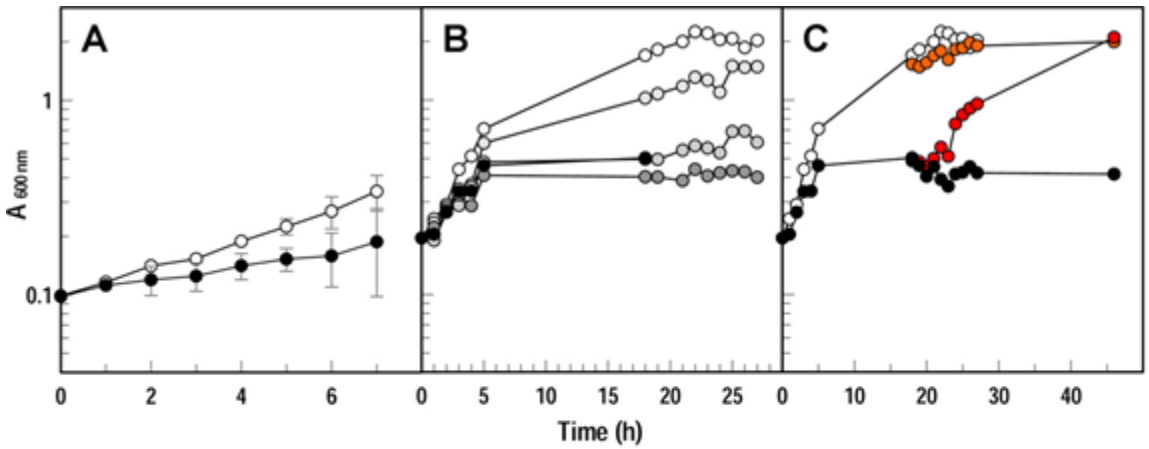

Growth of *C. crescentus* NA1000 in iron-deficient media. (A) Growth in NB (○) or NB containing 200 μM BP (●). Data points are means from two experiments; bars show the standard deviations. (B) Concentration dependence of inhibition by BP. White circles show growth in NB; darkening shades of gray circles show the effects of 50, 100, and 200 μM BP, and black circles show the effects of 100 μM enterobactin, added at 5 h. (C) Restoration of growth upon addition of ferrichrome. We added ferrichrome (10 μM) to NA1000 growing in NB (○) or NB plus 100 μM enterobactin (●) (from panel B) at 19 h (orange and red circles), and it restored the original growth rates. We repeated experiments shown in panels B and C several times; the plots represent a single experiment.

Figure 6-2: *C. crescentus* Growth in Iron limiting Conditions and Recovery when Supplemented with Utilizable Iron (Balhesteros et al, 2016. Figure 3).

Radioisotopic Measurements of Iron Binding and Transport. Nutrition tests indicated that *C. crescentus* NA1000 can take up many ferric hydroxamates (Figure 6-1). To verify and quantify this observation, the binding and transport of radiolabeled [^{59}Fe]-ferrichrome was evaluated. The K_m (0.03nM) and V_{max} (19pmol/min/10^9 cells) values were

determined for NA1000 uptake of [^{59}Fe]-ferrichrome (Figure 36-A/B). These values were found to be similar to those seen in *E. coli*, where strain AN193 with plasmid encoded FhuA was found to take up [^{59}Fe]-ferrichrome with a K_m = 0.6nM and V_{max} = 87nM (Scott et al, 2001). Furthermore, the strains ability to transport ferric citrate was tested using radioisotopic measurement (Figure 6-3C/D). Ferric citrate uptake couldn't be determined using siderophore nutrition tests as both Enterobactin and bipyridyl, the chelating agents used in the assay, can remove the ferric iron cation complexed by citrate. The binding and transport rates for ^{59}Fe-citrate had a K_m = 5nM and V_{max} = 29pmol/min/10^9 Compared to [^{59}Fe]-ferrichrome, NA1000 transported ^{59}Fe-citrate with a higher rate, but the K_m was two orders of magnitude higher, indicating higher affinity for [^{59}Fe]-ferrichrome. Depleting the proton motive force using the energy poison *m*-chlorophenyl hydrazine (CCCP) significantly inhibited transport of ^{59}Fe-citrate, indicating that transport of ferric-citrate was utilizing TonB-dependent transporters (Figure 6-3D).

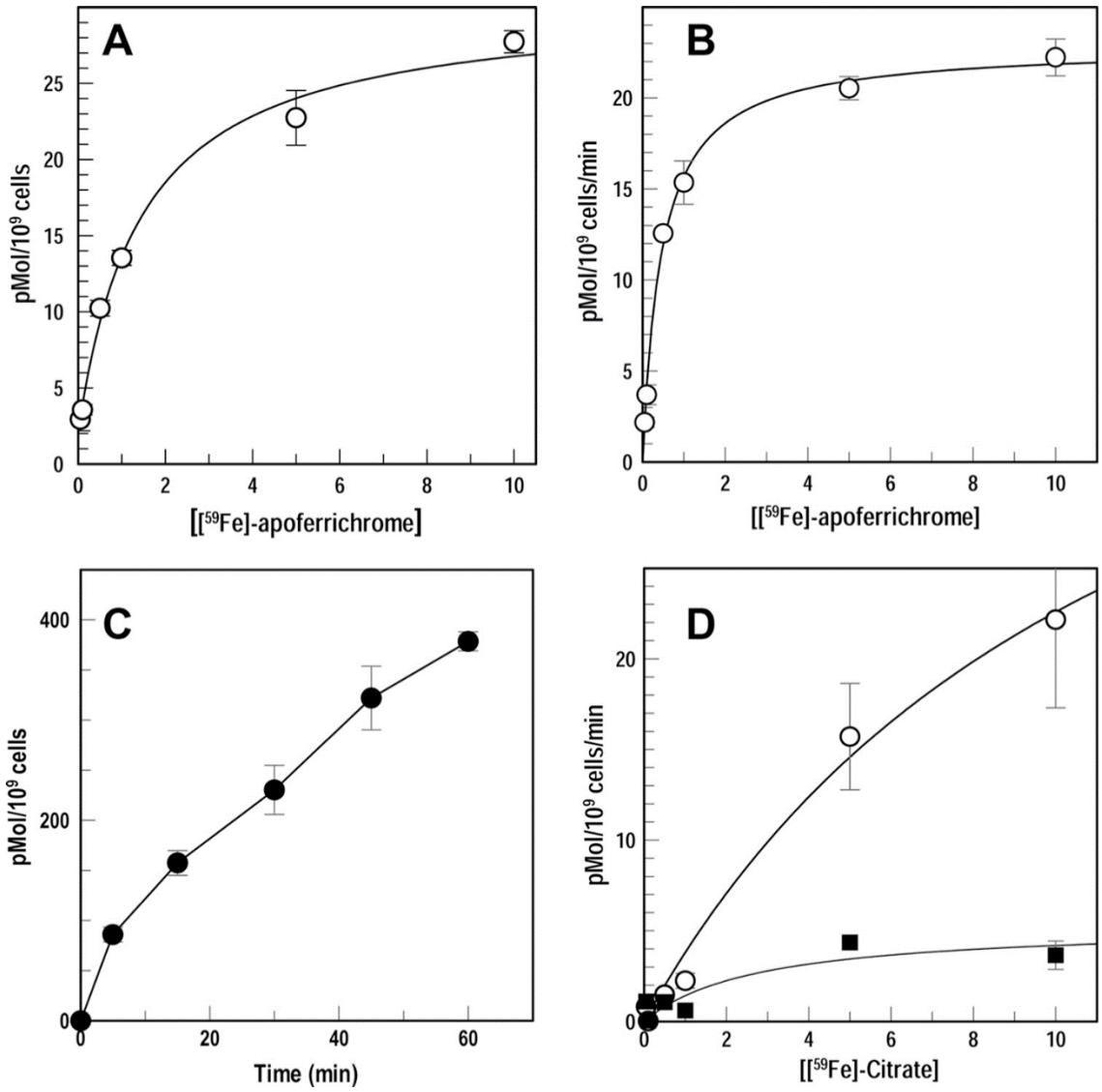

Figure 6-3: Binding and Transport of Radiolabeled Ferrichrome and Ferric-citrate (Balhesteros et al, 2016. Figure 4).

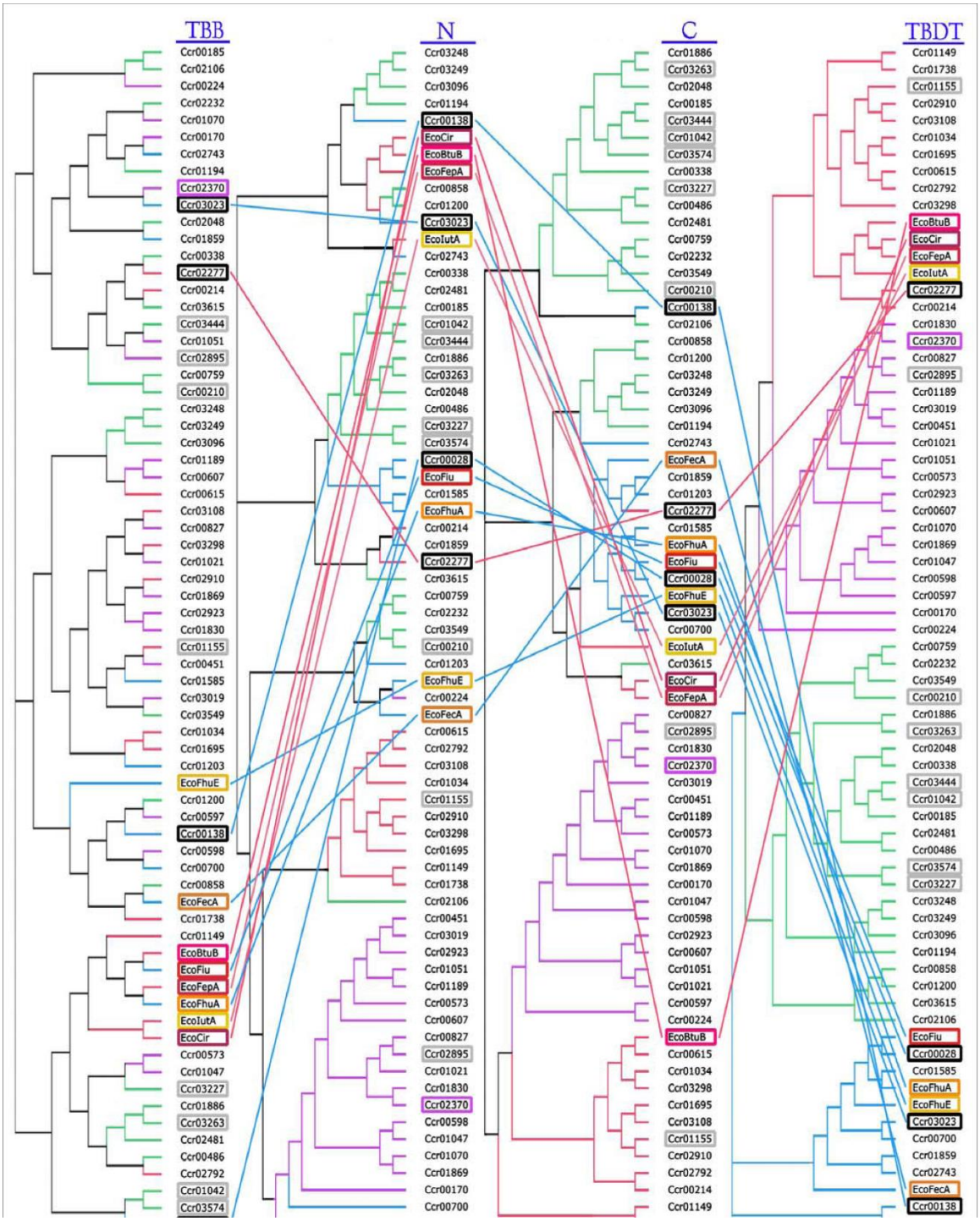

Figure 6-4: Phylogenetic Analysis of TBDTs from *E. coli* and *C. crescentus* (Balhesteros et al, 2016. Figure S2).

Identification of Potential Iron Transporters: The TBDT sequences of *E. coli* and *C. crescentus* were compared using a CLUSTALW2 alignment. Alignment was evaluated

using either the entire TBDT, the TonB-box (TBB) of the TBDT, the N-terminal "plug" domain and the C-terminal β-barrel domain. Based on the full-length TBDT, the transporters clustered into four branches which were colored magenta, purple, green and blue (Figure 6-4). *E. coli* TBDTs separated into two branches, with BtuB, Cir, FepA and IutA in the magenta branch, and Fiu, FhuA, FhuE and FecA separating into the blue branch. When aligned solely by their C-terminal β-barrel domains, seven *E. coli* C-termini clustered together and BtuB was in a separate group. The four TBDTs in *C. crescentus* that are negatively iron regulated include Ccr00028, Ccr00138, Ccr02277, Ccr03023 and each of these clustered with *E. coli* TBDTs. Ccr02277 clustered in the magenta branch along with BtuB, Cir, FepA and IutA, and Ccr00028, Ccr00138 and Ccr03023 clustered in the blue branch along with Fiu, FhuA, FhuE and FecA.

Iron Regulated Cell Envelope Proteins: To further characterize and quantify TBDTs in *C. crescentus*, separation of the NA1000 cell envelope into outer membranes and inner membranes was performed using sucrose gradients and sarkosyl extraction. NA1000 was grown up in NB and $FeSO_4$ was added to 50uM to simulate iron-rich conditions or Enterobactin was added to 100nM to simulate iron-starvation at the start of the exponential growth phase of the culture. After around six hours of growth, the cells were pelleted and French pressed. Unlysed cells were removed with a low-speed spin and then the cell envelope was collected with a high-speed spin (100000g). Separation of the cell envelope was not effective with the sucrose gradient as the same proteins were observed in different parts of the gradient (Figure 6-5B). Sarkosyl extraction was performed initially

with 0.5% sarkosyl, and resulted in a better separation than with sucrose gradients, but some proteins were still observed in both the inner and outer membrane fractions (Figure 6-5A). Considering that a 0.5% sarkosyl extraction for Gram-negative organisms, like *E. coli*, is considered standard, I hypothesized that the free-living *C. crescentus* encounters a more dilute and less noxious (from the view of the bacteria) environment in fresh-water lakes than the human digestive system, and therefore it's outer membrane might solubilize at lower concentrations of detergents like sarkosyl. When I repeated the sarkosyl extraction using 0.1% sarkosyl, I could separate the outer and inner membranes effectively, generating a sarkosyl fractionation typical of *E. coli* with 0.5% sarkosyl (Figure 6-6B).

Following SDS-Page and coomassie staining, bands that were over-expressed in the outer membrane in iron rich and iron-starved conditions were cut out from the gel and subject to mass spec analysis following tryptic digestion. Bands R1 and R2 were overexpressed in iron-rich conditions and were identified as Ccr00210 and Ccr01196, respectively. Ccr00210 has an estimated mass of 85,581Da and Ccr01196 had an estimated mass of 69,198Da, and these masses matched their migration by SDS-Page gel. Ccr01196 was previously characterized as an outer membrane virulence protein, and this study identified Ccr01196 as a TBDT for the first time. Bands B1, B2 and B3 were overexpressed in iron-starved conditions, and were identified as Ccr00028 (78,234Da), Ccr02277 (75,525Da) and Ccr03023 (74,322Da). Ccr02277 exhibited a high level of identity to the *E. coli* citrate TBDT Cir (25%), the *E. coli* ferric Enterobactin TBDT FepA (23%) and *E. coli* cobalamin transporter BtuB (22%). We deleted *ccr02277* from the *C. crescentus*

chromosome and tested the Δ02277 strain using the siderophore nutrition test (Figure 6-7A). The mutant lost the ability to take up iron from heme or hemoglobin, therefore we named *ccr02277* as *hutA* after its heme/hemoglobin utilization deficient phenotype. As expected, the deletion of this gene resulted in a lack of a 75,525Da band as seen in the SDS-PAGE gel (Figure 6-7B).

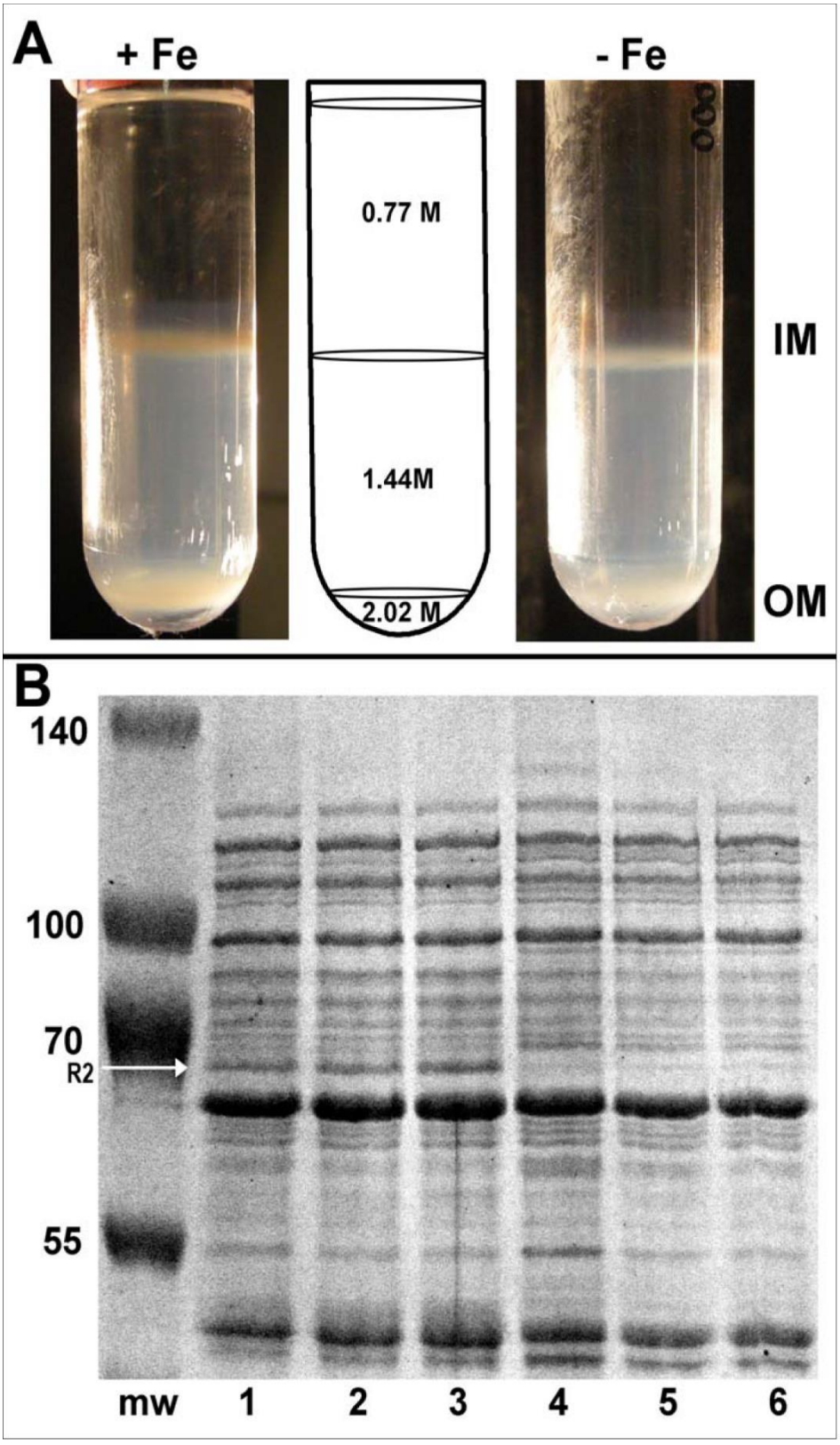

Figure 6-5: Sucrose Gradient Separation of *C. crescentus* Cell Envelope (Balhesteros et al, 2016. Figure S1).

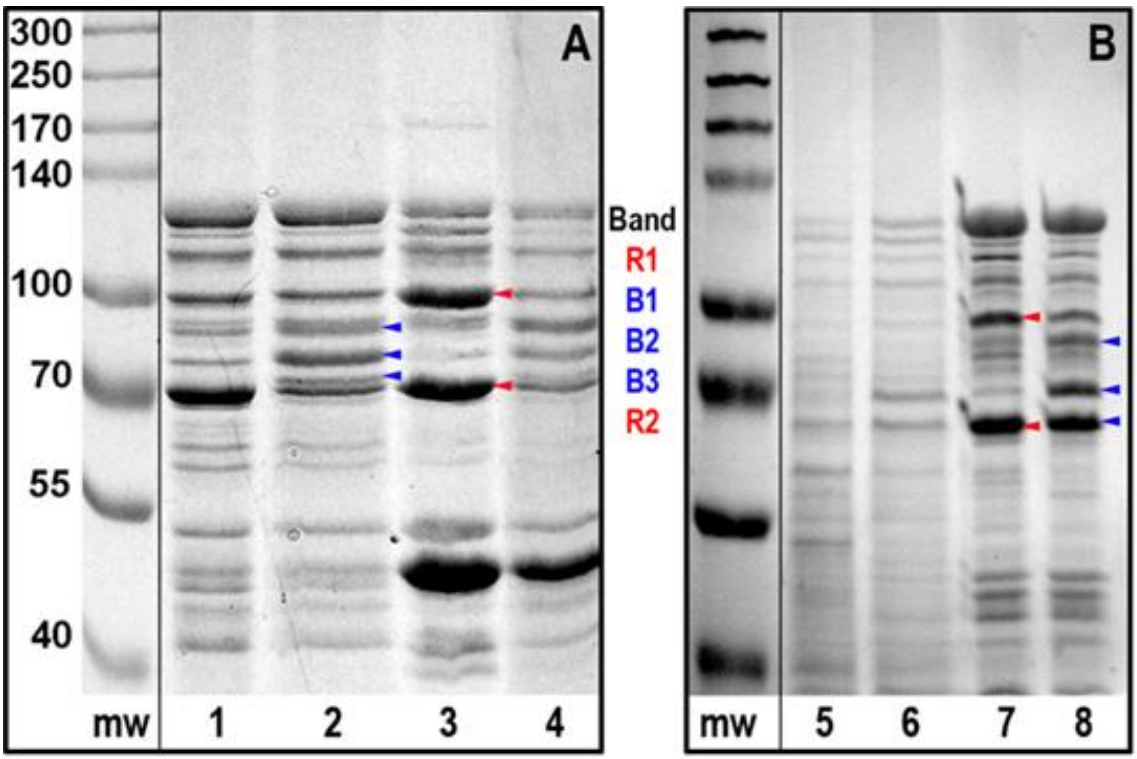

Band	Mass	Coverage (%)	Intensity (%)	Identity
R1	85,581	65.0	66.0	00210
B1	78,234	59.1	51.5	00028
B2	75,525	70.7	48.6	02277
B3	74,322	83.9	50.9	03023
R2	69,198	65.7	15.4	01196

Figure 6-6: Separation of *C. crescentus* Cell Envelope into Inner and Outer Membrane Fractions (Balhesteros et al, 2016. Figure 5).

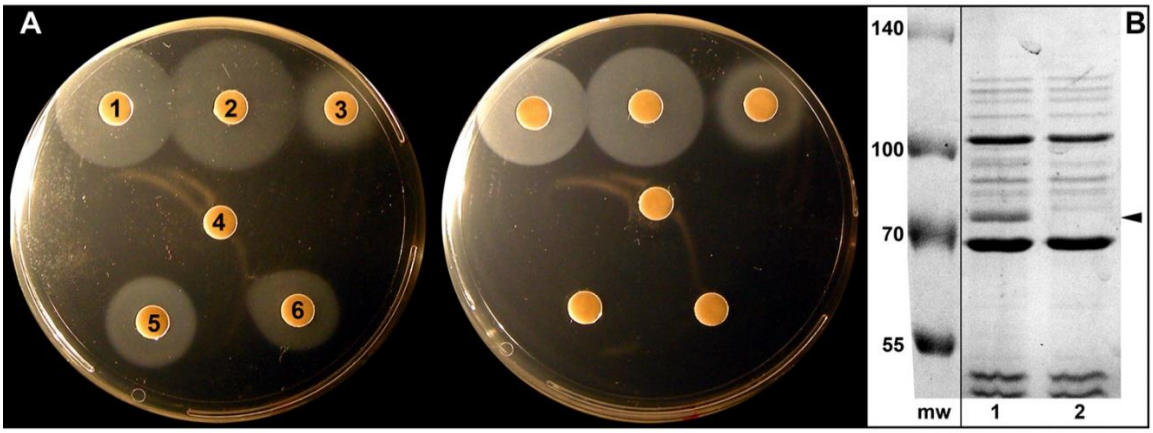

Figure 6-7: Deletion of ccr02277 Shows a Loss of Ability for *C. crescentus* to Produce HutA or Take up Heme (Balhesteros et al, 2016. Figure 6).

My personal contributions to Balhesteros et al 2016 include the lysis of *C. crescentus* and fractionation of the inner and outer membranes from the cell envelope. Methods attempted for separating the two membranes included sucrose gradient, 0.5% sarkosyl extraction and 0.1% sarkosyl extraction. The idea to lower the sarkosyl concentration to achieve more effective membrane separation. Preparing the acrylamide gels and running SDS-PAGE on the samples, and coomassie staining the gels. The work resulted in Figure 6-5 (Figure S1 in the supplemental of the original publication), Figure 29 (Figure 5 in the original publication) and Figure 6-7B (Figure 6-B in the original publication).

References

Allen CE, and Schmitt MP. 2011. Novel Hemin Binding Domains in the *Corynebacterium diphtheriae* HtaA Protein Interact with Hemoglobin and are Critical for Heme Iron Utilization by HtaA. J Bacteriol. **193**(19):5374-5385.

Annamalai R, Jin B, et al. 2004. Recognition of Ferric Catecholates by FepA. J Bacteriol. **186**(11):3578-3589.

Aranda IV R, Worley CE, et al. 2008. Bis-methionyl Coordination in the Crystal Structure of the Heme-Binding Domain of the Streptococcal Cell Surface Protein Shp. J Mol Biol. **374**(2):374-383.

Ascoli F, Fanelli MRR and Antonini E. 1981. Preparation and Properties of Apohemoglobin and Reconstituted Hemoglobins. Methods Enzymol. **76**:72-87.

Asuthkar S, Velineni S, et al. 2007. Expression and Characterization of an Iron-Regulated Hemin-Binding Protein, HbpA, from *Leptospira interrogans* Serovar Lai. Infection and Immunity. **75**(9):4582-4591.

Baichoo N and Helmann JD. 2002. Recognition of DNA by Fur: A Reinterpretation of the Fur Box Consensus Sequence. J Bacteriol. **184**(21):5826-5832.

Baker KR and Postle K. 2013. Mutations in *Escherichia coli* ExbB Transmembrane Domains Identify Scaffolding and Signal Transduction Functions and Exclude Participation in a Proton Pathway. J. Bacteriol. **195**(12):2898-2911.

Balderas MA, Nobles CL, et al. 2012. Hal is a *Bacillus anthracis* Heme Acquisition Protein. J Bacteriol. **194**(20):5513-5521.

Balhesteros H, Shipelskiy Y, et al. 2016. TonB-Dependent Heme/Hemoglobin Utilization by *Caulobacter crescentus* HutA. J Bacteriol. **199**(6): e00723-16.

Bates CS, Montañez GE, et al. 2003. Identification and Characterization of a *Streptococcus pyogenes* Operon Involved in Binding of Hemoproteins and Acquisition of Iron. Infection and Immunity. **71**(3):1042-1055.

Beddek AJ, Sheehan BJ, et al. 2004. Two TonB Systems in *Actinobacillus pleuropneumoniae*: Their Roles in Iron Acquisition and Virulence. Infection and Immunity. **72**(2):701-708.

Bierne H, Garandeau C, et al. 2004. Sortase B, A New Class of Sortase in *Listeria monocytogenes.* J Bacteriol. **186:**1972-1982.

Braun V and Hantke K. 2011. Recent Insights into Iron Import by Bacteria. Current Opinion in Chemical Biology. **15**:328-334.

Braun V, Pramanik A, et al. 2009. Sideromycins: Tools and Antibiotics. Biometals. **22**:3-13.

Bruck S, Personnic N, et al. 2011. Regulated Shift from Helical to Polar Localization of *Listeria monocytogenes* Cell Wall-Anchored Proteins. J Bacteriol. **193**(17):4425-4437.

Buchanan SK, Smith BS, et al. 1999. Crystal Structure of the Outer Membrane Active Transporter FepA from *Escherichia coli*. Nature. **56**(1):56-63.

Cadieux N, Bradbeer C and Kadner RJ. 2000. Sequence Changes in the Ton Box Region of BtuB Affect Transport Activities and Interaction with TonB Protein. J Bacteriol. **182**(21):5954-5961.

Cao Z, Warfel P, Newton SMC and Klebba, PE. 2003. Spectroscopic Observations of Ferric Enterobactin Transport. J Biol Chem. **278**(2):1022-1028.

Cao Z, Qi Zengbiao et al. 2000. Aromatic components of two ferric Enterobactin binding sites in *Escherichia coli* FepA. Molecular Microbiology. **37**(6):1306-1317.

Caux-Thang C, Parent A, et al. 2014. Single Asparagine to Arginine Mutation Allows PerR to Switch from PerR Box to Fur Box. ACS Chemical Biology. **10**:682-686.

Celia H, Noinaj N, et al. 2016. Structural Insight into the Role of the Ton Complex in Energy Transduction. Nature. **538**(7623):60-65.

Chan ACK, Lelj-Garolla B, et al. 2006. Cofacial Heme Binding is Linked to Dimerization by a Bacterial Heme Transport Protein. J Mol Biol. **362**:1108-1119.

Chimento DP, Mohanty AK, Kadner RJ and Wiener MC. 2003. Substrate-Induced Transmembrane Signaling in the Cobalamin Transporter BtuB. Nature Structural Biology. **10**(5):394-401.

Chung CC, Ohwaki K, et al. 2008. A Fluorescence-Based Thiol Quantification Assay for Ultra-High-Throughput Screening for Inhibitors of Coenzyme A Production. ASSAY and Drug Development Technologies. **6**(3):361-374.

Cobessi D, Meksem A and Brillet K. 2009. Structure of the Heme/Hemoglobin Outer Membrane Receptor ShuA from *Shigella dysenteriae*: Heme Binding by an Induced Fit Mechanism. Proteins. **78**(1):286-294.

da Silva Neto JF, Braz VS, Italiani VCS and Marques MV. 2009. Fur Controls Iron Homeostasis and Oxidative Stress Defense in the Oligotrophic Alpha-Proteobacterium *Caulobacter crescentus*. Nucleic Acids Research. **37**(14):4812-4825.

da Silva Neto JF, Lourenço RF and Marques MV. 2013. Global Transcriptional Response of *Caulobacter crescentus* to iron availability. BMC Genomics. **13**:549

de Lorenzo V, Bindereif A, Paw BH and Neilands JB. 1986. Aerobactin Biosynthesis and Transport Genes of Plasmid ColV-K30 in *Escherichia coli* K-12. J Bacteriol. **165**(2):570-578.

Dickson CF, Jacques DA, et al. 2015. The Structure of Haemoglobin Bound to the Haemoglobin Receptor IsdH from *Staphylococcus aureus* shows disruption of the Native α-globin Haem Pocket. Biological Crystallography. **D71**:1295-1306.

Dixon SD, Janes BK, et al. 2012. Multiple ABC Transporters are Involved in the Acquisition of Petrobactin in *Bacillus anthracis*. Mol Microbiol. **84**(2):370-382.

Drazek ES, Hammack CAS and Schmitt MP. 2000. *Corynebacterium diphtheriae* Genes Required for Acquisition of Iron from Haemin and Haemoglobin are Homologous to ABC Haemin Transporters. Molecular Microbiology. **36**(1):68-84.

Duong T, Park K, et al. 2013. Structural and Functional Characterization of an Isd-Type Haem-Degradation Enzyme from *Listeria monocytogenes*. Acta Crystallogr D Biol Crystallogr. **70**(Pt 3):615-626.

Escolar L, Perez-Martin J and de Lorenzo V. 1998. Binding of the Fur (Ferric Uptake Regulator) Repressor of *Escherichia coli* to Arrays of the GATAAT Sequence. J Mol Biol. **283**(3):537-547.

Evinger M, and Agabian N. 1977. Envelope-Associated Nucleoid from *Caulobacter crescentus* Stalked and Swarmer Cells. J Bacteriol. **132**(1):294-301.

Faulkner MJ, Ma Z, Fuangthong M and Helmann JD. 2012. Depression of the *Bacillus subtilis* PerR Peroxide Stress Response Leads to Iron Deficiency. J. Bacteriol. **194**(5):1226-1235.

Fedhila S, Daou N, Lereclus D and Nielsen-LeRoux C. 2006. Identification of *Bacillus cereus* Internalin and Other Candidate Virulence Genes Specifically Induced During Oral Infection in Insects. Mol. Micro. **62**(2):339-355.

Ferguson AD, Chakraborty R, et al. 2002. Structural Basis of Gating by the Outer Membrane Transporter FecA. Science. **295**:1715-1719.

Fonner BA, Tripet BP, et al. 2014. Solution Structure and Molecular Determinants of Hemoglobin Binding of the First NEAT Domain of IsdB in *Staphylococcus aureus*. Biochemistry. **53:**3922-3933.

Fukushima T, Allred BE and Raymond KN. 2014. Direct Evidence of Iron Uptake by the Gram-positive Siderophore-Shuttle Mechanism without Iron Reduction. ACS Chemical Biology. **9**(9):2092-2100.

Fusco WG, Coudhary NR, et al. 2013. Mutational Analysis of Hemoglobin Binding and Heme Utilization by a Bacterial Hemoglobin Receptor. J Bacteriol. **195**(13):3115-3123.

Gaspar AH, Marraffini LA, et al. 2005. *Bacillus anthracis* Sortase A Anchors LPXTG Motif-Containing Surface Proteins to the Cell Wall Envelope. J. Bacteriol. **187**(13):4646-4655.

Grandchamp GM, Caro L and Shank EA. 2017. Pirated Siderophores Promote Sporulation in *Bacillus subtilis*. Applied and Environmental Microbiology. **83**(10):e03293-16.

Gresock MG and Postle K. 2017. Going Outside the TonB Box: Identification of Novel FepA-TonB Interactions *In Vivo*. J Bacteriol. **199**(10): e00649-16.

Grigg JC, Cheung J, Heinrichs DE and Murphy MEP. 2010. Specificity of Staphyloferrin B Recognition by the SirA Receptor from *Staphylococcus aureus*. J Biol Chem. **285**(45):34579-34588.

Grigg JC, Ukpabi G, Gaudin CFM and Murphy MEP. 2010. Structural Biology of Heme Binding in the *Staphylococcus aureus* Isd system. J. Inorganic Biochemistry. **104**:341-348.

Hagan EC and Mobley HLT. 2009. Heme Acquisition is Facilitated by a Novel Receptor Hma and Required by Uropathogenic *Escherichia coli* for Kidney Infection. Mol Microbiol. **71**(1):79-91.

Hanahan D. 1983. Studies on Transformation of *Escherichia coli* with Plasmids. J Mol Biol. **166**:557-580.

Hanks TS, Liu M, McClure MJ and Lei B. 2005. ABC Transporter FTSABCD of *Streptococcus pyogenes* Mediates Uptake of Ferric Ferrichrome. BMC Microbiology. **5**:62.

Hanson M, Jordan LD, et al. 2016. High-Throughput Screening Assay for Inhibitors of TonB-Dependent Iron Transport. Journal of Biomolecular Screening/SLAS Discovery. **21**(3):316-322.

Hantke K. 1983. Identification of an Iron Uptake System Specific for Coprogen and Rhodotorulic Acid in *Escherichia coli* K12. Molecular & General Genetics. **191**(2):301-306.

Harro C, Betts R, et al. 2010. Safety and Immunogenicity of a Novel *Staphylococcus aureus* Vaccine: Results from the First Study of the Vaccine Dose Range in Humans. Clinical and Vaccine Immunology. **17**(12):1868-1874.

Higgs PI, Larsen RA, Postle K. 2002. Quantification of Known Components of the *Escherichia coli* TonB Energy Transduction System: TonB, ExbB, ExbD and FepA. Molecular Microbiology. **44**(1):271-281.

Honsa ES, Fabian M, et al. 2011. The Five Near-iron Transporter (NEAT) Domain Anthrax Hemophore, IsdX2, Scavenges Heme from Hemoglobin and Transfers Heme to the Surface Protein IsdC. J. Biol Chem. **286**(38):33652-33660.

Honsa ES, Maresso AW and Highlander SK. 2014. Molecular and Evolutionary Analysis of NEAr-Iron Transporter (NEAT) Domains. PLoS ONE. **9**(8): e104794.

Honsa ES, Owens CP, et al. 2013. The Near-iron Transporter (NEAT) Domains of the Anthrax Hemophore IsdX2 Require a Critical Glutamine to Extract Heme from Methemoglobin. J Biol Chem. **288**(12):8479-8490.

Huché F, Delepelaire P, Wandersman C and Welte W. 2006. Purification, Crystallization and Preliminary X-ray Analysis of the Outer Membrane Complex HasA-HasR from *Serratia marcescens.* Acta. Cryst. **F62**:56-60.

James KJ, Hancock MA, et al. 2008. TonB Induced Conformational Changes in Surface-Exposed f of FhuA, Outer Membrane Receptor of *Escherichia coli*. Protein Science. **17**:1679-1688.

Janulczyk R, Ricci S and Bjorck L. 2003. MtsABC is Important for Manganese and Iron Transport, Oxidative Stress Resistance, and Virulence of *Streptococcus pyogenes*. Infection and Immunity. **71**(5):2656-2664.

Jiang X, Payne MA, et al. 1997. Ligand-Specific Opening of a Gated-Porin Channel in the Outer Membrane of Living Bacteria. Science. **276**:1261-1264.

Jin B, Newton SMC, et al. 2006. Iron Acquisition Systems for Ferric Hydroxamates Haemin and Haemoglobin in *Listeria monocytogenes.* Molecular Microbiology. **59**(4):1185-1198.

Jordan LD, Zhou Y, et al. 2013. Energy-Dependent Motion of TonB in the Gram-negative Bacterial Inner Membrane. PNAS. **110**(28):11553-11558.

Joshi A, Pancari G et al. 2012. Immunization with *Staphylococcus aureus* Iron Regulated Surface Determinant B (IsdB) Confers Protection via Th17/IL17 Pathway in a Murine Sepsis Model. Human Vaccines and Immunotherapeutics. **8**(3):336-346.

Kim M, Hwang S, Ryu S and Jeon B. 2011. Regulation of *perR* Expression by Iron and PerR in *Campylobacter jejuni*. J Bacteriol. **193**(22):6171-6178.

Klebba PE. 2016. ROSET Model of TonB Action Gram-negative Bacterial Iron Acquisition. J. Bacteriol. **198**(7): 1013-1021.

Klebba PE, Charbit A, et al. 2012. Mechanisms of Iron and Haem Transport by *Listeria monocytogenes*. Molecular Membrane Biology. **29**(3-4):69-86.

Klebba PE, McIntosh MA and Neilands JB. 1982. Kinetics of Biosynthesis of Iron-Regulated Membrane Proteins in *Escherichia coli*. J Bacteriol. **149**:880-888.

Krieg S, Huché F, et al. 2009. Heme Uptake Across the Outer Membrane as Revealed by Crystal Structures of the Receptor-Hemophore Complex. PNAS. **106**(4):1045-1050.

Lauer P, Chow MY, et al. 2002. Construction, Characterization, and Use of Two *Listeria monocytogenes* Site-Specific Integration Vectors. J Bacteriol. **184**(15):4177-4186.

Lechowicz J and Krawczyk-Balska A. 2015. An Update on the Transport and Metabolism of Iron in *Listeria monocytogenes:* The Role of Proteins Involved in Pathogenicity. Biometals. **28**:587-603.

Ledala N, Pearson SL, Wilinson J and Jayaswal RK. 2007. Molecular Characterization of the Fur protein of *Listeria monocytogenes*. Microbiology. **153**:1103-1111.

Lee JW and Helmann JD. 2007. Functional Specialization within the Fur Family of Metalloregulators. Biometals. **20**:485-499.

Lee YL, Passalacqua KD, Hanna PC and Sherman DH. 2011. Regulation of Petrobactin and Bacillibactin Biosynthesis in *Bacillus anthracis* Under Iron and Oxygen Variation. PLOS ONE. **6**(6): e20777.

Lei B, Liu M, et al. 2003. Identification and Characterization of HtsA, a Second Heme-Binding Protein Made by *Streptococcus pyogenes*. Infect Immun. **71**(10):5962-5969.

Lei B, Smoot LM, et al. 2002. Identification and Characterization of a Novel Heme-Associated Cell Surface Protein Made by *Streptococcus pyogenes*. Infect Immun. **70**:4494-4500.

Létoffé S, Delepelaire P and Wandersman C. 2004. Free and Hemophore-Bound Heme Acquisition through the Outer Membrane Receptor HasR Have Different Requirements for the TonB-ExbB-ExbD Complex. J Bacteriol. **186**(13):4067-4074.

Lewinson O, Lee AT, Locher KP and Rees DC. 2010. A Distinct Mechanism for the ABC Transporter BtuCD-BtuF Revealed by the Dynamics of Complex Formation. Nature Structural and Molecular Biology. **17**(3):332-338.

Locher KP. 2009. Structure and Mechanism of ATP-binding Cassette Transporters. Phil Trans R Soc B. **364**:239-245.

Locher KP, Rees B, et al. 1998. Transmembrane Signaling Across the Ligand-Gated FhuA Receptor: Crystal Structures of Free and Ferrichrome-Bound States Reveal Allosteric Changes. Cell. **95**:771-778.

Lu C, Xie G, et al. 2012. Direct Heme Transfer Reactions in the Group A *Streptococcus* Heme Acquisition Pathway. PLOS ONE. **7**(5): e37556.

Ma L, Kaserer W, et al. 2007. Evidence of Ball-and-Chain Transport of Ferric Enterobactin through FepA. J Biol Chem. **282**(1):397-406.

Ma L, Terwiliger A and Maresso AW. 2015. Iron and Zinc Exploitation during Bacterial Pathogenesis. Metallomics. **7**(12):1541-1554.

Malmirchegini GR, Sjodt M, et al. 2014. Novel Mechanism of Hemin Capture by Hbp2, the Hemoglobin-Binding Hemophore from *Listeria monocytogenes.* J Biol Chem. **289**(50):34886-34899.

Maltais TR, Adak AK, et al. 2016. Label-Free Detection and Discrimination of Bacterial Pathogens Based on Hemin Recognition. Bioconjugate Chemistry. **27:** 1713-1722.

Maresso AW, Chapta TJ and Schneewind O. 2006. Surface Protein IsdC and Sortase B are Required for Heme-Iron Scavenging of *Bacillus anthracis*. J Bacteriol. **188**(23):8145-8152.

Maresso AW, Garufi G and Schneewind O. 2008. *Bacillus anthracis* Secretes Proteins That Mediate Heme Acquisition from Hemoglobin. PLOS Pathogen. **4**(8): e1000132.

Maresso AW and Schneewind O. 2006. Iron Acquisition and Transport in *Staphylococcus aureus*. BioMetals. **19**:193-203.

Marsay L, Dold C, et al. 2015. A Novel Meningococcal Outer Membrane Vesicle Vaccine with Constitutive Expression of FetA: A Phase I Clinical Trial. J Infect. **71**(3):326-337.

May JJ, Wendrich TM and Marahiel MA. 2001. The *dhb* Operon of *Bacillus subtilis* Encodes the Biosynthetic Template for the Catecholic Siderophore 2,3-Dihydrixybenzoate-Glycine-Threonine Trimeric Ester Bacillibactin. J Biol Chem. **276**(10):7209-7217.

Mazmanian SK, Skaar EP, et al. 2003. Passage of Heme-Iron Across the Envelope of *Staphylococcus aureus*. Science. **299**:906-909.

McLaughlin HP, Xiao Q, et al. 2012. A Putative P-Type ATPase Required for Virulence and Resistance to Haem Toxicity in *Listeria monocytogenes*. PLOS ONE. **7**(2): e30928.

McNeely TB, Shah NA, et al. 2014. Mortality Among Recipients of the Merck V710 *Staphylococcus aureus* Vaccine After Postoperative *S. aureus* Infections: An Analysis of Possible Contributing Host Factors. Human Vaccines and Immunotherapeutics. **10**(12):3513-3516.

Merchant AT and Spatafora GA. 2014. A Role for the DtxR Family of Metalloregulators in Gram-positive Pathogenesis. Mol Oral Microbiol. **29**(1)1-10.

Mesnage S, Fontaine T, et al. 2000. Bacterial SLH Domain Proteins are Non-Covalently Anchored to the Cell Surface via a Conserved Mechanism Involving Wall Polysaccharide Pyruvylation. The EMBO Journal. **19**(17):4473-4484.

Michelini E, Cevenini L, et al. 2010. Cell-Based Assays: Fueling Drug Discovery. Anal Bioanal Chem. **398**: 227-238.

Mike LA, Smith SN, et al. 2016. Siderophore Vaccine Conjugates Protect Against Uropathogenic *Escherichia coli* Urinary Tract Infection. PNAS. **113**(47):13468-13473.

Miller JH. 1972. Experiments in Molecular Genetics. Cold Spring Harbor Laboratory, Cold Spring Harbor, NY.

Mirus O, Strauss S, et al. 2009. TonB-Dependent Transporters and their Occurrence in Cyanobacteria. BMC Biology. **7**:68.

Montañez GE, Neely MN and Eichenbaum Z. 2005. The Streptococcal Iron Uptake (Siu) Transporter is Required for Iron Uptake and Virulence in a Zebrafish Infection Model. Microbiology. **151**:3749-3757.

Moriwaki Y, Terada T, et al. 2013. Heme Binding Mechanism of Structurally Similar Iron-Regulated Surface Determinant Near Transporter Domains of *Staphylococcus aureus* Exhibiting Different Affinities for Heme. Biochemistry. **52**:8866-8877.

Moriwaki Y, Terada T, Tsumoto K and Shimizu K. 2015. Rapid Heme Transfer Reactions between NEAr Transporter Domains of *Staphylococcus aureus*: A Theoretical Study Using QM/MM and MD Simulations. PLOS ONE. **10**(12): e0145125.

Nairn BL, Eliasson OS, et al. 2017. Fluorescence High-Throughput Screening for Inhibitors of TonB Action. J Bacteriol. **199**(10): e00889-16.

Neidhardt FC, Bloch PL and Smith DF. 1974. Culture Medium for Enterobacteria. J Bacteriol. **119**(3): 736-747.

Neilands JB. 1981. Microbial Iron Compounds. Ann Rev Biochem. **50**:715-731.

Neugebauer H, Herrmann C, et al. 2005. ExbBD-Dependent Transport of Maltodextrins through the Novel MalA Protein across the Outer Membrane of *Caulobacter crescentus*. J Bacteriol. **187**(24):8300-8311.

Newton SMC, Igo JD, et al. 1999. Effect of Loop Deletions on the Binding and Transport of Ferric Enterobactin by FepA. Molecular Microbiology. **32**(6):1153-1165.

Newton SMC, Klebba PE, et al. 2005. The *svpA-srtB* locus of *Listeria monocytogenes* Fur-Mediated Iron Regulation and Effect on Virulence. Molecular Microbiology **55**(3):927-940.

Newton SMC, Trinh V, Pi H and Klebba PE. 2010. Direct Measurements of the Outer Membrane Stage of Ferric Enterobactin Transport. J Biol Chem. **285**(23):17488-17497.

Nierman WC, Feldblyum TV, et al. 2001. Complete Genome Sequence of *Caulobacter crescentus*. PNAS **98**(11):4136-4141.

Nikaido H and Rosenberg EY. 1990. Cir and Fiu Proteins in the Outer Membrane of *Escherichia coli* Catalyze Transport of Monomeric Catechols: Study with β-Lactam Antibiotics Containing Catechol and Analogous Groups. J Bacteriol. **172**(3):1361-1367.

Noinaj N, Guillier M, Barnard TJ and Buchanan SK. 2010. TonB-Dependent Transporters: Regulation, Structure, and Function. Annu Rev Microbiol. **64**:43-60.

Nygaard TK, Blouin GC, et al. 2006. The Mechanism of Direct Heme Transfer from the Streptococcal Cell Surface Protein Shp to HtsA of the HtsABC Transporter. J. Biol. Chem. **281**(30):20761-20771.

Occhino DA, Wyckoff EE, et al. 1998. *Vibrio cholera* Iron Transport: Haem Transport Genes are Linked to One of Two Sets of *tonB, exbB, exbD* Genes. Molecular Microbiology. **29**(6):1493-1507.

Ouattara M, Pennati A, et al. 2013. Kinetics of Heme Transfer by the Shr NEAT Domains of Group A Streptococcus. Arch Biochem Biophys. **538**(2):71-79.

Page MGP, Dantier C and Desarbre E. 2010. *In Vitro* Properties of BAL30072, a Novel Siderophore Sulfactam with Activity Against Multiresistant Gram-negative Bacilli. Antimicrobial Agents and Chemotherapy. **54**(6):2291-2302.

Pancari G, Fan H, et al. 2012. Characterization of the Mechanism of Protection Mediated by CS-D7, a Monoclonal Antibody to *Staphylococcus aureus* Iron Regulated Surface Determinant B (IsdB). Front Cell Infect Microbiol. **2**:36.

Pawelek PD, Croteau N, et al. 2006. Structure of TonB in Complex with FhuA, *E. coli* Outer Membrane Receptor. Science. **312**:1399-1402.

Payne MA, Igo JD, et al. 1997. Biphasic Binding Kinetics Between FepA and its Ligands. J. Biol. Chem. **272**:21950-21955.

Phadke ND, Molloy MP, et al. 2001. Analysis of the Outer Membrane Proteome of *Caulobacter crescentus* by Two-Dimensional Electrophoresis and Mass Spectrometry. Proteomics. **1**:705-720.

Pi H, Patel SJ, et al. 2016. The *Listeria monocytogenes* Fur-regulated Virulence Protein FrvA is an Fe(II) efflux P_{1B4}-type ATPase. Molecular Microbiology. **100**(6):1066-1079.

Pilpa RM, Robson SA, et al. 2008. Functionally Distinct NEAT (NEAr Transporter) Domains within the *Staphylococcus aureus* IsdH/HarA protein Extract Heme from Methemoglobin. J Biol Chem. **284**(2):1166-1176.

Pishchany G, Sheldon JR, et al. 2014. IsdB-Dependent Hemoglobin Binding is Required for Acquisition of Heme by *Staphylococcus aureus*. Journal of Infectious Diseases. **209**(11):1764-1772.

Proctor RA. 2012. Challenges for a Universal *Staphylococcus aureus* Vaccine. Clinical Infectious Diseases. **54**(8):1179-1186.

Raymond KN, Dertz EA and Kim SS. 2003. Enterobactin: An Archetype for Microbial Iron Transport. PNAS. **100**(7):3584-3588.

Roe KL, Hogle SL and Barbeau KA. 2013. Utilization of Heme as an Iron Source by Marine *Alphaproteobacteria* in the *Roseobacter* Clade. Applied and Environmental Microbiology. **79**(18):5753-5762.

Ruhr E and Sahl HG. 1985. Mode of Action of the Peptide Antibiotic Nisin and Influence on the Membrane Potential of Whole Cells and on Cytoplasmic and Artificial Membrane Vesicles. Antimicrobial Agents and Chemotherapy. **27**(5):841-845.

Rutz JM, Liu J, et al. 1992. Formation of a Gated Channel by a Ligand-Specific Transport Protein in the Bacterial Outer Membrane. Science. **258**:471-475.

Sæderup KL, Stødkilde K, et al. 2016. The *Staphylococcus aureus* Protein IsdH Inhibits Host Hemoglobin Scavenging to Promote Heme Acquisition by the Pathogen. J Biol Chem. **291**(46):23989-23998.

Schauer K, Rodinov DA and de Reuse H. 2008. New Substrates for TonB-Dependent Transport: Do We Only See the 'Tip of the Iceberg'? Cell. **33**(7):330-338.

Schmitt MP and Holmes RK. 1994. Cloning, Sequence, and Footprint Analysis of Two Promoter/ Operators from *Corynebacterium diphtheriae* that are Regulated by the Diphtheria Toxin Repressor (DtxR) and Iron. J Bacteriol. **176**(4):1141-1149.

Scott DC, Cao Z, et al. 2001. Exchangeability of N Termini in the Ligand-gated Porins of *Escherichia coli*. J Biol Chem. **276**(16)13025-13033.

Scott DC, Newton SMC and Klebba PE. 2002. Surface Loop Motion in FepA. J Bacteriol. **184**(17):4906-4911.

Sharp KH, Schneider S, Cockayne A and Paoli M. 2007. Crystal Structure of the Heme-IsdC Complex, the Central Conduit of the Isd Iron/Heme Uptake System in *Staphylococcus aureus*. J Biol Chem. **282**(14):10625-10631.

Sheldon JR and Heinrichs DE. 2015. Recent Developments in Understandings the Iron Acquisition Strategies of Gram-positive Pathogens. FEMS Microbiology Reviews. **39**:592-630.

Shultis DD, Purdy MD, et al. 2006. Outer Membrane Active Transport: Structure of the BtuB:TonB Complex. Science. **312**:1396-1399.

Sjodt M, Macdonald R, et al. 2016. The PRE-Derived NMR Model of the 38.8kDa Tri-Domain IsdH Protein from *Staphylococcus aureus* Suggests that it Adaptively Recognizes Human Hemoglobin. J Mol Biol. **428**(6):1107-1129.

Skaar EP, Humayun M, et al. 2004. Iron-Source Preference of *Staphylococcus aureus* Infections. Science. **305**(5690):1626-1628.

Smallwood CR, Marco AG, et al. 2009. Fluoresceination of FepA During Colicin B Killing: Effects of Temperature, Toxin and TonB. Mol Microbiol. **72**(5):1171-1180.

Smallwood CR, Jordan L, et al. 2014. Concerted Loop Motion Triggers Induced Fit of FepA to Ferric Enterobactin. J Gen Physiol. **144**(1):71-80.

Spirig T, Malmirchegini R, et al. 2013. *Staphylococcus aureus* Uses a Novel Multidomain Receptor to Break Apart Human Hemoglobin and Steal Its Heme. J Biol Chem. **288**(2):1065-1078.

Sprencel C, Cao Z, et al. 2000. Binding of Ferric Enterobactin by the *Escherichia coli* Periplasmic Protein FepB. J Bacteriol. **182**(19):5359-5364.

Tarlovsky Y, Fabian M, et al. 2010. A *Bacillus anthracis* S-Layer Homology Protein that Binds Heme and Mediates Heme Delivery to IsdC. J Bacteriol. **192**(13):3503-3511.

Thomas X, Destoumieux-Garzón D, et al. 2004. Siderophore Peptide, a New Type of Post-Translationally Modified Antibacterial Peptide with Potent Activity. J Biol Chem. **279**(27):28233-28242.

Torres VJ, Pishchany G, et al. 2006. *Staphylococcus aureus* IsdB is a Hemoglobin Receptor Required for Heme Iron Utilization. J Biol Chem. **188**(24):8421-8429.

Toukoki C, Gold KM, McIver KS and Eichenbaum Z. 2010. MtsR is a Dual Regulator that Controls Virulence Genes and Metabolic Functions in Addition to Metal Homeostasis in GAS. Mol Microbiol. **76**(4):971-989.

Trieu-Cuot P, Carlier C, Poyart-Salmeron C and Courvalin P. 1990. A Pair of Mobilizable Shuttle Vectors Conferring Resistance to Spectinomycin for Molecular Cloning in *Escherichia coli* and in Gram-positive Bacteria. Nucleic Acid Research. **18**(14):4296.

Uluisik RC, Akbas N, et al. 2017. Characterization of the Second Conserved Domain in the Heme Uptake Protein HtaA from *Corynebacterium diphtheriae*. Journal of Inorganic Biochemistry. **167**:124-133.

Van Delden C, Page MGP and Köhler T. 2013. Involvement of Fe Uptake Systems and AmpC β-Lactamase in Susceptibility to the Siderophore Monosulfactam BAL30072 in *Pseudomonas aeruginosa*. Antimicrobial Agents and Chemotherapy. **57**(5):2095-2102.

Villareal VA, Spirig T, et al. 2011. Transient Weak Protein-Protein Complexes Transfer Heme Across the Cell Wall of *Staphylococcus aureus*. J Am Chem Soc. **133**(36):14176-14179.

Wencewicz TA. 2016. New Antibiotics from Nature's Chemical Inventory. Bioorganic and Medicinal Chemistry. **24**:6227-6252.

White P, Joshi A, et al. 2017. Exploitation of an Iron Transporter for Bacterial Protein Antibiotic Import. PNAS. pii:201713741. Doi10.1073/pnas.1713741114. [Epub ahead of print].

Wolff N, Izadi-Pruneyre N, et al. 2008. Comparative Analysis of Structural and Dynamic Properties of the Loaded and Unloaded Hemophore HasA: Functional Implications. J Mol Biol. **376**:517-525.

Yeowell HN and White JR. 1982. Iron Requirements in the Bactericidal Mechanism of Streptonigrin. Antimicrob Agens Chemother. **22**:961-968.

Yep A, McQuade T, et al. 2014. Inhibitors of TonB Function Identified by a High-Throughput Screen for Inhibitors of Iron Acquisition in Uropathogenic *Escherichia coli* CFT073. mBio. **5**(2): e01089-13.

Yukl ET, Jepkorir G, et al. 2010. Kinetic and Spectroscopic Studies of Hemin Acquisition in the Hemophore HasAp from *Pseudomonas aeruginosa*. Biochemistry. **49**:6646-6654.

Xiao Q, Jiang X, et al. 2011. Sortase Independent and Dependent Systems for Acquisition of Haem and Haemoglobin in *Listeria monocytogenes*. Mol Microbiol. **80**(6):1581-1597.

Zhang J, Chung TDY and Oldenburg KR. 1999. A Simple Statistical Parameter for Use in Evaluation and Validation of High Throughput Screening Assays. Journal of Biomolecular Screening. **4**(2):67-73.

Zhu H, Li D, et al. 2014. Non-Heme-Binding Domains and Segments of the *Staphylococcus aureus* IsdB Protein Critically Contribute to the Kinetics and Equilibrium of Heme Acquisition from Methemoglobin. PLOS ONE. **9**(6): e100744.

Zhu H, Liu M and Lei B. 2008. The Surface Protein Shr of *Streptococcus pyogenes* Binds Heme and Transfers it to the Streptococcal Heme-Binding Protein Shp. BMC Microbiology. **8**:15.